AQUATIC RESEARCH

AQUATIC RESEARCH

AQUATIC RESEARCH

Aims and Scope

"**Aquatic Research**" journal is the official publication of ScientificWebJournals (SWJ) and it is published quarterly on January, April, July, and October. The publication language of the journal is English or Turkish and continues publication since 2018.

"**Aquatic Research**" journal aims to contribute to the literature by publishing manuscripts at the highest scientific level on all fields of marine and aquatic sciences. The journal publishes original research and review articles that are prepared in accordance with the ethical guidelines.

Aquatic Biology, Aquatic Ecology, Aquatic Environment and Pollutants, Aquaculture, Conservation and Management of Aquatic Source, Economics and Managements of Fisheries, Fish Diseases and Health, Fisheries Resources and Management, Genetics of Aquatic Organisms, Limnology, Maritime Sciences, Marine Accidents, Marine Navigation and Safety, Marine and Coastal Ecology, Oseanography, Seafood Processing and Quality Control, Seafood Safety Systems, Sustainability in Marine and Freshwater Systems The target audience of the journal includes specialists and professionals working and interested in all disciplines of marine and aquatic sciences.

Manuscripts submitted to "**Aquatic Research**" journal will go through a double-blind peer-review process. Each submission will be reviewed by at least two external, independent peer reviewers who are experts in their fields in order to ensure an unbiased evaluation process. The editorial board will invite an external and independent editor to manage the evaluation processes of manuscripts submitted by editors or by the editorial board members of the journal. Our journal will be published quarterly in English or Turkish language.

The target audience of the journal includes specialists and professionals working and interested in all disciplines of marine and aquatic Sciences.

The editorial and publication processes of the journal are shaped in accordance with the guidelines of the International Committee of Medical Journal Editors (ICMJE), World Association of Medical Editors (WAME), Council of Science Editors (CSE), Committee on Publication Ethics (COPE), European Association of Science Editors (EASE), and National Information Standards Organization (NISO). The journal is in conformity with the Principles of

Transparency and Best Practice in Scholarly Publishing (doaj.org/bestpractice).

"**Aquatic Research**" journal is indexed in FAO/AGRIS, SciLit and Bielefeld Academic Search Engine (BASE).

Processing and publication are free of charge with the journal. No fees are requested from the authors at any point throughout the evaluation and publication process. All manuscripts must be submitted via the online submission system, which is available at

http://dergipark.gov.tr/journal/2277/submission/start

The journal guidelines, technical information, and the required forms are available on the journal's web page.

Statements or opinions expressed in the manuscripts published in the journal reflect the views of the author(s) and not the opinions of the ScientificWebJournals, editors, editorial board, and/or publisher; the editors, editorial board, and publisher disclaim any responsibility or liability for such materials.

OPEN ACCESS

Editor in Chief: Prof. Nuray ERKAN

Address: Istanbul University, Faculty of Aquatic Sciences, Department of Seafood Processing Technology, Ordu Cad. No: 8, 34134 Fatih/Istanbul, Turkey

E-mail: nurerkan@istanbul.edu.tr

Contents/İçerik

Research Article

THE INHIBITORY SITUATIONAL ANALYSIS OF SOME FEED INGREDIENTS FOR MEAGRE, *Argyrosomus regius* (Asso 1801) LARVAE AND EVALUATION FOR DIET FORMULATIONS

Gürkan Diken[1] , Orhan Demir[1] , Mehmet Naz[2]

[1] Isparta University of Applied Sciences, Faculty of Eğirdir Fisheries, Isparta, 32260 Turkey

[2] Iskenderun Technical University, Marine Science and Technology Faculty, İskenderun, Hatay, 31200, Turkey

ORCID IDs of the authors:
G.D. 0000-0002-3386-3676
O.D. 0000-0002-1230-8489
M.N. 0000-0002-5129-8498

Correspondence:

Gürkan DİKEN
E-mail: gurkandiken@isparta.edu.tr

ABSTRACT

Meagre, *Argyrosomus regius* (Asso 1801) is an important alternative species in aquaculture. The *in vitro* assay provides practical assessments for the evaluation of feed ingredients. In this study, the inhibition degrees of feed ingredients (fish meal-FM, fish hydrolysate-FH, krill meal-KM, soybean meal-SM, wheat gluten-WG, corn gluten-CG and sunflower meal-SF) on protease activities of meagre larvae were determined. Larvae were sampled from the first day of opening the mouth (3 days after hatching-DAH) until the end of the weaning (32 DAH) from the Egemar Hatchery (Aydın-Turkey). Larvae of the total length were measured as 3.19 ±0.02-21.61 ±0.22 mm and weights were calculated as 0.53 ±0.02-118.00 ±1.09 mg at 3 and 32 DAH, respectively. Protease activities of larvae were the lowest as 5.95 ±0.60 U/mg protein (15 DAH) and the highest as 211.21 ±12.56 U/mg protein (7 DAH), respectively ($P<0.05$). The lowest inhibitions degrees of feed ingredients were observed at 15 DAH except for SF. The use of FH in the diet formulations of meagre larvae should be paid attention. While CG and SF are advised, SM does not seem to be suitable.

Keywords: *Argyrosomus regius,* Meagre, Protease activities, Inhibitions, Feed ingredients

Introduction

Mediterranean marine aquaculture production in Turkey, Greece, France, Italy, Spain, Croatia and Cyprus based on total juvenile production reached to 1.3 billion number in gilthead bream (*Sparus aurata*) and European sea bass (*Dicentrarchus labrax*) production (FEAP, 2016). Aquaculture requires low cost inputs and high productivity and needs to focus on the introduction of new candidate species. Meagre is an important species in diversification of Mediterranean aquaculture (El-Shebly et al., 2007; Monfort, 2010; Kružić et al., 2016). Because of its high pace of growth, it has significant advantages in aquaculture (Quemener, 2002; Duncan and Myrseth, 2011; Parisi et al., 2014). The sciaenid meagre is a Mediterranean species and distributed in the Atlantic coasts of Europe and the northwest coast of Africa (Whitehead et al., 1986; Haffray et al., 2012).

A better understanding of the nutrient requirement of larvae, the absolute requirement of nutrient concentrations and the determination of optimal intervals will provide significant contributions to larval feeding studies (Person-Le Ruyet and Bergot, 2001; Holt et al., 2011; Southgate, 2012). *In vivo* methods used in the aquaculture feeding experiment expressed that the evaluation of nutritional value of the feed is time-consuming and the results can be affected by environmental factors. *In vitro* methods were described as rapid, reproducible and allowed only small quantities of raw materials to be used (Ezquerra et al., 1997; Garciá-Ortega et al., 2000). *In vitro* methods commonly used in the evaluation of nutrition and nutritional qualities of humans and terrestrial animals had the potential to be used in determining the feed components and production methods of fish larvae (Holt et al., 2011; Moyano et al., 2015). It was found that *in vitro* methods of extracting larval digestive enzymes and mixing with food and hydrolysis measured were used to determine the digestibility of fish larvae (Holt et al., 2011). *In vitro* techniques were reported to be important for the development of larval artificial feeds and in recent years *in vitro* techniques were assessed for pre-protein digestibility of larval microcapsules (Cahu and Zambonino Infante, 1994). Inhibitors of proteases in fish diet revealed different sensitivity for the preliminary evaluation of the usability of the ingredients in feed (Moyano et al., 1998; Alarcón et al., 1999). The effects of feed ingredients on protease activities of *Sparus aurata* larvae and shrimps were determined (Alarcón et al., 1997, 1999). In addition, trials were carried out to evaluate cheap and sustainable alternative protein sources such as soybean meal in diets. However, the main obstacles to the use of high amounts of plant protein sources in fish diets were at low protein quality due to the amino acid imbalances and the availability of antinutritional component decreasing

the activity of enzymes (Tacon, 1997; Krogdahl et al., 2003).

Researchers focused on growth, survival and larval rearing of meagre, the histology and ontogeny of digestive system of larval meagre and the effects of different levels of plant proteins on juvenile meagre (Fernández-Palacios et al., 2007; Roo et al., Arda, 2011; 2010; Estévez et al., 2011; Schiavone et al., 2012; Papadakis et al., 2013; Vallés and Estévez, 2013, 2015). Also, digestive enzymes of marine fish larvae such as European seabass, gilthead seabream, Senegalese sole, white seabream, redbanded seabream, meagre were studied (Zambonino Infante and Cahu, 1994; Moyano et al., 1996; Ribeiro et al., 1999; Cara et al., 2003; Moyano et al., 2005; Süzer et al., 2013; Solovyev et al., 2016).

We identified studies on inhibition effects of feed ingredients and microdietes related to marine fish (Kuzu and Naz, 2012; Naz and Yúfera, 2012; Yıldız et al., 2012; Yılmaz et al., 2012; Haközü, 2014). We could only find few studies on the inhibitory effects of microdiets and feed ingredients on protease activities of meagre larvae (Diken et al., 2016a, b, c; 2017; Diken et al., 2018). Therefore, the aim of this research was to determine the potential inhibitory effects of commonly used feed ingredients on protease activities of meagre larvae using *in vitro* techniques and suggested for microdiet formulations of larvae of meagre.

Material and Methods

Larvae Culture and Sampling

Larval rearing was conducted in EGEMAR Aquaculture Food Industry and Commercial Incorporated Company (Aydın/TURKEY). Eggs were obtained by hormone injection which fertilized ones were incubated at conical fiberglass tank and 23.6±0.5ºC (GnRH; 20 µg/kg ♀ and 10 µg/kg ♂). Larvae were fed between 0-15 DAH, in 7 m³ ellipsoidal fiberglass tank and the rate of 75-80 larvae/L in the larva unit. Larvae weaning were taken at 16-32 DAH, in 27 m³ raceway made of concrete and the rate of 10-12 larvae/L in the weaning unit. The water used in the aquaculture was filtered by sand, bag and UV filters. Environmental conditions of larval cultures were determined at 20.8-24.1ºC temperature, 27.0-40.0 g/L salinity, 8.4-14.4 mg/L O_2, and 7.5-7.9 pH. Air and water was entered from the surface until 15 DAH and it was applied to 18light:6dark photoperiod (18L:6D h). The feeding protocol is at Table 1. Prior to feeding, samples were taken from 3, 5, 7, 10, 12, 15, 17, 20, 22, 25, 27, 30, 32 DAH larvae triplicates and taken to protection in liquid nitrogen tank (-196 ºC).

In Vitro Assay

Extracts of larvae

The larvae were thawed by maintaining the cold chain and rinsed in distilled water, and the whole body was homogenized (400 mg/mL in distilled water) and centrifuged (16,000 g, 30 minutes at 4 °C) to extract the larvae.

Extracts of feed ingredients

Extracts of feed ingredients (fish meal, fish hydrolysate, krill meal, soybean meal, wheat gluten, corn gluten, and sunflower meal) were prepared by homogenization (100 mg/mL in distilled water) followed by centrifugation (15,000 g, 10 minutes).

Determination of protease activities of larvae

Total protease activities of larvae were measured as described by Walter (1984), using casein (10 mg/mL) in 50 mM Tris-HCl buffer at pH 8.5 as the substrate. The mixtures including extracts of larvae and substrate were incubated and then the reaction was stopped by addition of 500 μL trichloroaceticacid (TCA) (concentration of TCA, 120 g/L). Total protease activities were determined as spectrophotometrically (Shimadzu UV mini 1204). One unit of enzyme activity was defined as 1 μg of tyrosine release per minute. The soluble protein concentrations of larvae were determined according to Bradford (1976).

Effects of feed ingredients on protease activities of larvae

The inhibitory effects of feed ingredients on protease activities of meagre larvae were determined by measuring the reduction in protease activity of extracts using a modification of the method described by García-Carreno (1996). The method was based on the measurement of residual protease activity remaining after preincubation with feed ingredients. Values were calculated as inhibition degrees %.

Statistical Methods

Larval measurements were made on 30 samples. *In vitro* assays were performed in triplicates. The experimental data, the larval total length and weight and larvae's protease and the inhibition degrees of feed ingredients were subjected to one-way ANOVA and mean ±standard error (SE) differences were calculated by using SPSS software (v21, IBM, USA) statistical package. Statistical significance of larvae's protease was tested by Duncan test at P=0.05 content level.

Results and Discussion

Meagre is an important species because of market preferences and product diversity in various sizes with rapid development production in Mediterranean marine aquaculture (Monfort, 2010). Studies on this important and potential cultivation have been continuing at a considerable level in recent years (Fernández-Palacios et al., 2007; Gil Oviedo and Gracia and Jofre, 2013; Bodur et al., 2014; Vargas-Chacoff et al., 2014; Velazco-Vargas et al., 2014; Candeias-Mendes et al., 2015; Saavedra et al., 2016; Campoverde et al., 2017). Among these studies, diet and nutrition relationship are the main research topics. In addition, meagre is a species that has the potential to evaluate vegetable feed ingredients (Bestin et al., 2014; Dias et al., 2014; Ribeiro et al., 2015). Our study, is a research that supports investigations in which we conducted *in vitro* studies to determine the feed ingredients of the meagre larvae. *In vitro* techniques have been used and recommended by many investigators (Eid and Matty 1989; Ezquerra et al., 1998; Alarcón et al., 1999; Ali et al., 2009; Kuzu and Naz, 2012; Yıldız et al., 2012; Yılmaz et al., 2012). Significant results have been achieved with this method for determining potential inhibitory effects of feed ingredients (fish meal, fish hydrolysate, krill meal, soybean meal, wheat gluten, corn gluten, and sunflower meal) on protease activities of larvae of meagre.

Total length and wet weight gains were obtained from 3 DAH to 32 DAH of the meagre larvae (Figure 1, 2). It determined that these values have increased from 0.53 ±0.02 mg to 118.00± 1.09 mg and 3.19 ±0.02 mm to 21.61 ±0.22 mm, respectively. These results indicated that the larval stage of meagre is a species with a high rate of development. The results of the study revealed that larvae had high growth rates. These results were similar to the larval stage results of Gamsız and Neke (2008), Arda (2011) and Papadakis et al., (2013) and support the expression that Quemener (2002), and Gamsız and Neke (2008)'s meagre larvae had a high rate of development.

Changes in protease activity of larvae of meagre were calculated at the highest value at 7 DAH (211.21 ±12.56 U/mg protein) and the lowest at 15 DAH (5.95 ±0.6 U/mg protein) (Figure 3). Sharper decreases and increases were observed in protease activity changes on days 3, 5, 7, and 10, and these values were determined at statistical differences at significant levels on the 4 measurement days (P<0.05). From 10 DAH to 32 DAH, there were no significant differences in protease activity changes and calculated lower before 10 DAH. The protease activity changes of meagre larvae supported that the fluctuations in the protease activities of the larvae of gilthead seabream was not related to the decrease in enzyme synthesis but reflected an increase in tissue proteins (Zambonino Infante and Cahu, 2001).
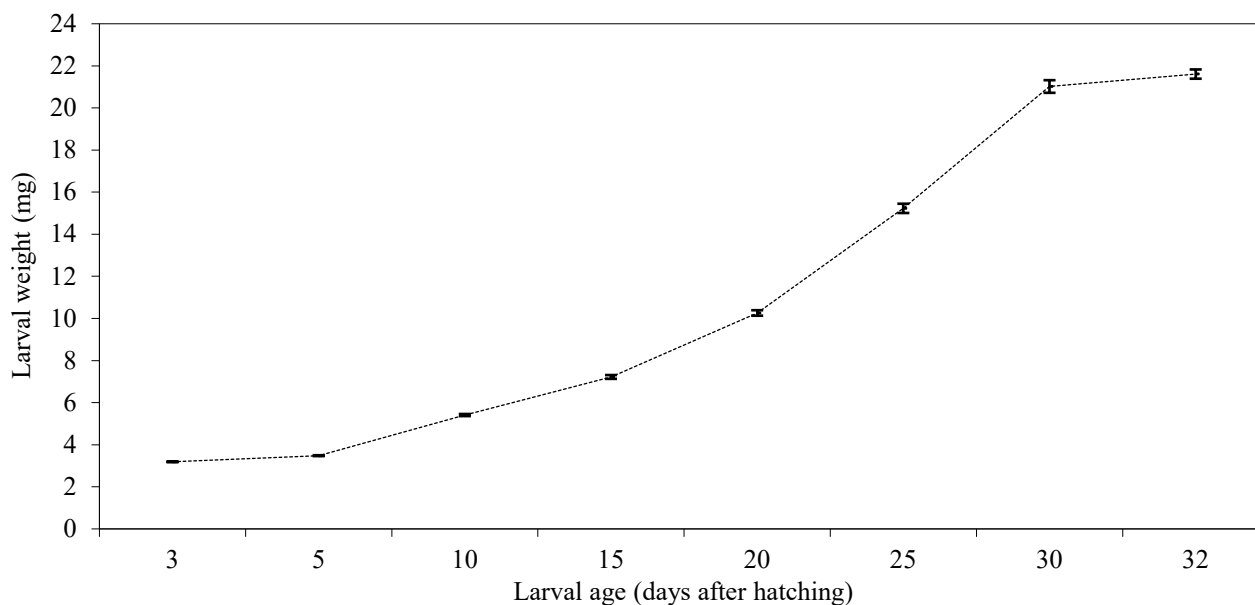
Figure 1. Weight changes of larvae of meagre (*A. regius*) (wet weight mean ±SE mg n=30)
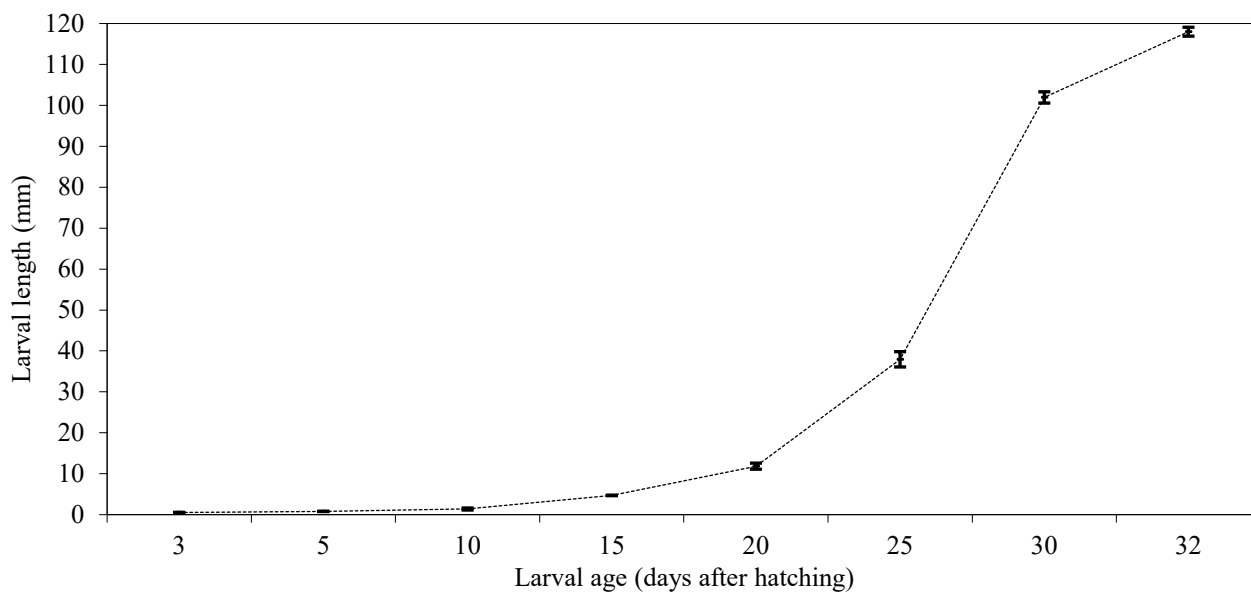
Figure 2. Lenght changes of larvae of meagre (*A. regius*) (total lenght mean ±SE mm n=30)
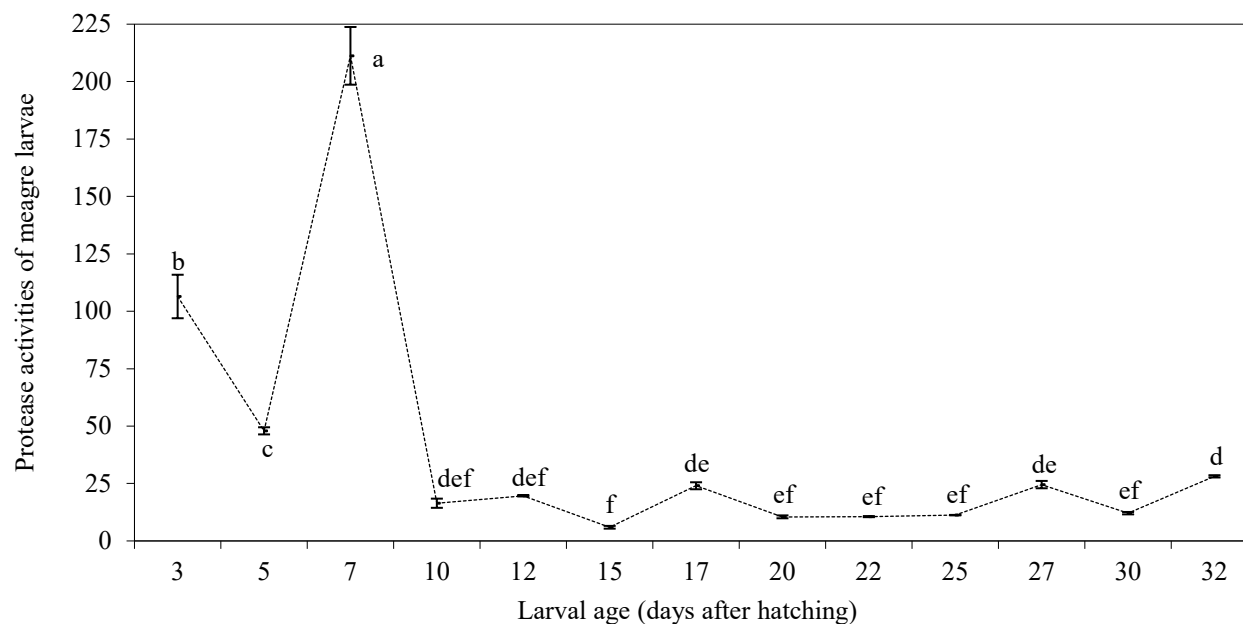
Figure 3. The changes of protease activities of larvae of meagre (*A. regius*) (U/mg protein mean ±SE mg). Different superscripts show significant differences between means of protease activities

The mean values of inhibition levels of feed ingredients at 3-32 DAH were calculated high in fish hydrolysate from animal sources and in soybean meal and wheat gluten from vegetable sources (Figure 4, 5). However, in these assessments, 3, 5, 7, 10, 12, 15, 17, 20, 22, 25, 27, 30, and 32 DAH of the analysis should be evaluated separately.

Results of inhibition analysis revealed that fish meal had low inhibitions until 10 DAH while it was expected that larvae offered fish hydrolysate would exhibit worse performance than fish meal (Figure 4). Fish meal, fish hydrolysate and krill meal showed the lowest inhibitions at 15 DAH and then, followed by a sharp increase from 15 to 17 DAH. The inhibitions of fish meal and krill meal tended to increase until 20 DAH but not fish hydrolysate. After 20 DAH, fish hydrolysate had the highest inhibitions. Fish meal exhibited lower inhibitions at 17, 22, 27, and 32 DAH than those of both fish hydrolysate and krill meal. However, fish hydrolysate at 12, 20, 25, and 30 DAH exhibited lower inhibitions than those of fish meal. Kolkovski and Tandler (2000) reported even 50% replacement of the dietary protein with hydrolysed squid meal was associated with a decline in seabream larval growth. This study clearly reveals the suitability of fish meal for critical larval stages but not fish hydrolysate except for the mentioned days above.

The results demonstrate that krill meal had low inhibitions in critical larval stage except for 5 DAH. After 15 DAH,

krill meal showed better performance than those of fish hydrolysate except for 20 DAH and also, fish meal at 25 and 30 DAH. Kolkovski et al. (2000) reported that feed attractants such as krill can play an important role in acceptance of dry diets in fish larvae during the weaning period as well as enhancing growth due to higher consumption. They showed that, coating dry diets with liquid krill hydrolysate can improve dry diet attractiveness, increase in larval growth and can potentially decrease the duration of weaning period. Our results revealed that krill meal is a good candidate to be used in microdiets of meagre larvae except for the mentioned days above.

The inhibitions of soybean meal on protease activities of larvae were high except for 15 and 25 DAH (Figure 5). In addition, wheat gluten on protease activities of larvae had the high inhibitions except for 15, 20, 22, 25, and 30 DAH. Corn gluten had lower inhibitions than those of soybean meal and also wheat gluten except for 30 DAH. Sunflower meal had low inhibitions except for 5, 15, and 25 DAH. The lowest inhibition of sunflower meal was measured at 3 DAH. The lowest inhibitions of soybean meal, wheat gluten, and corn gluten were determined at 15 DAH except for sunflower meal. The highest inhibitions of soybean meal, wheat gluten were observed at 3 DAH and corn gluten at 17 DAH. Soybean meal and wheat gluten exhibited high inhibitions until 12 DAH. However, corn gluten and sunflower meal in these days had better performance except for 5 DAH of sunflower. Inhibition results indicated that soybean meal is not suitable

for microdiets of meagre larvae. However, corn gluten could be used as feed ingredient in microdiets of meagre larvae. Soy protein concentrate and corn gluten have been researched as possible fish meal replacement in aquaculture feeds. Complete substitution of fish meal with soy protein has been achieved only in rainbow trout (Kaushik et al., 1995; Rodehutscord et al., 1995). In addition, a similar study has been reported that soy protein concentrate and vegetable protein concentrate do not appear to be suitable for meagre larvae (Diken et al., 2016c). The use of soy protein or corn gluten as the sole protein source in diets for gilthead seabream is not recommended (Kissil and Lupatsch, 2004). Hence the replacement of fish meal with a mixture of several vegetable protein sources is a common approach in order to minimize the amino acid deficiencies in fish diet and meet the nutritional requirements of fish species (De Francesco et al., 2007). Kissil and Lupatsch (2004) reported that processing of soybean meal (heating, defattening or germination) does not guarantee the elimination of antinutritional factors. Moyano et al. (1999) showed that protease inhibitors in soybeans and corn gluten reduce the activity of proteolytic enzymes in seabream and also soybean inhibitors have a stronger effect than those in corn gluten. Results obtained positive effects of corn gluten and negative effects of soybean meal on protease activities of meagre larvae and was supported by Moyano et al. (1999). On the other hand, it was reported that meagre larvae of soybean meal (defatted soybean meal) can be used at the level that can substitute fish meal in their growing feed (Velazco-Vargas et al., 2013).

Wheat gluten was researched as possible fish meal replacement in aquaculture feeds. Complete substitution of fish meal with wheat gluten was achieved only in rainbow trout (Kaushik et al., 1995; Rodehutscord et al., 1995). Kaushik et al. (2004) recently suggested that the use of wheat gluten in combination with other plant proteins may be economically feasible as a fish meal substitute for European seabass. Results of the present study indicated that wheat gluten is not suggested until 12 DAH. After 12 DAH, wheat gluten can be used up to 32 DAH except for 17 and comparatively 27 DAH. Sunflower meal and corn gluten had lower inhibitions when compared with other plant protein sources. According to the results of this study, sunflower meal is moderately advisable as feed ingredient in microdiets of meagre larvae except for 5 and 25 DAH.

On the protease activities of gilthead seabream larvae corn gluten, and on the protease activities of European seabass larvae wheat gluen and protease activities of both marine fish larvae soybean meal have not been recommended due to inhibition effects. However, wheat gluten for gilthead seabream larvae and corn gluten for European seabass larvae have been recommended (Kuzu and Naz, 2012; Yıldız et al., 2012). Our study results also suggest that soybean meal has not been recommended for meagre larvae, marine fish larvae are important for feed formulations. On the other hand, the preference for meagre larvae supports the availability of vegetable feed ingredients in microdiet formulations of the meagre larvae of corn and wheat gluten.
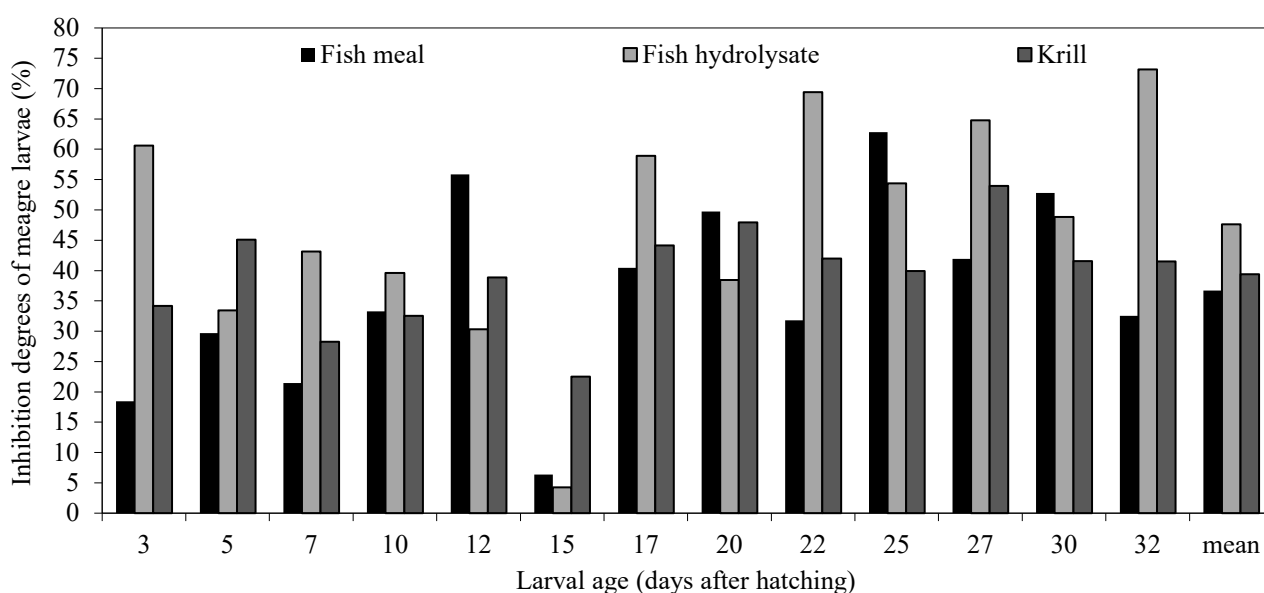
Figure 4. The inhibitory effects of feed ingredients such as fish meal, fish hydrolysate, and krill meal on protease activities of larvae of meagre (*A. regius*) (%)
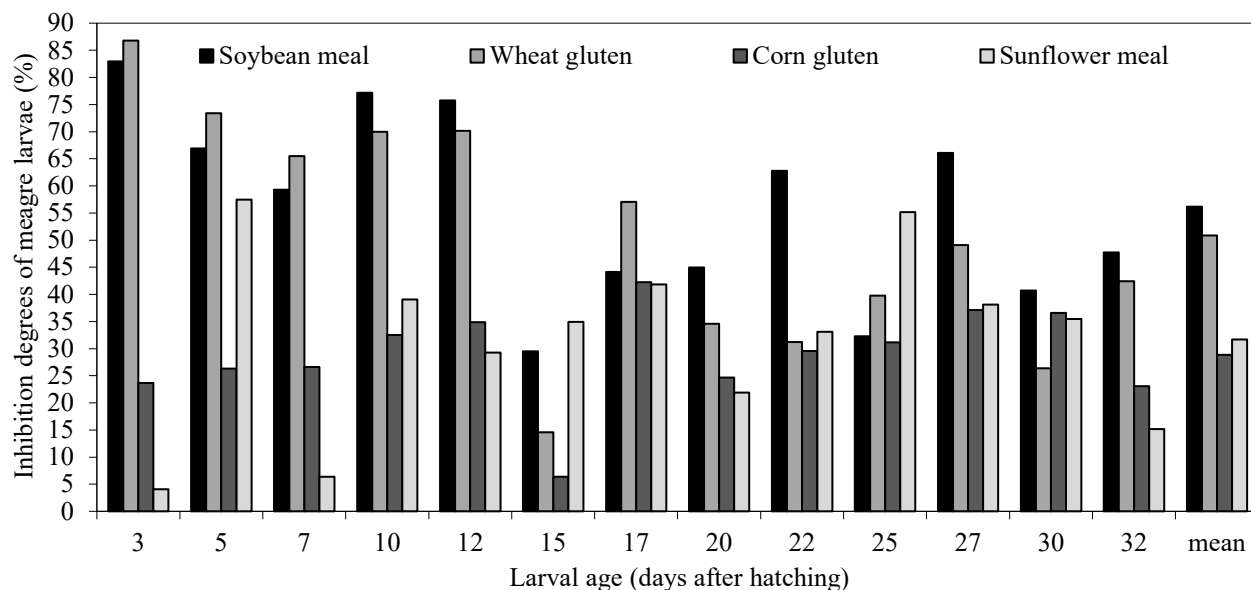
Figure 5. The inhibitory effects of feed ingredients such as soybean meal, wheat gluten, corn gluten, and sunflower meal on protease activities of larvae of meagre (*A. regius*) (%)

Table 1. Meagre (*A.regius*) larvae's feeding protocol

DAH	Practice
3-15	**Green water**
	(Commercial powder microalgae-Sanolife GWS; Inve Aquaculture, NV Hoogveld, 91 9200, Dendermonde, Belgium or ω3 Algae®; Bernaqua, NV Hagelberg, 3 B-2250, Olen, Belgium)
16-26	Sanolife GWS
	Live food
3-9	Rotifer, *Brachionus plicatilis*
	Culture (Commercial culture diets-Algamac Protein Plus; Aquafaune Bio-Marine Inc. Hawthorne USA and Sparkle, INVE Aquaculture)
	Enrich (Commercial enriched diet-Spresso; INVE Aquaculture) 10-15 prey/mL
6	*Artemia* nauplii (AF480; Inve Aquaculture) 2-4 prey/mL
10	*Artemia* metanauplii 1.5-6 prey/mL
	Enrich
	(Artemia EG; Great Salt Lake Brine Shrimp Cooperative Inc., Utah, USA),
	(Commercial enriched diets-Algamac 3050-Aquafaune, Red Papper-Bernaqua, and Spresso-INVE Aquaculture, 26 ºC and 28 g/L)
16-32	**Microdiets**
	(Orange Start-S,100-200 μ, Orange Start-L, 200-300 μ, Orange Nurse-XS, 300-500 μ, Orange Grow-S, 300-500 μ, Orange Grow-L, 500-800 μ; INVE Aquaculture)

Conclusion

In conclusion, fish meal and krill meal is advised to be used as feed ingredient in microdiets of meagre larvae but not for fish hydrolysate except for the mentioned days (12, 15, and 20 DAH) and the use of fish hydrolysate should be paid attention. Second, soybean meal seems not to be a good candidate as feed ingredient due to having higher inhibitions on protease activities. Third, wheat gluten is not recommended until 12 DAH. Fourth, corn gluten and sunflower meal could be used as feed ingredient in formulations of meagre larvae. Fifth, the highest resistance to protease inhibitors found in feed ingredients was observed at 15 DAH. When such data become available, they will serve the replacement of fish meal with alternative and sustainable feed ingredients. These results are also recommended in future studies, as it will be an important factor in determining inhibitory effects on the protease activities of marine fish larvae.

References

Alarcón, F.J., Díaz, M., Moyano, F.J. (1997). Feeding tomorrow's fish. In A.G.J. Tacon & B. Basurco (Eds.), *Studies of digestive enzymes in fish: Characterization and practical applications* (p. 113-121). Zaragoza Mazarrón, Spain: CHIEM-Cahiers Options Meditérranéennes n.22.

Alarcón, F.J., Moyano, F.J.M., Díaz, M., Fernández-Díaz, C., Yúfera, M. (1999). Optimization of the protein fraction of microcapsules used in feeding of marine fish larvae using *in vitro* digestibility techniques. *Aquaculture Nutrition*, 5(2), 107-113.

Ali, H., Haque, M.M., Chowdhury, M.M.R., Shariful, M.I. (2009). *In vitro* protein digestibility of different feed ingredients in Thai koi (*Anabas testudineus*). *Journal of the Bangladesh Agricultural University*, 7(1), 205-210.

Arda, G. (2011). Sarıağız (*Argyrosomus regius)* larvalarında gastrointestinal tüpün histolojik gelişimi. MSc Thesis: Ege Üniversitesi, Fen Bilimleri Enstitüsü, İzmir.

Bestin, A., Dupont-Nivet, M., Médale, F., Quillet, E., Vandeputte, M., Cariou, S., Desgranges, A., Laureau, S., Ricoux R., Beutin, C., Haffray, P. (2014). Comparative additive genetic basis of high feed substitution by plant ingredients in four major fish species farmed in temperate and Southern Europe. Aquaculture Europe 14, Donostia-San Sebastián, Spain, 14-17 Oct 2014, pp. 136-137.

Bodur, T., Günaydın, C.O., Toplu, S. (2014). A preliminary research on Meagre (*Argyrosomus regius*, Asso 1801) culture in earthen pond during summer season in Turkey. Aquaculture Europe 14, Donostia-San Sebastián, Spain, 14-17 Oct 2014, pp. 150-151.

Bradford, M.M. (1976). A rapid sensitive method for the quantification of microgram quantities of protein utilizing the principle of protein-dye binding. *Analytical Biochemistry*, 72(1-2), 248-254.

Cahu, C.L., Zambonino Infante J.L. (1994). Early weaning of sea bass (*Dicentrarchus labrax*) larvae with a compound diet: effect on digestive enzymes. *Comparative Biochemistry and Physiology Part A: Physiology*, 109(2), 213-222.

Cara, J.B., Moyano, F.J., Cárdenas, S., Fernández-Díaz, C., Yúfera, M. (2003). Assessment of digestive enzyme activities during larval development of white bream. Journal of *Fish Biolgy,* 63(1), 48-58.

Campoverde, C., Estevez, A. (2017). The effect of live food enrichment with docosahexaenoic acid (22:6n-3) rich emulsions on growth, survival and fatty acid composition of meagre (*Argyrosomus regius*) larvae. *Aquaculture*, 478, 16-24.

Candeias-Mendes, A., Castanho, S., Ribeiro, L., Conceição, L.E.C., Dias, J., Costa, S., Bandarra, N.M., Pousão-Ferreira, P. (2015,). Melhoramento do cultivo larvar de corvina, *Argyrosomus regius*. XV Congreso Nacional y ı Congreso Ibérico de Acuicultura, Huelva, España 13-16 Oct 2015, pp. 536-537.

De Francesco, M., Parisi, G., Pérez-Sánchez, J., Gómez-Réqueni, P., Médale, F., Kaushik, S.J., Mecatti, M., Poli, B.M. (2007). Effect of high-level fish meal replacement by plant proteins in gilthead sea bream (*Sparus aurata*) on growth and body/fillet quality traits. *Aquaculture Nutritional*, 13(5), 361-372.

Dias, J., Ribeiro, L., Soares, F., Barata, M., Bandarra, N., Rodrigues, V., Colen, R., Amoedo, A., Moura, J., Fernandes, J., Narciso, L., Cunha, M., Conceição, L., Pousão Ferrera, P. (2014). Nutritional basis of meagre (*Argyrosomus regius)* a candidate species for mass production in the mediterranean. Aquaculture Europe 14, Donostia-San Sebastián, Spain, 14-17 Oct 2014, pp. 327-328.

Diken, G., Demir, O., Naz, M. (2016a). The potential effects of commercial feeding protocol on protease activities

and cortisol stress responses of meagre (*Argyrosomus regius*). *Agriculture&Food*, 4, 460-472.

Diken, G., Demir, O., Naz, M. (2016b). The potential inhibitory effects of microalgae and macroalgae on protease activities of *Argyrosomus regius* (Pisces, Scianidae) larvae using *in vitro* assays. *Agriculture&Food*, 4, 473-483.

Diken, G., Demir, O., Naz, M. (2016c). The inhibition effects of different protein sources on protease activities of meagre larvae (*Argyrosomus regius* Asso, 1801). FABA 2016, 3-5 Nov 2016, Antalya, Turkey, pp. 85.

Diken, G., Demir, O., Naz, M. (2017). Determination of the inhibitory effects of microdiets used in routine commercial feeding protocols on protease activities of *Argyrosomus regius* (Asso, 1801) larva. *Iranian Journal of Fisheries Sciences*, 16(1), 96-107.

Diken, G., Demir, O., Naz, M. (2018). The inhibitory effects of different diets on the protease activities of *Argyrosomus regius* (Pisces, *Scianidae*) larvae as a potential candidate species. *Journal of Applied Animal Research*, 46(1), 94-99.

Dimes, L.E., Haard, N.F. (1994). Estimation of protein digestibility, I. development of an *in vitro* method for estimating protein digestibility of salmonids. *Comparative Biochemistry and Physiology Part A: Physiology*, 108(2-3), 349-362.

Duncan, N., Myrseth, B. (2011). European Aquaculture Socitey Web. *New species for aquaculture production including ornamentals.* Retrieved December 20, 2015, from http://www.aquaeas.eu/images/stories/Meetings/AE2011/New_species_Duncan.pdf (accessed 03.01.19).

Eid, A.E., Matty, A.J. (1989). A simple *in vitro* method for measuring protein digestibility. *Aquaculture*, 79, 111-119.

El-Shebly, A.A., El-Kady, M.A.H., Hussin, A.B., & Hossain, Md.Y. (2007). Preliminary observations on the pond culture of meagre *Argyrosomus regius* (Asso, 1801) (*Sciaenidae*) in Egypt. *Journal of Fisheries and Aquatic Science*, 2(5), 345-352.

Estevéz, A., Treviño, L,, Kotzamanis, Y., Karacostas, I., Tort, L., Gisbert, E. (2011). Effects of different levels of plant proteins on the ongrowing of meagre (*Argyrosomus* regius) juveniles at low temperatures. *Aquaculture Nutritional*, 17(2), e572-e582.

Ezquerra, J.M., García-Carreño, F.L., Civera, R., Haard, N.F. (1997). pH-stat method to predict protein digestibility in white shrimp *(Penaeus vannamei)*. *Aquaculture*, 157(3-4), 251-262.

Ezquerra, J.M., García-Carreño, F.L., Carrillo, O. (1998). *In vitro* digestibility of dietary protein sources for white shrimp (*Penaeus vannamei*). *Aquaculture*, 163(1-2), 123-136.

Federation of European Aquaculture Producers-FEAP. (European Aquaculture Production Report 2008-2016). Retrieved June 26, 2018 from http://blancchamp.be/wp-content/uploads/2018/05/production-report-2017_web.pdf (accessed 03.01.19).

Fernández-Palacios, H., Schuchardt, D., Roo, J., Borrero, C., Hernández-Cruz, C.M., Socorro, J. (2007). Estudio morfométrico de la corvina (*Argyrosomus regius* Asso, 1801) durante el primer mes de vida. XI Congreso Nacional de Acuicultura, Vigo, Española, 24-28 Sept 2007, pp. 755-758.

Gamsız, K., Neke, M. (2008). Embryonic development stages of meagre *Argyrosomus regius Asso* 1801 under rearing conditions. 8th Larval Biology Symposium, Lisbon, Portugal, 6-11 July 2008, poster session.

García-Carreño, F.L. (1996). Proteinase inhibitors. *Trends* in *Food Science and Technology,* 7(6), 197-204.

García Mesa, S., Suárez, M.D., Rincón Cervera, M.A., Guil Guerrero, J.L., González, G., Cárdenas, S., García Gallego, M. (2014). Time course of muscle fatty acid composition of cultured meagre (*Argyrosomus regius*) during the first sixteen months of a cage culture. *Grasas Aceites*, 65(1), e006.

Gracia, E.P., Jofre, A.G. (2013). Diversificación de especies en la piscicultura marina Española. In: E.A. Martínez & I.A. Atarés (Eds.), *Cultivo de esciénidos. I: La corvina* (p. 117-153). Madrid, Española: Fundación Observatorio Español de Acuicultura Instituto Español de Oceanografía. ISBN: 978-84-939800-1-6

García-Ortega, A., Koussoulaki, A., Boer, H., Verreth, J. (2000). *In vitro* protein digestibility of *artemia* decapsulated cysts and nauplii, and of microbound diets for larval fish. *Aquaculture Research*, 31(5), 475-477.

Gil Oviedo, M.M. (2013). Recovery of meagre (*Argyrosomus regius*) population in the Balearic Coastal ecosystem (Western Mediterranean). PhD Thesis: University of the Balearic Islands, Palma.

Haffray. P., Malha, R., Sidi, M.O.T., Prista, N., Hassan, M., Castelnaud, G., Karahan-Nomm, B., Gamsız, K., Sadek, S., Bruant, J-S., Balma, P., Bonhomme, F. (2012). Very high genetic fragmentation in a large marine fish, the meagre *Argyrosomus regius* (Sciaenidae, Perciformes): Impact of reproductive migration, oceanographic barriers and ecological factors. *Aquatic Living Resources*, 25(2), 173-183.

Haközü, G. (2014). Çipura (*Sparus aurata*, Linneaus 1758) larvalarının kortizol seviyeleri üzerine ticari besleme prosedürünün etkileri. MSc Thesis: Mustafa Kemal Üniversitesi, Fen Bilimleri Enstitüsü, Hatay.

Holt, G.J., Webb, K.A., Rust, M.B. (2011). Larval fish nutrition. In: G.J. Holt (Ed.), *Microparticule diets: testing and evaluating success*, (p. 353-372). Chichester, UK: John Wiley & Sons Inc. ISBN: 978-0-8138-1792-7.

Kaushik, S.J., Cravedi, J.P., Lalles, J.P., Sumpter, J., Fauconneau, B., Laroche, M. (1995). Partial or total replacement of fish meal by soybean protein on growth, protein utilization, potential estrogenic or antigenic effects, cholesterolemia and fresh quality in rainbow trout, *Oncorhynchus mykiss*. *Aquaculture*, 133, 257-274.

Kaushik, S. J., Covès, D., Dutto, G., Blanc, D. (2004). Almost total replacement of fishmeal by plant protein sources in the diet of a marine teleost, the European seabass, *Dicentrarchus labrax*. *Aquaculture*, 230, 391-404.

Kolkovski, S., Tandler, A. (2000). The use of squid protein hydrolysate as a protein source in microdiets for gilthead seabream *Sparus aurata* larvae. *Aquaculture Nutritional*, 6(1), 11-15.

Kolkovski, S., Czesny, S., Dabrowski, K. (2000). Use of krill hydrolysate as a feed attractant for fish larvae and juveniles. *Journal of the World Aquaculture Society*, 31(1), 81-88.

Kissil, G.W., Lupatsch, I. (2004). Successful replacement of fishmeal by plant proteins in diets for the gilthead seabream, *Sparus aurata* L. *The Israeli journal of aquaculture-Bamidgeh*, 56(3), 188-199.

Krogdahl, Å., Bakke-McKellep, A. M., Baevefjordi, G. (2003). Effects of graded levels of standard soybean meal on intestinal structure, mucosal enzyme activities, and pancreatic response in Atlantic salmon (*Salmo salar* L.). *Aquaculture Nutritional*, 9(6), 361-371.

Kružić, N., Mustać, B., Župan, I., Čolak, S., 2016. Meagre (*Argyrosomus regius Asso*, 1801) aquaculture in Croatia. Croatian Journal of Fisheries, 74, 14-19.

Kuzu, E., Naz, M. (2012). Çipura (*Sparus aurata* L., 1758) larvalarında proteaz aktiviteleri üzerine farklı protein kaynaklarının inhibisyon etkileri. FABA 2012, 21-24 Nov Eskişehir, Turkey, pp. 33.

Monfort, M.C. (2010). *Present Market Situation and prospects of Meagre (Argyrosomus regius), as an emerging species in Mediterranean Aquaculture*. Rome, Italy: FAO. ISBN: 978-92-5-106605-8.

Moyano, F.J., Díaz, M., Alarcón, F.J., Sarasquete, M.C. (1996). Characterisation of digestive enzyme activity during larval development of gilthead seabream (*Sparus aurata*). *Fish Physiology and Biochemistry,* 15(2), 121-130.

Moyano, F.J., Alarcón, F.J., Díaz, M. (1998). Comparative biochemistry of fish digestive proteases applied to the development of *in vitro* digestibility assays. *Trends in Comparative Biochemistry and Physiology,* 5, 136-143.

Moyano López, F.J., Martínez Díaz, I., Díaz López, M., & Alarcón López, F.J. (1999). Inhibition of digestive proteases by vegetable meals in three species (*Sparus aurata*), tilapia (*Oreochromis niloticus*) and African sole (*Solea senegalensis*). *Comparative Biochemistry and Physiology Part B: Biochemistry and Molecular Biology*, 122(3), 327-332.

Moyano, F.J., Barros, A.M., Prieto, A., Cañavate, J.P., Cárdenas, S. (2005). Evaluación de la ontogenia de enzimas digestivas en larvas de hurta, *Pagrus auriga* (Pisces: Sparidae). *Revista AquaTIC*, 22, 39-47.

Moyano, F., Saénz de Rodrigáñez, M.A., Díaz, M., Tacon, A.G.J. (2015). Application of *in vitro* digestibility methods in aquaculture: constraints and perspectives. *Reviews in Aquaculture*, 7(4), 223-242.

Naz, M., Yúfera, M. (2012). The potential ınhibitory effects of the commercial diets on protease activities of larvae and live foods. *Journal of FisheriesSciences.com*, 6(3), 224-231.

Papadakis, I.E., Kentouri, M., Divanach, P., Mylonas, C.C. (2013). Ontogeny of the digestive system of meagre *Argyrosomus regius* reared in a mesocosm, and quantitative changes of lipids in the liver from hatching to juvenile. *Aquaculture*, 388-391, 76-88.

Parisi, G., Terova, G., Gasco, L., Piccolo, G., Roncarati, A., Moretti, V.M., Centoducati, G., Gatta, P.P., Pais, A. (2014). Current status and future perspectives of Italian finfish aquaculture. *Reviews in Fish Biology and Fisheries*, 24(1), 15-73.

Person-Le Ruyet, J., Bergot, P. (2001). Nutrition and feeding of fish and crustaceans. In: J. Guillaume & S. Kaushik & P. Bergot & R. Métailler (Eds.), *Artificial food for fish larvae* (p. 229-238). Chichester, UK: Praxis Publishing Ltd. ISBN: 978-1-85233-241-9.

Quéméner, L. (2002). *Le maigre commun (Argyrosomus regius) Biologie, pêche, marché et potential aquacole*. Ifremer, Plouzané, France. ISBN: 2-84433-074-6

Ribeiro, L., Zambonino-Infante, J.L., Cahu, C., Dinis, M.T. (1999). Development of digestive enzymes in larvae of *Solea senegalensis*, Kaup 1858. *Aquaculture*, 179, 465-473.

Ribeiro, L., Moura, J., Santos, M., Colen, R., Rodrigues, V., Bandarra, N., Soares, F., Ramalho, P., Barata, M., Moura, P., Pousão-Ferreira, P., Dias, J. (2015). Effect of vegetable based diets on growth, intestinal morphology, activity of intestinal enzymes and haematological stress indicators in meagre (*Argyrosomus regius*). *Aquaculture*, 447, 116-128.

Rodehutscord, M., Mandel, S., Pack, M., Jacobs, S., Pfeffer, E. (1995). Free amino acids can replace protein-bound amino acids in test diets for studies in rainbow trout (*Oncorhynchus mykiss*). *Journal of Nutrition*, 125(4), 956-963.

Roo, J., Hernández-Cruz, C.M., Borrero, C., Schuchardt, D., Fernández-Palacios, H. (2010) Effect of larval density and feeding sequence an meagre (*Argyrosomus regius*; Asso, 1801) larval rearing. *Aquaculture*, 302, 82-88.

Schiavone, R., Zilli, L., Storelli, C., Vilella, S. (2012). Changes in hormonal profile, gonads and sperm quality of *Argyrosomus regius* (Pisces, Scianidae) during the first sexual differentiation and maturation. *Theriogenology*, 77, 888-898.

Saavedra, M., Grade, A., Candeias-Mendes, A., Pereiraa, T.G., Teixeiraa, B., Yúfera, M., Conceiçãoc, L.E.C., Mendesa, R., Pousão-Ferreira, P. (2016). Different dietary protein levels affect meagre (*Argyrosomus regius*) larval survival and muscle cellularity. *Aquaculture*, 450, 89-94.

SPSS Inc. (2015). SPSS for IBM Version 23.0. Chicago, IL, USA.

Solovyev, M.M., Campoverde, C., Öztürk, S., Moreira, C., Diaz, M., Moyano, F.J., Estévez, A., Gisbert, E. (2016). Morphological and functional description of the development of the digestive system in meagre (*Argyrosomus regius*): An integrative approach. Aquaculture, 464, 381-391.

Southgate, P.C. (2012). Aquaculture farming aquatic animals and plant. In: J.S. Lucas & P.C. Southgate (Eds.), *Foods and feeding*, (p. 188-213). Chichester, UK: A John Wiley & Sons Ltd. Publication. ISBN: 978-1-4051-8858-6.

Süzer, C., Kamacı, H.O., Çoban, D., Yıldırım, Ş., Fırat, K., Saka, Ş. (2013). Functional changes in digestive enzyme activities of meagre (*Argyrosomus regius*; Asso, 1801) during early ontogeny. *Fish Physiology and Biochemistry,* 39(4), 967-977.

Tacon, A.G.J. (1997). Feeding tomorrow's fish. In A.G.J. Tacon & B. Basurco (Eds.), *Fishmeal replacers: review of antinutrients within oilseeds and pulses. A limiting factor for the aquafeed green revolution?* (p 153-

182). Zaragoza, Mazarrón: CHIEM-Cahiers Options Meditérranéennes n:22.

Vallés, R., Estévez, A. (2013). Light conditions for larval rearing of meagre (*Argyrosomus regius*). *Aquaculture*, 376-379, 15-19.

Vallés, R., Estévez, A. (2015). Effect of different enrichment products rich in docosahexaenoic acid on growth and survival of meagre, *Argyrosomus regius* (Asso, 1801). *Journal of the World Aquaculture Society*, 46(2), 191-200.

Vargas-Chacoff, L., Ruiz-Jarabo, I., Páscoa, I., Gonçalves, O., Mancera, J.M. (2014). Yearly growth and metabolic changes in earthen pond-cultured meagre *Argyrosomus regius*. *Scientia Marina*, 78(2), 193-202.

Velazco-Vargas, J., Martínez-Llorens, S., Cerda, M.J., Tomás-Vidal, A. (2013). Evaluation of soybean meal as protein source for *Argyrosomus regius* (Asso, 1801) (*Sciaenidae*). *International Journal of Fisheries and Aquaculture*, 5(3), 35-44.

Velazco-Vargas, J., Tomás-Vidal, A., Hamdan, M., Moyano López, F.J., Cerda, M.J., Martínez-Llorens, S. (2014). Influence of digestible protein levels on growth and feed utilization of juvenil meagre *Argrysomus regius*. *Aquaculture Nutrition*, 20(5), 520-531.

Walter, H.E. (1984). Methods of enzymatic analysis. In: H.U. Bergmeyer, J. Bergmeyer, M. Graßl (Eds.), *Proteinases: methods with haemoglobin, casein and azocoll as substrates* (p. 270-277). Weinheim, Florida: Verlag Chemie ISBN: 270-277; 3-527-26045-5.

Whitehead, P.J.P., Bauchot, M.L., Hureau, J.C., Nielsen, J., Tortonese, E. (1986). Fishes of the North-Eastern Atlantic and the Mediterranean. Paris, France: UNESCO. ISBN: 978-0119111590.

Yıldız, G., Ateş, G., Ünal, C., Kuzu, E., Naz, M. (2012). Levrek (*Dicentrarchus labrax* L., 1758) larvalarının proteaz aktiviteleri üzerine farklı protein kaynaklarının inhibisyon etkileri. FABA 2012, 21-24 Nov Eskişehir, Turkey, pp. 41.

Yılmaz, E., Naz, M., Sayın, S., Töre, Y. (2012). Çipura (*Sparus aurata* L., 1758) larvalarının proteaz aktiviteleri üzerine *Chlorella* spp. ve *Spirulina platensis*'in inhibisyon etkileri. FABA 2012, 21-24 Nov Eskişehir, Turkey, pp. 87.

Zambonino Infante, J.L., Cahu, C.L. (1994). Development and response to a diet change of some digestive enzymes in sea bass (*Dicentrarchus labrax*) larvae. *Fish Physiology and Biochemistry*, 12(5), 399-408.

Zambonino Infante, J.L., Cahu, C.L. (2001). Ontogeny of the gastrointestinal tract of marine fish larvae. *Comparative Biochemistry and Physiology Part C: Toxicology & Pharmacology*, 130(4), 477-487.

Research Article

PRESENT STATUS OF STURGEON IN THE LOWER SAKARYA RIVER IN TURKEY

Devrim Memiş[1] , **Deniz Devrim Tosun[1]** , **Güneş Yamaner[1]** , **Gökhan Tunçelli[1]** ,
Jörn Gessner[2]

[1] Istanbul University Aquatic Sciences Faculty, Ordu Str. No:8 Laleli, Istanbul, Turkey

[2] Leibniz-Institute for Freshwater Ecology and Inland Fisheries Müggelseedamm 310, Berlin, Germany

ORCID IDs of the authors:

D.M. 0000-0003-2616-3601
D.D.T. 0000-0001-6612-6624
G.Y. 0000-0003-1886-4985
G.T. 0000-0003-1708-7272
J.G. 0000-0002-1675-0549

C**orrespondence:**

Devrim MEMİŞ

E-mail: mdevrim@istanbul.edu.tr

ABSTRACT

The Hydro development started in the 1960s with building 3 major dams in the upstream section of the Sakarya River. During the 1980s the development of the floodplain sections of the river had its onset. Under these altered conditions *Huso huso, Acipenser nudiventris*, and *Acipenser sturio* disappeared from the river until the 1980s but *Acipenser gueldenstaedtii, as well as Acipenser stellatus,* were shown to still reproduce in the remaining section of the river by 2013. The construction of three additional HEPPs begun in the river section below Pamukova, blocking migration and cutting off major spawning sites. While fish passage facilities were included in the construction of the HEPPs since the 1980s, their design and location, as well as the maintenance rendered them completely dysfunctional. A survey was carried out in the remaining free flowing section of the lower river in 2014 to determine fish community composition and water quality at 4 stations below Adasu HEPP. While a few *A. gueldenstaedtii* juveniles were observed in Sakarya River mouth close to the Black Sea, only one young-of-the- (YOY) (*A. stellatus*; W:25g; TL:28cm) was reported which was captured from the Lower Sakarya River.

Keywords: Lower Sakarya River, Sturgeon, HEPP, Fish Passage

Introduction

Sakarya River is the third largest river in Turkey, its springs are located in the Anatolian mountains approx. 400 km west of Ankara and enters the Black Sea approx. 100 km east of Istanbul. It is 810 km long and up to-150 m wide. Sakarya River is defined hydrologically in three parts: upper, middle and lower. Sakarya River Basin is characterized by flood plain areas separated through mountain ridges. Sturgeon fishery was important in the Sakarya River mouth area (Karasu- Yenimahalle region) until the 1970ies (Anon, 1992). Arısoy (1968) reported that sturgeons spawned in the Sakarya River between February and June, while one month later, in August, sturgeon fingerlings were observed in the lower reaches to enter the Black Sea.

Over the past 50 years, hydropower was considered a priority development in Turkey, facilitating the supply of an industrializing society while minimizing the running cost and interdependence from oil and gas supplies. As a result, the first hydropower dams were constructed in the 1950s on the large rivers in Turkey, mainly those entering the Black Sea.

Dam constructions started in the middle part of Sakarya River basin after the 1950s, for hydropower generation, flood control and the management of the flow regime in the lower Sakarya River. After construction of the three dams Sarıyar Dam (1956), Gökçekaya Dam (1972) and the most upstream Yenice Dam (1985-2000), flow and sediment transport characteristics of the river changed drastically. It was observed that sediment transport was decreased by 40-65% after the construction of Gökçekaya Dam (Saltabaş et al., 2003; Doğan et al., 2016). By comparison of cross section measurements in 1965 and 2003, an enlargement in the width and scouring in the depth of the river up to 7 m were reported (Işık et al., 2006; Doğan et al., 2016).

Şengörür and İsa (2001) recorded that the Sakarya River basin is polluted by industrial wastes and sewer system, especially heavy metals such as Iron (Fe), Copper (Cu), Lead (Pb), Mercury (Hg) from the Çarksuyu area to the Black Sea. Gümrükçüoğlu and Baştürk (2007) reported that water quality levels in the lower section of Sakarya River below the Gökçekaya Dam to River Mouth were evaluated as 3rd class (polluted) based upon the NO2-N and BOD5 levels according to the Ministry of Environment and Urbanization (Official Gazette, 2004). Lower Sakarya River is classified as 3 and 4 (polluted to highly polluted) water quality due to the Nitrate and Total Phosphorus pollution (Anon. 2013).

Habitat degradation resulting from river gravel extraction, diking, as well as chemical load due to sewage, agricultural and communal nutrient input and industrial pollution decreased fish populations of Sakarya River. Besides human-made obstructions, toxins and heavy metals, pesticides and other polychlorinated hydrocarbons impose a major impact upon the fish communities (Anon. 2013).

Human activities on river including hydropower stations, water diversion, and over-fishing have resulted in the interruption of migration routes and effectuated a significant decline in the range and population sizes of sturgeon species in Turkey (Anon. 2013; Edwards and Dorosov, 1989; Rosenthal et al., 2015).

The development of hydroelectric power plants (HEPP) in the remaining floodplain sections started in the 1980s when low-head dams such as the Pamukova HEPP were constructed 150 km upstream from the sea to increase the energy yield. After the construction of migratory obstructions, A. gueldenstaedtii and A. stellatus were shown to still reproduce in the remaining section of the river by 2011. In 2012 the construction of three additional HEPPs (Doğançay I-II and Adasu) started in the river section below Pamukova, further reducing the remaining section of the free-flowing river to approx. 90 km. In the light of this development, this study focused the effects of the impoundments upon the fish community in the lower river section, the effect upon the water quality and the state of the nursery grounds to assess the potential of the remaining river section as sturgeon habitat.

Material and Methods

The sampling took place from April 2014 to September 2014 in a first attempt to evaluate the effects of the anthropogenic impacts upon the remaining sturgeon populations and their available habitat.

Study Area

This study was conducted in the lower Sakarya River in the Karasu Region at four stations (Figure 1). The first station was on the right bank of the river at 2.6 km from the Black Sea in Yenimahalle District (41°06'15.883"N; 30°38'45.023"E); The second station was 6 km on the left bank in Tuzla District (41°04'37.350"N; 30°38'14.234"E); The third station was at 17 km on the left bank in Akkum District (41°04'00.450"N; 30°36'14.593"E); And the fourth station was located at around 18 km on the left bank in Ferizli-Adatepe District (41°03'52.745"N; 30°36'28.250"E). The stations were chosen based on the experience of local fishermen about river fish catching areas.
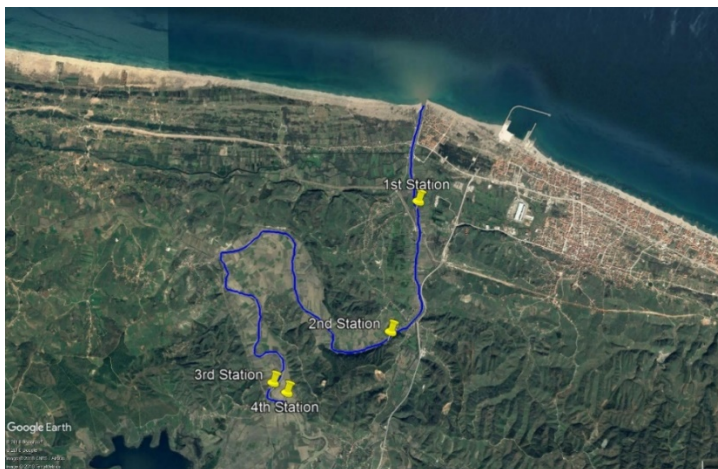
Figure 1. Sampling stations in the lower Sakarya River Basin (Google Earth Map)

Fish Presence

Fyke nets were used at all four stations. The fyke nets were fixed on the bottom (180 cm depth) by stakes and had wings which guide the fish towards the entrance of the bags (FAO, 2001; Buysse et al., 2008). The nets had a mesh size of 70 mm and were made of polyfil nylon. The nets were produced by a local fisherman according to meet the size requirements for migrating mature sturgeon. The fyke net entrance was 140 cm in diameter; the nets were cone-shaped and had a length of 5 m and were equipped with 6 chambers. In order to catch sturgeons moving from the Black Sea to the Sakarya River between April and September (6 months), the net-openings were positioned to face the sea. Nets were checked once every week. Fish were identified as species level.

Additional sturgeon catch data were collected from regional fishermen after carrying out an information campaign. Fishermen were contacted individually and a reward for the catch information was established.

Water Quality

Dissolved oxygen (DO), temperature (°C) and pH were measured in situ by a portable WTW Multi-Parameter Instrument (Multi 3430 MultiLine IDS) in the late morning. A secchi disc (30 cm diameter) was used to determine water transparency. River depth of the sampling area was measured by a meter.

Benthos

The sampling stations were sampled for benthic fauna by using an Ekman-Birge grab (15x15 cm), sieved on a 0.5 mm mesh size and kept individually in plastic bottles preserved in 70% ethanol. Sediment samples were taken at triplicate at

each station in every survey. Samples were washed with 0.5 microns 30 cm radius filters. Individual organisms were counted in 100g subsamples. Organisms were determined according to Brinkhurst (1963).

Statistical Analysis

The results were statistically analysed using SPSS v21.0 for Windows software. The statistical differences were determined using a one-way analysis of variance (ANOVA) followed by a Tukey's comparison test at $p<0.05$.

Results and Discussion

Physico-chemical parameters, transparency, depth of water and sediment sampling

The water quality (temperature, dissolved oxygen, and pH), transparency and depth at the sampling points in the Lower Sakarya River revealed that water temperature, dissolved oxygen and pH levels were similar between the four stations. There were no significant differences between water quality parameters of the sampling stations ($p>0.05$). Water temperature showed an average of 22.6 ±0.99°C between May and August and showed a marked decrease after August. The pH values reveal a stable level at around 7.7 ±0.1 but their development shows marked differences with larger fluctuations in the first 3 months of the sampling period in the upper three stations while the lower river values are rather stable. The oxygen contents at all 4 stations are low with an average of 4 ±1.16 mg/l (Figure 2). At mean water temperatures of 22.6°C, this reflects saturation levels of 50-55% indicating massive oxygen consumption through sewage and nutrient discharge.

On a monthly base, a gradual decrease in water transparency was observed for 4 stations with the highest values in April (53.7 ±13.7 cm) to the lowest in September (24.5 ±4.27 cm). Monthly changes in discharge were related to HEPP operation and did result in fluctuations of up to 80 cm between April and September.

Sampled sediment consisted of mud was dark coloured with organic decay odour. Bottom and turbidity surveys showed that from the Black Sea up to Akkum region (3rd station) there are high amounts of debris and decaying organic materials (plants, leaves, seeds, litter etc.) (Table 1).

During sampling, sediment samples from the sampling stations were analysed to evaluate the presence and composition of the macrozoobenthos serving as important feed organisms for sturgeon (Table 2). The samples taken were only comprised of oligochaete larvae (Brinkhurst 1963).
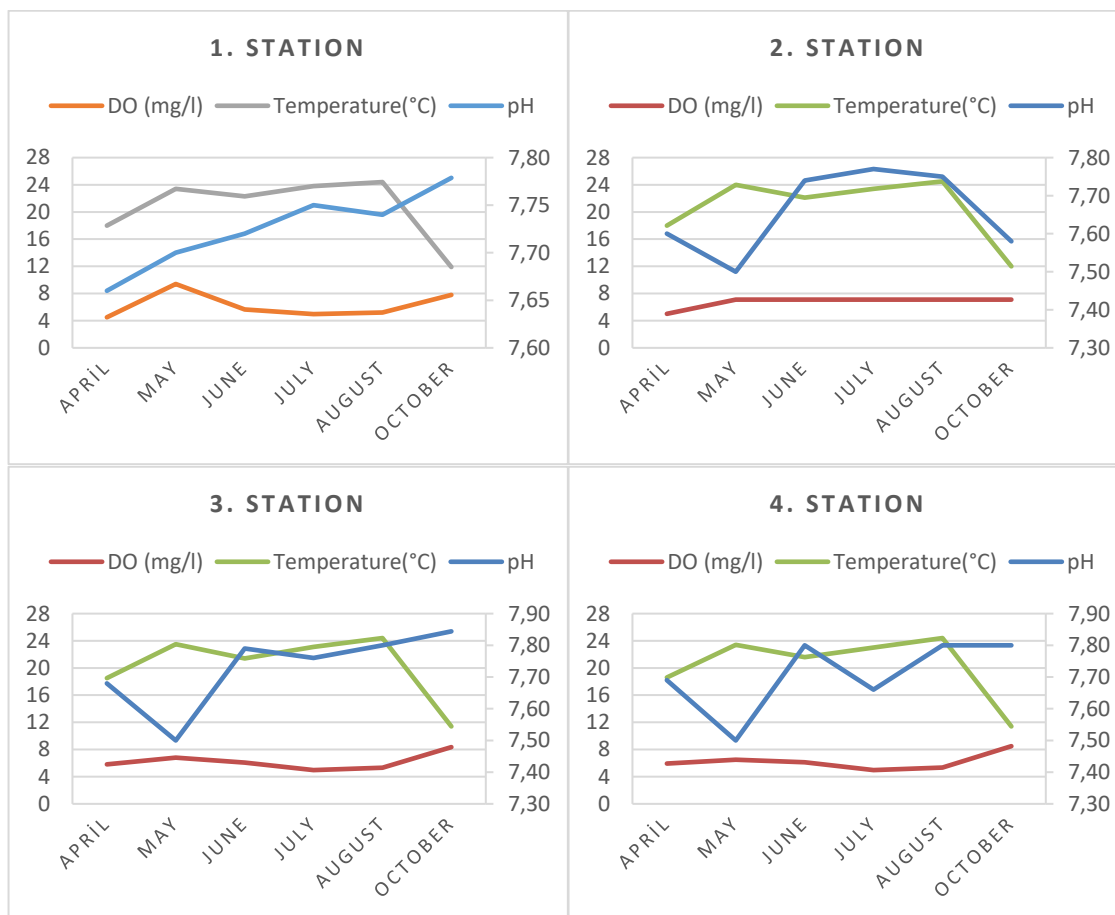
Figure 2. Water quality parameters (temperature (°C), dissolved oxygen (mg/L), pH) during the stations throughout the study.

Table 1. Description of the sediment sampling in stations in Sakarya River.

Stations	Sediment	Macrophytes
1	Mud	+
2	Mud	+
3	Organic mud	+
4	Mud	+

Table 2. Zoobenthic fauna (oligochaete larvae) and monthly changes of the Lower Sakarya River (mean number of individuals/$100g/m^2$).

Months	1.Station	2.Station	3.Station	4.Station
April	-	-	-	-
May	-	-	-	-
June	2	-	-	17
July	-	-	-	-
August	1	9	-	24
September	-	-	-	-

High population density in Sakarya River basin results in industrial and agricultural pollution in Sakarya River. Chemical parameters of the river are adversely affected by the pollutants as well as high heavy metal contents. Treatment facilities for industrial establishments and urban wastes should be mandatory and minimum discharge should be allowed to decrease pollution in this river. Erosion, silt, and sand coming from the river bed results in elevated turbidity and high suspended solid load in the water. Many sand quarries operating on Sakarya River, removing gravel from the river bed or from adjacent pits adversely affect the natural river bed through the removal of gravel and the input of fines (Anon, 2013). In the current study, we determined structural and physical activities on the Sakarya River and their adverse effects on fish populations and most importantly sturgeon fish populations.

Fish Composition

Fyke nets located at the four stations during the study determined nine fish species including; pike (*Esox lucius*)*,* wels catfish *(Silurus glanis),* tench (*Tinca tinca),* common carp (*Cyprinus carpio*)*,* Prussian carp *(Carassius gibelio),* mullet (*Mugil sp.*)*,* common bream (*Abramis brama*)*,* white bream *(Blicca bjoerkna)* and rudd (*Scardinius erythrophthalmus)*. The catches of the nine fish species mostly comprise a few or single individuals during the sampling periods (Table 3). There was no captured fish in fyke nets in April because of overflow. One fyke net was lost in the 2nd station. It was drifted by flood and a substitute fyke net was put at the same point. Sturgeons were the most famous and valuable fish in Sakarya River in the past 50 years. Recently, 11 fish species were reported from the lower part of the Sakarya River between 2011 and 2013 using fyke nets and gill nets (Akmirza

and Yardımcı, 2014). *Rutilus rutilus* and *Barbus barbus* species were not found in all stations in this study.

Buysse et al. (2008) captured diadromous fishes with fyke nets in the Scheldt River (Belgium). They reported that exotic Siberian sturgeon (*Acipenser baerii*) were captured during downstream migration using mesh sizes of 8 mm. Fyke nets located on the migration route proved to be ineffective to capture sturgeons during the sampling period in the Sakarya River. The catch of other fish species by local fishermen varies largely between sites and months. Since a lot of sturgeons captured in the coastal waters were close to the Sakarya River mouth, it seems probable that both *A. gueldenstadtii* and *H. huso* originate from stocking or natural reproduction in the Danube and Ukrainian waters. The only exception is YOY *A. stellatus* caught on 31.09.2014 in the freshwater section of Sakarya River close to the river mouth (Table 4). Since the fish are caught in freshwater and are too small (25 g) to have migrated through full strength seawater over such a considerable distance (Khodorevskaya et al., 2009) it is most probable that this individual originated from reproduction in the river of the same year. Fishermen told that the catch of sturgeon with fishing rods and gill nets between the second and the third stations during the sampling period. Most fish were caught in brackish water along the coast at left and right side of Sakarya River Mouth.

This is verified for the tagged sturgeons with a CTW tag (Present or absent) in Table 4 which released from Danube River in Romania. During the study, a larger number of small stellate sturgeons were caught by local fishermen in the catching area out of which only one *A. stellatus* of 25g was made available (Table 4).

Table 3. Fish species captured with fyke nets between April and September 2016 at four sampling stations through the down Sakarya River

Months	1st Station	2nd Station	3rd Station	4th Station
April	-	-	-	-
May	Pike	-	-	Wels, Prussian carp, Tench
June	-	Wels, Common carp	Wels, Common carp	White bream
July	-	Chub	wels	
August	-	-	Chub	Common bream
September	-	-	Common bream, Mullet	-

Table 4. Reported by-catch sturgeon species inside and around Sakarya River mouth.

Date	Species	Live Weight (g)	Total Lenght (cm)	CTW tag Present (P) or Absent (A)
24 August 2013	*A.stellatus**	1000	30	A
15 May 2014	*H.huso*	1520	65	P
July/September 2014	*A.stellatus***	-	-	A
31 September 2014	*A.stellatus****	25	28	A
7 November 2014	*A.stellatus*****	-	-	A
28 November 2014	*A.stellatus*	258	48	A
25 November 2015	*A. gueldenstaedtii*	300	46	P
25 November 2015	*A. gueldenstaedtii*	245	43	P
25 November 2015	*A. gueldenstaedtii*	285	47	P
25 November 2015	*A. gueldenstaedtii*	265	45	P
24 February 2016	*A. gueldenstaedtii*	812	61	P
24 February 2016	*A. gueldenstaedtii*	504	51	P
24 February 2016	*A. gueldenstaedtii*	411	47	P
24 February 2016	*A. gueldenstaedtii*	538	49	A
02 March 2016	*A. gueldenstaedtii*	-	-	A

*Stellat sturgeon captured by amateur fishermen by fishing rod inside the river.

**All *A.stellatus* samples informed by fishermen inside the Lower Sakarya River and they released them (around 40 individuals) during these periods.

***Only one small live stellat sturgeon which captured from the Sakarya River with a gill net.

**** This fish reported by Adasu HEPP's worker which they saw dead stellat sturgeon below the Adasu HEPP.

Investigated HEPPs and Man-Made Structures on Sakarya River

The investigation of HEPPs was conducted between the Sakarya River mouths to Pamukova Regulator. This covered 154 km river length. Pamukova Regulator and HEPP, Doğançay Regulator and HEPP I, Doğançay Regulator and HEPP II, Adasu Regulator and HEPP were investigated onsite for suitability of sturgeon migration and fish passage availability. Details of the design of fish passages were not shared by the companies during the investigations. All passages were either vertical slot designs or baffle designs and comprised two passes, one with 20 m length to overcome the spillway and the second pass of 50 m lengths that was intended to overcome the dam section. Passage facilities covered a height of 10m over 50m length, were equipped with very small chambers of 0.6m length and 20X20cm baffles which were not suitable for sturgeon. In all passage facilities, the migration pathways were either not connected to the downstream aggregation areas, were blocked by building material, did not receive sufficient water flow or were disconnected from the water level upstream of the HEPPs. The legislation states that "water discharge from a HEPP construction should at least be 10% of the last 240 decade's average natural water flow". In addition, upstream fish passages/ladders are mandatory to ensure uninterrupted fish migration for HEPPs and regulators (Anon, 2013). Yet, their functionality is not monitored and the enforcement of retrofitting is missing. As such the biggest problem on Turkish inland water resources in the last decade had resulted from the energy production with HEPP installations. Emerging need for energy resulted in a disregard for the environment and lack of planning about ecosystem interactions of these HEPPs.

In addition, water quality is low, largely impacted by wastewater loads from rural, industrial and agricultural sources, reducing the oxygen contents to levels at which embryonic development becomes inhibited (Delage, 2015). Also, the bottom characteristics pose a risk for sturgeon reproduction with a high percentage of the fish prefers to lay their eggs on gravel. Additionally, the surveyed area had sand most probably gener-

ated by the sand quarries operating on the river. As revealed by the reported catch of a 25 g YOY stellate sturgeon in 2014 mature fish still reproduce in Lower Sakarya River and young fish are returning to the sea.

Both EU Water Directive (EU Directive 60/2000/EG), CITES agreement and Turkish legislation (Fisheries Law No. 1380) dictates that any activity which adversely affects the life cycle of sturgeon fish should be under control and migration of this fish should not be obstructed. Also, the location of the HEPP should provide sufficient habitat for the fish to reproduce and grow up rather than reflecting only the maximum utilization of the hydropower potential available. In the past, these precautionary approaches have not been taken into consideration.

Conclusion

Sakarya River has lost the majority of the functional spawning and nursery habitats between Adasu HEPP and Pamukova HEPP (Rosenthal et al., 2015). After the construction of 3 HEPPs 90 km of free river flow remains. But, with anymore HEPP projects, access to this last breeding ground will be impossible and the population will finally be lost. The last free 90 km river must be left alone and further monitoring of this species must continue in the river. In addition, proper criteria for the construction of functional sturgeon migration facilities both upstream (DWA, 2014; Tiril and Memiş, 2018) and downstream are not available on present structures. These must be implemented in a timely fashion to reopen the important habitats upstream of Adasu HEPP's. HEPPs which has dysfunctional fish passages should be revised for sturgeon species at least for *A. stellatus*. And, according to Anon (2018) there is an urgent need for coordinated efforts and centralized facilities in order to save this species which one may be the last living sturgeon species in Lower Sakarya River habitat.

Compliance with Ethical Standard

Conflict of interests: The authors declare that for this article they have no actual, potential or perceived conflict of interests.

Ethics committee approval: All procedures were performed involving fish were in accordance Law on Veterinary and Medical Activities and National Animal Welfare Act, thus ethical approval was not required.

References

Akmirza, A., Yardımcı R.E. (2014). Fish parasites of the Sakarya River, Turkey. *Journal of Academic Documents for Fisheries and Aquaculture*, 1(1), 23-29.

Anon (1992). General directorate of the state water, investigation of pollution aspects of Sakarya–Seyhan Basins and report of determination of quality classes of this basins, 5, General Directorate of the State Water, Ankara.

Anon (2013). Preparation Project of Action Plan of River Basin Protection; Proposal Report of Sakarya River Basin. 5118601 (Çtüe.13.134). Türkiye Bilimsel Ve Teknolojik Araştırma Kurumu Marmara Araştırma Merkezi Çevre Enstitüsü. Temmuz, 2013 Gebze, Kocaeli.

Anon (2018). Pan-European Action Plan For Sturgeon. Convention on the Conservation of European Wildlife and Natural Habitats. Standing Committee 38th Meeting Strasbourg, 27-30 November 2018. Document prepared by the World Sturgeon Conservation Society and WWF, Strasbourg, France.

Arısoy, S. (1968). *Fisheries in Sakarya (Sakarya vilayeti çevresinde su ürünleri ekonomisi ve kooperatiflesme ile kalkinma imkan ve problemleri)*. Istanbul University Economics Faculty Publication No: 1391, Istanbul, 182 p. 182.

Brinkhurst R.O. (1963). *A Guide for the Identification of British Aquatic Oligochaeta*, Freshwater Biological Associaton Scientific Publication, 22:55.

Buysse, D., Coeck, J., Maes, J. (2008). Potential re-establishment of diadromous fish species in the River Scheldt (Belgium). *Hydrobiologia*, 602(1), 155-159.

Delage, N. (2015). Experimental study of environmental conditions effects (temperature, oxygen, pollutants) on survival, development and behaviour of European sturgeon, Acipenser sturio, embryo-larval stages (PhD Thesis). Bordeaux University, French.

Doğan, E., Çeribaşı, G., Akkaya, U. (2016). Investigation for Effecting of Dam to River Flow Regime by Trend Analysis Method: Case Study of Sakarya River. *Karaelmas Fen ve Mühendislik Dergisi*, 6(1), 50-55. (In Turkish).

DWA, (2014). Fischaufstiegsanlagen und fischpassierbare Bauwerke-Gestaltung, Bemessung, Qualitätssicherung., Mai, Hennef, Deutschland, 334 pp.

Edwards, D., Doroshov, S. (1989). Sturgeon and Seatrout Fisheries Development, FAO, Turkey Technical Cooperations Programme. Appraisal of the Sturgeon and Seatrout Fisheries and Proposals for a Rehabilitation Programme, Rome, 35 pp.

FAO, (2001). Fishing Gear types. Fyke nets. Technology Fact Sheets. Retrieved from http://www.fao.org/fishery/ (accessed 10.10.2013).

Gümrükçüoğlu, M., Baştürk, O. (2007). Coğrafi bilgi sistemleri kullanılarak Sakarya nehri kirlilik yükünün belirlenmesi. In TMMOB Harita ve Kadastro Mühendisleri Odası Ulusal Coğrafi Bilgi Sistemleri Kongresi (pp. 1-5). Trabzon, Turkey.

Işık, S., Şaşal, M., Doğan, E. (2006). Investigation on downstream effects of dams in the Sakarya River. *Gazi University Journal of Engineering and Architecture*, 21(3), 401-408.

Khodorevskaya, R.P., Ruban, G.I., Pavlov, D.S. (2009). Behaviour, migrations, distribution, and stocks of Sturgeons in the Volga-Caspian Basin. Neu Wulmstorf; World Sturgeon Conservation Society Special Publication, No. 3, p.233

Official Gazette. (2004). Water Pollution and Control Regulations. Ministry of Environment and Urbanization, No: 25687, 31.12.2004. http://www.mevzuat.gov.tr (accessed 20 January 2018).

Rosenthal, H., Gessner, J., Deniz, H.; Memiş, D., Ustaoğlu Tırıl, S., Zengin, M., and Altan, Ö. (2015). National Action Plan for the Conservation and Restoration of the Sturgeons of Turkey. (Edits: Rosenthal, H., Gessner, J), Ministry of Food, Agriculture and Livestock, Ankara.

Saltabaş, L., Şaşal, M., Işık, S., Doğan, E. (2003). Examination of the current changes in the Lower Sakarya River. *Sakarya Üniversitesi, Fen Bilimleri Enstitüsü Dergisi,* 7(2), 9-15.

Şengörür, B., İsa, D. (2001). Factor analysis of water quality observations in the Sakarya River. *Turkish Journal of Engineering and Environmental Sciences*, 25(5), 415-426.

Tırıl Ustaoğlu, S., Memiş, D. (2018). An Overview of the Factors Affecting the Migration of Sturgeons in Yeşilırmak. *Aquatic Sciences and Engineering*, 33(4), 138-144.

Research Article

POTENTIAL ENVIRONMENTAL IMPACTS OF TUNA CAGE FARMING IN THE AEGEAN SEA

Rıdvan Kaan Gürses[1] ⓘ, Yeşim Büyükateş[1] ⓘ, Murat Yiğit[2] ⓘ, Sebahattin Ergün[3] ⓘ, A. Suat Ateş[1] ⓘ, H. Göksel Özdilek[4] ⓘ

[1] Canakkale Onsekiz Mart University, Faculty of Marine Science, Department of Marine Science, 17100 - Canakkale, Turkey

[2] Canakkale Onsekiz Mart University, Faculty of Marine Science, Department of Marine Technology Engineering, 17100 - Canakkale, Turkey

[3] Canakkale Onsekiz Mart University, Faculty of Marine Science, Department of Aquaculture, 17100 - Canakkale, Turkey

[4] Canakkale Onsekiz Mart University, Faculty of Engineering, Department of Environmental Engineering, 17100 - Canakkale, Turkey

ORCID IDs of the authors:
R.K.G. 0000-0001-5951-2308
Y.B. 0000-0002-4402-4587
M.Y. 0000-0001-8086-9125
S.E. 0000-0002-9077-9438
A.S.A. 0000-0002-4682-1926
H.G.Ö. 0000-0001-9740-9758

Correspondence:

Yeşim BÜYÜKATEŞ

E-mail: ybuyukates@comu.edu.tr

ABSTRACT

The present study aimed to investigate the potential impacts of Atlantic Bluefin Tuna (*Thunnus thynnus*) farming in offshore cage systems in the Aegean Sea (Sığacık Bay-Izmir, Turkey), in respect to physico-chemical water quality parameters, nutrient loads, chlorophyll-*a*, total suspended solids, zooplankton groups, and TRIX index calculations for the potentially affected cage farm area and an unaffected reference site. Concentrations of physico-chemical variables (temperature, salinity, dissolved oxygen, pH) in the study carried out in May and August 2018, were within the acceptable limits for marine aquaculture in terms of water quality characteristics. The concentrations of PO_4-P, NH_4-N, and NO_2-N showed no temporal or spatial changes, and were recorded below 0.01 mg/L (<0.01) for PO_4-P and NH_4-N, whereas lower than 0.005 mg/L (<0.005) for NO_2-N values in both cage and reference stations in May and August 2018 periods. Results showed low levels of TSS (0.33-11.87 mg/L), both in the cage farm area and the reference site, remaining below the general quality criteria of 30 mg/L for marine environment. No eutrophication risk (TRIX index, *T<4*) was observed around the Tuna Cage Farm Site in Sığacık Bay, according to the legislations enacted for "Sensitive Areas of Enclosed Bays where fish farms are not allowed". Based on these findings, demonstrating highly interactive trophic level variability, it can be concluded that the impacts of the Tuna Cage Farm were not significant, possibly due to the consistent movement of the water in currents in the study area.

Keywords: Tuna farming, Cage aquaculture, Environmental impact, Water quality

Introduction

The traditional fish production has become a growing industry with the development of new production systems and marine technologies in fish farming facilities. As a rapid growing industry, the aquaculture sector today reached a global fish production of nearly 54.091.148 tons worldwide with about 138.537.398.000 USD economic value (FAO, 2019a) and aims to provide high quality protein for the increasing demand of the world population that is expected to reach around 9.8 billion in 2050, and 11.2 billion in 2100 (UN-WPP, 2017). However, the rapid growth in intensive culture conditions arise significant risks and pressure on the marine environment. Since water resources are limited and vital for human beings, the sustainable use of water is an important matter that needs to be considered for the future of marine resources in the world. The assessment of potential productivity without significant negative impacts on the marine environment caused by the production activities (Beveridge and Phillips, 1993; Beveridge, 1996; Kautsky et al., 1997; Pittroff and Pedersen, 2001), and the maximum sustainable nutrient input that the water body can receive without exposing any eutrophication signs (Ganguly et al., 2015), are important issues for sustainable development of the cage farming industry, which can only be achieved when the farm loads are kept below the carrying capacity limitations of the water environment. Farm impacts could be reduced or minimized via proper site selection, stock density management, optimization of feed formulations using well selected ingredients and the integration of multi-trophic aquaculture production systems such as mussels, oysters, seaweed, etc. Environmental monitoring and control of farm sites are important in terms of assuring maximum fish biomass to be maintained in a water environment without negatively influencing ecological conditions of the water body (Granada et al., 2015).

Besides the mainly produced fish species of seabream and seabass, tuna farming is a growing aquaculture industry in the Mediterranean with a production of 6.089 tons and a value of 102.308.000 USD in 2016, among which the Turkish Tuna farming covers 13% with a production of 770 tons of the total harvest with a value of 11.422.000 USD (FAO, 2019b). The difference in tuna cage farming compared to seabream or seabass is that fish caught from the wild and fattened with trash fish to larger size in one season and then harvest. The sustainable growth of the Tuna farm operations can only be ensured with environmental control of the marine sites in the Aegean and the Mediterranean. Therefore, the present study aimed to investigate potential environmental impacts of a tuna farm site in the Aegean Sea (Turkish coast) in respect to Turkish environmental legislations.

Material and Methods

Study Area and Sampling Period

The study was conducted in the potential cage farm site area No: 9 in Sığacık Bay (Seferihisar town, Izmir province, Turkey), determined and established by the Ministry of Environment and Urban Development (Figure 1, 2).

This study was conducted at 2 different sampling stations determined as "Cage and Reference" stations, with 3 different water depths of "surface (5 m), mid layer (35 m), and bottom (80 m)" in the study area of Sığacık Bay – Tuna Cage Farm Site. The "Cage Station" was designated as a sampling location next to the farm site, whereas the "Reference Station" was assigned an unaffected location of the upstream area 150 m in distance from the cage site. The study was conducted in two periods May 2018 and August 2018, which was assumed to be the highest season in terms of temperature, presence of tuna biomass and active feeding progress in the cage systems, nutritional inputs via fish feeding, and nitrogen or phosphorous loads due to excretory waste outputs, as well as plankton production in the study area.

Layout and Design of Tuna Cage Farm System

A 2x4 bay submerged grid-mooring system was used to set the Tuna cages consisting of single pipe floatation as the main upper rim, anchored to sea bottom with 16 deadweight anchors. The layout design of the Tuna cage farm operating in the study area of Sığacık Bay (Seferihisar-Izmir, Turkey) is demonstrated in Figure 3.

Analyses of Water Samples

Water Quality Analyses

In the sampling locations, seawater quality parameters such as temperature, salinity, pH, dissolved oxygen (% saturation and mg/L level) were measured *insitu* using a YSI 600QS model multi probe system. Seawater visibility was measured *insitu* using a Secchi disk.

Nutritional Element Analyses

Among the nutrients, soluble reactive phosphorus (PO_4-P), total phosphorus (TP), nitrite (NO_2^-), nitrate (NO_3^-), ammonia (NH_4) and total nitrogen (TN) were sampled from designated sampling locations and depths, and transferred to GEMAR laboratories (GEMAR, Environmental Measurements and Analyses Laboratory - Çevre Ölçüm ve Analiz Laboratuarı, Canakkale-Turkey). Consequently, spectrophotometric analyses were performed according to ISO, EPA, TS and EN standards using methods SM 4500-P E for PO_4-P and SM 4500-P B, E for TP, SM 4500-NO_2. B for NO_2^-, EPA 352.1 for NO_3^-, SM 4500-NH3 B, F for NH_4 and SM 4500-NO2 B- EPA 352.1-SM4500-Norg B for TN.

For the analyses of silicate (SiO₂) values in the samples collected from the study area in different depth were conducted spectrophotometrically according to the methods for seawater analyses described by Strickland and Parsons (1972) in the Planktonology Laboratory of Canakkale Onsekiz Mart University, Faculty of Marine Science and Technology (Canakkale, Turkey). For the silicate analyses, water samples were kept in room temperature. A water sample of 25 mL was added on a 10 mL-molybdate solution within a 50 mL flask, stirred and kept for 10 min (waiting time should not exceed 30 min). Then the flask was filled up to 50 mL with using a reducing reactive and stirred immediately, remained for 2-3 hours in order to complete the reduction, and reading was conducted spectrophotometrically at 810 nm wave length.

Total Suspended Solids (TSS) Analyses

Sampling for the determination of total suspended solids (TSS) was conducted from the water column and sea bottom using a 5-L volume Nansen bottle. The TSSs, composed by both organic and inorganic compounds and influencing light penetration an important criterion for photosynthesis, were analyzed gravimetrically according to Clesceri et al. (1998).

Chlorophyll-a Analyses

Water samples for determining the chlorophyll-*a* concentrations, an indication of primary productivity and phytoplankton density, were taken from designated depths via a 5-L Nansen bottle. Each of the 1.5 L water samples were *in situ* vacuum-filtered using a 47 mm GF/F filter paper, which were then places in glass tubes after filtration and covered by aluminum folio and kept frozen until analysis. Then, the spectrophotometric analysis after 90% acetone extraction was performed according to Greenberg et al. (1992).
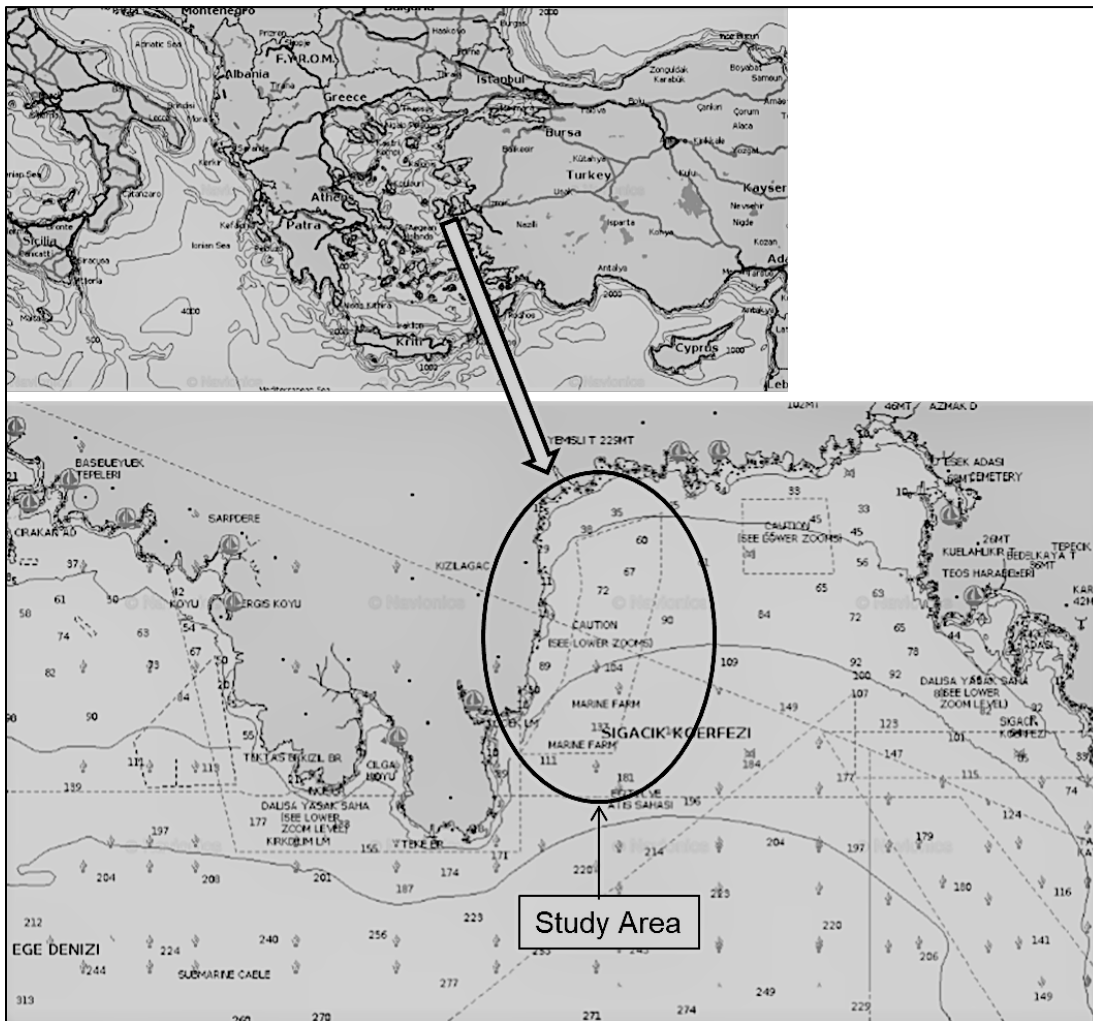
Figure 1. Location of the study area; Sığacık Bay, Izmir-Turkey (https://sailingheaven.com/nautical-map/)
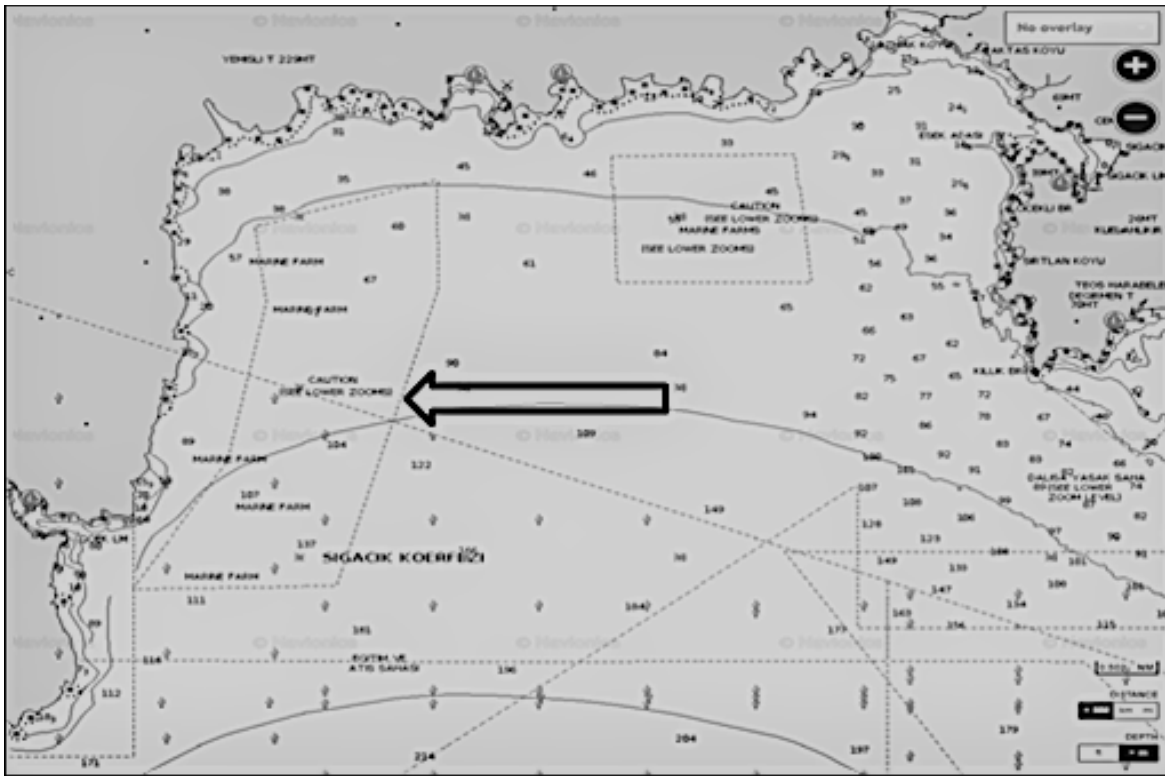
Figure 2. Sığacık Bay and site No: 9 (https://sailingheaven.com/nautical-map, July 2018)
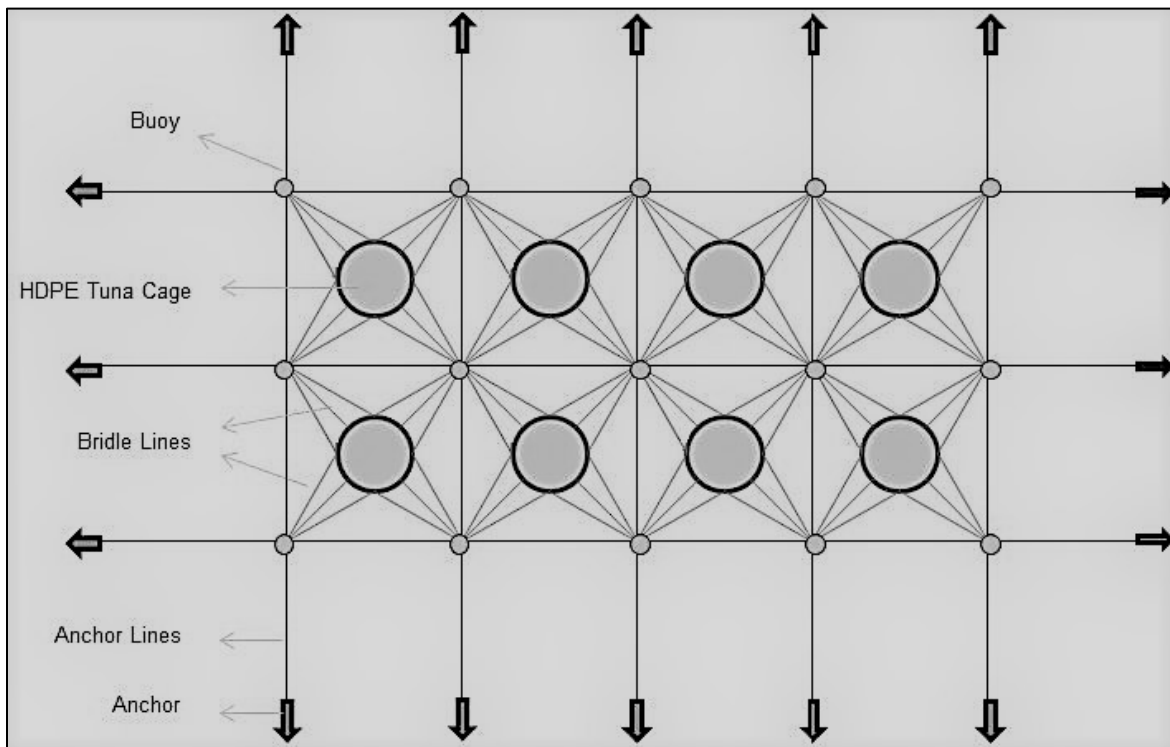
Figure 3. Layout design of the Tuna cage farm in Sığacık Bay (Seferihisar-Izmir, Turkey), HDPE: High density polyethylene

Zooplankton Analyses

In the present study, 200 µm mesh diameter standard plankton net was used for zooplankton samplings. In each of the designated sampling depths, samples were obtained through vertical towing and retained with 4% end volume buffered formaldehyde. Qualitative analyses on the zooplankton were performed in the laboratory, where the excess water was syphoned and samples transferred into smaller flasks. The distribution rate of groups and species was done using unit-sample methods (Ozel, 1998). In this point, samples were homogenous distributed on a container with a known surface area, and the sub-samples with smaller scale obtained via unit-sample method were transferred on a lamella and zooplankton analyses conducted. For the quantitative analyses, a certain volume out of the total homogeny sample was taken and the unit-sample method applied (Ozel, 1998). For the systematic classification of the species, earlier reports of Tregouboff and Rose (1957), Todd et al. (2006), and Young et al. (2006) were followed, as well as the web site of European Register of Marine Species (MarBEF, 2008) in order to check most recent additions. A trinocular stereo-zoom research microscope Olympus brand SZX7 model was used for determining the zooplankton species.

TRIX Index and Calculation

In the present study, TRIX index calculations were performed using measured values of Chlorophyll-*a*, % dissolved oxygen saturation, total dissolved inorganic nitrogen (TIN) and total phosphorous (TP) concentrations. The TRIX indexes were calculated according to the guidelines for "Sensitive Areas of Enclosed Bays where Fish Farms are not allowed" entered into force on 24.01.2017 with the law no: 26413 by of the Turkish Ministry of Environment and Forest, using following equation:

TRIX Index= (Log (Chlorophyll-*a* x %O$_2$ x TIN x TP) + 1.5) x 0.833 (4)

where,

Chlorophyll-*a* : Chlorophyll-*a* concentration in water body (µg/L),

%O2 (The absolute percent value deviated from the saturated oxygen rate) = |%DO – 100|,

TIN (Total dissolved inorganic nitrogen, µg/L) = N - (NO$_3$ + NO$_2$ + NH$_4$),

TP : Total phosphorous (µg/L)

Results and Discussion

In the present study, seawater temperatures in different depths of the designated study area were recorded between 17.70-21.22 °C in May 2018, and between 18.69-24.85 °C in August 2018. Salinity was recorded as 38 ppt in May 2018, while it was around 31 ppt in August 2018. The percent dissolved oxygen (% DO) saturation and DO level were measured as 98-107.8 % and 7.20-7.74 mg/L in May, whereas these values were recorded as 97.50-99 % and 6.29-8.20 mg/L in August 2018, respectively. The pH values varied between 7.78-8.38 and 8.07-8.22 for the May and August 2018 terms, respectively. The values for seawater temperature, salinity, DO concentration, and pH were within the acceptable limits for marine aquaculture in terms of water quality characteristics (Table 1).

The chlorophyll-*a* value as an indication of primary productivity and phytoplankton density in the present study was measured between 0.20-0.32 µg/L and the TSS, composed by both organic and inorganic compounds and influencing light penetration that is important for photosynthesis, was measured between 8.00-11.30 mg/L during the May 2018 study period. In the sampling period of August 2018 however, chlorophyll-*a* values were recorded between 0.04–0.41 µg/L, and the TSS varied between 0.33-11.87. The TSS measured from different sampling locations and water depths in both periods were below the general quality criteria of 30 mg/L for seawater, based on the WPCL (2004) (Table 2). The Secchi disk values for the May 2018 study period were recorded as 11.60 m in the Cage Station, while 16.00 m in the Reference Station. In the August 2018 sampling period, the Secchi disk values varied between 10.25-13.50 m (Table 3).

Silicate values in all sampling depths throughout the study period remained between 30-40 µg/L, which was far below the level supporting continuous growth of diatoms (Kocatas, 1993). As known, the silicate cycle in the aquatic systems is limited, and the silicate into the marine ecosystems transported from mainly rivers, rain falls, and winds in the area (Kocatas, 1993; Goldman and Horne, 1994). The "total inorganic dissolved nitrogen" to "phosphorous" ratio (TIN:P) obtained in the study period of May 2018 remained below the Redfield ratio of "16:1", suggesting a limitation of nitrogen forms such as nitrite + nitrate and ammonium on phytoplankton development. Besides, considering that the TIN:P ratio recorded in the August 2018 period being above the 16:1 ratio in some stations might be an indication of a potential limiting effect of phosphorous on phytoplankton growth. In some sampling stations, the TIN:Si ratios were reasonably higher than the Redfield ratio of 1:1, which is deterministic for diatoms. Therefore, this can be an indication that silicate might have a potential limiting effect on the diatom growth (Kocum, 2005). Considering these measurements, it was found that nutrient concentrations in both study periods of May and August 2018 were between acceptable ranges of water quality characteristics and within the limits suitable for marine aquaculture activities. Besides, our findings in terms of nutrients in this study were similar to those of previously conducted studies in the same study area (Palta, 2010; CSB, 2018).

Table 1. Sığacık Bay Tuna Cage Farm Site; temperature, salinity, dissolved oxygen (%), dissolved oxygen (mg/L), and pH values in sampling locations and variations with depth (May – August 2018)

Sampling Station	MAY - 2018		AUGUST – 2018	
	Cage	Reference	Cage	Reference
Temperature (°C)				
Surface	21.22	20.80	23.71	24.28
Mid Layer	20.00	20.00	21.88	22.75
Bottom	18.28	17.70	18.69	18.94
Salinity (ppt)				
Surface	38	38	31.25	31.41
Mid Layer	38	38	31.16	31.31
Bottom	38	38	31.11	31.21
Dissolved Oxygen (%)				
Surface	107.8	105.0	98.0	98.2
Mid Layer	102.0	102.0	97.0	99.0
Bottom	98.0	102.0	97.0	99.0
Dissolved Oxygen (mg/L)				
Surface	7.74	7.60	7.20	6.96
Mid Layer	7.50	7.60	7.60	6.96
Bottom	7.20	7.20	8.20	7.29
pH				
Surface	8.38	8.42	8.21	8.22
Mid Layer	8.20	8.20	8.21	8.21
Bottom	7.78	8.20	8.21	8.18

Table 2. Variations of chlorophyll-*a* and TSS values according to sampling stations and depth in Sığacık Bay – Tuna Cage Farm locations (May – August 2018). (---): not enough water samples available

Sampling Station	MAY - 2018		AUGUST - 2018	
	Cage	Reference	Cage	Reference
Chlorophyll-*a* (µg/L)				
Surface	0.25	0.28	0.04	0.05
Mid Layer	0.25	---	0.15	0.12
Bottom	0.20	0.32	0.22	0.15
TSS (mg/L)				
Surface	8.70	8.00	7.23	11.87
Mid Layer	10.20	---	7.28	4.29
Bottom	11.30	8.50	8.60	0.33

Table 3. Secchi disk values in Sığacık Bay–Tuna Cage Farm sampling stations (May – August 2018)

Sampling Station	Secchi Disk (m)	
	MAY - 2018	AUGUST - 2018
Cage	11.60	10.25
Reference	16.00	11.40

During the study period of May 2018, NO$_3$-N, NO$_2$-N, NH$_4$-N, and PO$_4$-P did not exceed 0.03 mg/L, 0.006 mg/L, 0.01 mg/L, and 0.01 mg/L, respectively, in the selected sampling stations and depths. The TN values were recorded between 0.3-0.8 m/L. The TP values were found to be below 0.029 mg/L, and SiO$_2$ values varied between 0.03-0.09 mg/L. In the sampling period of August 2018, NO$_3$-N, NH$_4$-N and TN were recorded as 0.08-0.18 mg/L, 0.01-0.03 mg/L, and 0.35-2.91 m/L, respectively, while the NO2-N values did not exceed 0.005 mg/L. The PO$_4$-P values were below 0.01 mg/L, and TP values were obtained between 0.01-0.12 mg/L. In the study period, the SiO$_2$ values were found as 0.03-1.15 mg/L in the selected sampling stations and depths (Table 4).

Nitrogen and phosphorous loads in the surrounding water environment occur due to the feed losses, fecal and other metabolic wastes (Yildirim and Korkut, 2004), and as results of domestic and industrial pollution. When comparing offshore systems with no coastal influences and coastal zone areas under coastal influence, the impact of phytoplanktonic production on TSS in the offshore marine systems is higher (Besiktepe et al., 1994). Therefore, considering chlorophyll-*a* concentrations and TSS values, it can be concluded that the TSS was controlled by coastal effluents and/or feeding activities in the study locations during the sampling periods.

The TRIX indexes obtained in the present study via calculation of measured values of chlorophyll-*a*, % DO saturation, TIN, TP concentrations for the study periods from May to August 2018 are given in Table 5.

According to the results obtained from sampling stations in Sığacık Bay – Tuna Cage Farm Site in the highest season from May to August, when potentially high impacts could be expected, Sığacık Bay – Tuna Cage Farm Site did not show any Eutrophication Risk, being below the Eutrophication Risk Scala of less than "4" (*T<4*), based on the legislations enacted for "Sensitive Areas of Enclosed Bays where Fish Farms are not allowed". Our results obtained here during the tuna production period from May to August 2018, are in close agreement with an earlier report on environmental impacts of a large-size tuna farm with a capacity of 1840 ton/year and operating in a water surface area of 30.000 m^2 in May and August 2015 (Kocak, 2018).

The abundance and distribution of zooplanktonic organisms in the study area and sampling locations are given in Table 6. Members of *Oithona* species among copepods and *Oikopleura dioica* species among appendicularians were dominant during the May 2018 study period. With the increase of the water temperature in August 2018, the abundance of *Cladocera* was found to be higher compared to the other groups. Especially, the abundance of *Penilia avirostris*, feeding on smaller-sized particles, was the highest in the study period compared to other species.

The *Penilia avirostris*, mainly distributed in temperate enclosed bays (DellaCroce and Venugopal, 1972; Aker and Ozel, 2006) are capable to feed and utilize on a variety of trophic sources (Turner et al., 1988), and can propagate easily in temperate areas with suitable trophic conditions. The *Evadne spinifera* is a warm-water species, appearing in oceanic or coastal waters (Aker and Ozel, 2006). Due to its ecological characteristics, it may show distribution during the spring and summer period, whereas disappearing during the autumn or winter periods. The copepods are selective feeders. Calanoid copepods prefer feeding on micro-plankton and larger particles such as ciliates (>20 μm) (Paffenhöfer and Knowles, 1980; Kleppel, 1993; Fessenden and Cowles, 1994; Sommer et al., 2000; Stibor et al., 2004). The *Centropages typicus* show both carnivorous and omnivorous characteristics, and can feed on phytoplankton, ciliates appendicularians, copepod eggs and nauplii, and even on fish larvae with yolk sack (Carlotti and Harris, 2007). With their specific characteristics, these species can live and distribute in large numbers in temperate climate, neritic coastal zones, especially in bays and shallow marine areas with high salinities, and can reach significant abundance during the spring season in the Northern Mediterranean. *Oithona* species have a wide range of trophic preference and may show aggressive feeding behavior, therefore phytoplankton, ciliates, detritus, naupliu and fecal pellets are within their feed-range (Nakamura and Turner, 1997; Atienza et al., 2006). Hence, in oligotrophic waters with low chlorophyll-a levels they can easily increase their numbers (Castellani et al., 2015). Appendicularians (*Oikopleura* species) however, are filter-feeders (Siokou-frangou et al, 1998; Stibor et al., 2004). They are one of the most important parts of the secondary production, due to their ability of capturing nano-pico particles, and shorter generation-cycle compared to copepods (Uye and Ichino, 1995; Spinelli et al., 2013), being among the feed sources of high-trophic ctenophores and several fish species (Uye and Ichino, 1995; Spinelli et al., 2013). *Sagitta* sp. is generally feeding on adult copepods. Further, *Oithona* and *Oikopleura* species as well as their own younger individuals are among their feed sources (Steele, 1970; Giesecke and Gonzalez, 2008).

Table 4. Sığacık Bay – Tuna Cage Farm sampling stations; NO_3-N, NO_2-N, NH_4-N, PO_4-P, SiO_2, TN and TP values and TIN*:P, TIN:Si ratios (May – August 2018)

Sampling Station	MAY – 2018						AUGUST - 2018						MMR
	Cage			Reference			Cage			Reference			
	Surface	MidL	Bottom	Surface	MidL	Bottom	Surface	MidL	Bottom	Surface	MidL	Bottom	
TP (mg/L)	0.023	0.01	0.01	0.029	0.011	btd	btd	btd	btd	0.06	0.12	0.12	0.01-6
PO_4-P (mg/L)	btd	btd	btd	btd	btd	btd	btd	btd	btd	btd	btd	btd	0.01-6
TN (mg/L)	0.3	0.7	0.7	0.7	0.8	0.8	0.66	0.74	0.37	0.35	0.75	2.91	-
NH_4-N (mg/L)	<0.01	<0.01	<0.01	<0.01	<0.01	<0.01	<0.01	<0.01	<0.01	<0.01	<0.01	<0.01	0.005-0.6
NO_2-N (mg/L)	btd	btd	btd	0.006	btd	bdt	btd	btd	btd	btd	btd	btd	0.005-1
NO_3-N (mg/L)	0.021	0.01	0.01	0.03	0.02	0.02	0.13	0.12	0.09	0.13	0.11	0.08	0.1-2
SiO_2 (mg/L)	0.03	0.05	0.05	0.7	0.7	0.9	0.09	0.07	0.05	0.03	0.04	0.04	-
TIN:P	3.60	2.50	2.50	4.60	3.50	3.50	14.50	13.50	10.50	14.50	12.50	9.50	
TIN:Si	1.20	0.50	0.50	0.07	0.05	0.04	1.61	1.93	2.10	4.83	3.13	2.38	

*TIN: Total inorganic dissolved nitrogen, N-(NO_3+NO_2+NH_4); MidL: Mid Layer; MMR: Method Measured Range; btd: below detection limits (<0.01 for TP and PO_4-P and <0.005 for NO_2-N)

Table 5. Trix index values in Sığacık Bay – Tuna Cage Farm sampling stations, May – August 2018

	TRIX Index	
Sampling Station	MAY - 2018	AUGUST – 2018
Cage Location		
Surface	3.92	2.97
Mid Layer	3.00	3.57
Bottom	2.92	3.57
Reference Location		
Surface	3.97	3.66
Mid Layer	---	3.97
Bottom	3.21	3.94

TRIX index calculated according to the guidelines for "Sensitive Areas of Enclosed Bays where fish farms are not allowed" entered into force on 24.01.2017 with the law no: 26413 by of the Turkish Ministry of Environment and Forest.

Table 6. Main zooplankton species in the study area of Sığacık Bay – Tuna Cage Farm Site, May – August 2018

	MAY – 2018		AUGUST - 2018	
Sampling Stations	**Cage**	**Reference**	**Cage**	**Reference**
Zooplankton Species (individuals / m³)				
Bivalvia veliger l.	Nd	2	18	5
Calanoida	Nd	Nd	125	75
Centropages typicus	62	33	Nd	Nd
Corycaeus sp.	Nd	3	18	23
Copepoda naupliu	5	9	53	35
Euterpina acutifrons	Nd	Nd	5	13
Evadne spinifera	Nd	Nd	118	129
Fritillaria sp.	Nd	2	Nd	Nd
Oithona similis	38	7	18	10
Oithona nana	6	4	Nd	Nd
Oithona plumifera	3	4	25	10
Oithona sp.	Nd	3	24	35
Oncaea sp.	Nd	2	Nd	Nd
Oikopleura dioica	42	Nd	Nd	Nd
Oikopleura longicauda	13	Nd	12	35
Oikopleura fusiformis	Nd	5	Nd	Nd
Penilia avirostris	Nd	Nd	231	385
Pleopsis polyphemoides	Nd	Nd	17	38
Sagitta sp.	2	3	15	15
Others*	19	3	8	5

* Gastropoda, Bivalvia, Polychaeta, Echinodermata, Siphonophora, Thaliacea, fish larvae and fish eggs; *Nd*: Not detected

Conclusion

As a conclusion of the present study in terms of water quality parameters, nutrient load, TIN:P ratio, TRIX index eutrophication risk, and zooplanktonic data evaluation, it can be concluded that highly interactive trophic level variability was observed in the study area of Sığacık Bay, during the sampling period. The Eutrophication Risks Scala of less than "4" (*T<4*) recorded in this study might indicate that there is no eutrophication risk in the Tuna Cage Farm Site of Sığacık Bay, according to the environmental legislations enacted for "Sensitive Areas of Enclosed Bays where Fish Farms are not allowed". Further investigations are encouraged in terms of continuous monitoring of cage farm sites in order to control water quality and potential farm effects for the sustainable growth of tuna aquaculture in the Mediterranean.

Compliance with Ethical Standard

Conflict of interests: The authors declare that for this article they have no actual, potential or perceived conflict of interests.

Ethics committee approval: No Ethical committee approval is required for this study, since no experimental living organisms were used.

References

Aker, H.V., Ozel, İ. (2006). İzmir Körfezi Kladoserlerinde Mevsimsel Dağılım. *Ege Üniversitesi Su Ürünleri Dergisi,* 23, 17-22

Atienza, D., Calbet, A., Saiz, E., Alcaraz, M., Trepat, I. (2006). Trophic impact, metabolism and biogeochemical role of the marine cladoceran Penilia avirostris and the co-dominant copepod Oithona nana in NW Mediterranean coastal waters. *Marine Biology International Journal on Life in Oceans and Coastal Waters,* 15(2), 221-235.

Besiktepe, S., Sur, H.I., Ozsoy, E., Latif, M.A., Oguz, T., Unluata, U. (1994). The circulation and hydrography of the Marmara Sea. *Progress in Oceanography,* 34, 285-334.

Beveridge, M.C.M. (1996). *Cage Aquaculture*. Fishing News Books Ltd., London, UK, ISBN 0852382359

Beveridge, M.C.M., Phillips, M..J. (1993). Environmental Impact of Tropical Inland Aquaculture, In: R.S.V. Pullin, H. Rosenthal, J.L. Maclaen (Eds.), *Environment and Aquaculture in Developing Countries* (p. 213–236). International Center for Living Aquatic Resources Management, Manila, Philippines. ISBN 971-8709-05-3

Carlotti, F., Harris, R. (2007). The biology and ecology of *Centropages typicus* an introduction. *Progress in Oceanography,* 72, 117-120.

Castellani, C., Licandro, P., Fileman, E., DiCapua, I., Mazzocchi, M.G. (2015). *Oithona similis* likes it cool: evidence from two long-term time series. *Journal of Plankton Research,* 38, 703-717.

Clesceri, L.S., Greenberg, A.E., Eaton, A.E. (1998). *Standard Methods for the Examination of Water and Wastewater* 20th Edition [Method 2540 B. (Total Solids), Method 2540 C. (Total Dissolved Solids) and Method 2540 D. (Total Suspended Solids)]. American Public Health Association, Washington, p. 1325.

CSB (2018). Deniz kalitesi bülteni, Ege Denizi. T.C. Çevre ve Şehircilik Bakanlığı, Çevresel Etki Değerlendirmesi İzin ve Denetim Genel Müdürlüğü Yayınları, p. 21.

Della, Croce, N., Venugopal, P. (1972). Distribution of marine cladocerans in the Indian Ocean. *Marine Biology,* 15, 132-138.

FAO (2019a). UN, FAO Figis Online Statistical Query Results, Global Aquaculture Production. Retrieved from http://www.fao.org/fishery/statistics/global-aquaculture-production/query/en (accessed 10.02.19)

FAO (2019b). UN, FAO Figis Online Statistical Query Results, Atlantic Bluefin Tuna Production in the Mediterranean. Retrieved from http://www.fao.org/fishery/statistics/global-aquaculture-production/query/en (accessed 10.02.19)

Fessenden, L., Cowles, T.J. (1994). Copepod predation on phagotrophic ciliates in Oregon coastal waters. *Marine Ecology Progress Series,* 107, 103-111.

Ganguly, D., Patra, S., Muduli, P.R., Vardhan, K.V., Abhilash, R.K., Robin, R.S., Subramanian, B.R. (2015). Influence of nutrient input on the trophic state of a tropical brackish water lagoon. *Journal of Earth System Science,* 124, 1005-1017.

Giesecke, R., Gonzalez, H.E. (2008). Reproduction and feeding of Sagitta enflata in the Humboldt Current system off Chile. *ICES- Journal of Marine Science,* 65, 361-370.

Granada, L., Sousa, N., Lopes, S., Lemos, M.F.L. (2015). Is integrated multitrophic aquaculture the solution to the sectors' major challenges? – a review. *Reviews in Aquaculture*, 8(3), 283-300.

Greenberg, A.E., Clesceri, L.S., Eaton, A.D., Franson, M.A.H. (1992). *Standard Methods for the Examination of Water and Wastewater* 18th Edition. American Public Health Association, Washington. ISBN 0-87553-207-1

Goldman, C.R., Horne, A.J. (1994). *Limnology.* McGraw Hill Education ISE Editions, 2nd Edition, p. 736, ISBN 0071133593

Katechakis, A., Stibor, H., Sommer, U., Hansen, T. (2004). Feeding selectivities and food niche separation of *Acartia clausi*, *Penilia avirostris* (Crustacea) and *Doliolum denticulatum* (Thaliacea) in Blanes Bay (Catalan Sea, NW Mediterranean). *Journal of Plankton Research,* 26, 589-603.

Kautsky, N., Berg, H., Folke, C., Larsson, J., Troell, M. (1997). Ecological footprint for assessment of resource

use and development limitations in shrimp and tilapia aquaculture. *Aquaculture Research,* 28, 753–766.

Kleppel, G.S. (1993). On the diets of calanoid copepods. *Marine Ecology Progress Series*, 99, 183–195.

Kocak E., 2018. Açık-Deniz Orkinos Balık Yetiştiriciliği ve Yasal Sınırlamaların Büyük Ölçekli Bir Tesis Örneği Üzerinden İncelenmesi. Niğde *Ömer Halisdemir Üniversitesi Mühendislik Bilimleri Dergisi / OHU Journal of Engineering Science,* 7, 558-565.

Kocatas, A. (1993). *Oseanoloji.* Ege Üniversitesi Kitaplar Serisi, Bornova, İzmir. p. 358.

Kocum, E. (2005). Çanakkale Boğazında Klorofil-*a* ve Çözünmüş Mineral Besin Elementi Miktarlarının Analizi. *Ekoloji* 15, 1-6.

MarBEF (2008). MarBEF Data System, Retrieved from http://www.marbef.org/data (accessed 29.05.08)

Nakamura, Y., Turner, J.T. (1997). Predation and repiration by the small cyclopoid copepod *Oithona similis*: how important is feeding on cliates and heterotrophic flagellates? *Journal of Plankton Research,* 19, 1275-1288.

Ozel, İ. (1998). *Planktonoloji* 1. Ege Üniversitesi Su Ürünleri Fakültesi Yayınları, p. 2-88.

Paffenhöfer, G.A., Knowles, S.C. (1980). Omnivorousness in marine planktonic copepods. *Journal of Plankton Research,* 2, 355–365.

Palta, Z.H. (2010). Gerence ve Sığacık Körfez'inde (Ege Denizi), iki ağ kafes işletmesinde çevresel parametrelerin zooplankton dinamiğine etkisi. Yüksek Lisans Tezi, Çanakkale Onsekiz Mart Üniversitesi Fen Bilimleri Enstitüsü. p. 91.

Pittroff, W., Pedersen, E.K. (2005). *Ecological Modelling.* In eLS. John Wiley & Sons Ltd, Chichester. http://www.els.net (doi: 10.1038/npg.els.0003270)

Siokou-frangou, I., Papathanassiou, A.E., Lepretre Frontier S. (1998). Zooplankton assemblages and influence of environmental parameters on them in a Mediterranean coastal area. *Journal of Plankton Research,* 20, 847-870.

Sommer, F., Stibor, H., Sommer, U., Velimirov, B. (2000). Grazing by mesozooplankton from Kiel Bight, Baltic Sea, on different sized algae and natural seston size fractions. *Marine Ecology Progress Series,* 199, 43–53.

Spinelli, M., Guerrero, R., Pajaro, M., Capitanio, F. (2013). Distribution Of *Oikopleura dioica* (Tunicata, Appendicularia) Associated With A Coastal Frontal System (39°-41°S) of the SW Atlantic Ocean in the Spawning Area of *Engraulis anchoita* Anchovy. *Brazilian Journal of Oceanography,* 61, 141-148.

Steele, J.H. (1970). *Marine Food Chains*. University of California Press (Berkeley and Los Angeles). 1st ed.

Stibor, H., Vadstein, O., Lippert, B., Roederer, W., Olsen, Y. (2004). Calanoid copepods and nutrient enrichment determine population dynamics of the appendicularian *Oikopleura dioica*: a mesocosm experiment. *Marine Ecology Progress Series,* 270, 209–215.

Strickland, J.D.H., Parsons, T.R. (1972). A practical handbook of seawater analysis. 2nd ed. Bulletin, Ottowa: *Fisheries Research Board of Canada,* 167, 310.

WPCL (2004). Water Pollution Control Legislation, Su Kirliliği Kontrolü Yönetmeliği, Resmi Gazete: Tarih 31 Aralık Cuma Sayı: 25687.

Todd, C.D., Laverack, M.S., Boxshall, G.A. (2006). *Coastal Marine Zooplankton: A Practical Manual for Students*. 2nd ed. University Press, Cambridge.

Tregouboff, G., Rose, M. (1957). Manuel De Planctonologie Mediterranéenne. Tome I: Texte. Tome II: Planches. *Centre National De La Recherce Scientifique*. Paris.

Turner, J.T., Tester, P.A., Ferguson, R.L. (1988). The marine cladocerans *Penilia avirostris* and the "microbial loop" of pelagic food webs. *Limnology and Oceanography,* 33, 245-255.

UN-WPP (2017). World Population Prospects: The 2017 Revision. United Nations, Population Division, Department of Economic and Social Affairs. Retrieved from https://population.un.org/wpp/Download/Standard/Population/ (accessed 08.02.19)

Uye, S., Ichino, S. (1995). Seasonal variations in abundance, size composition, biomass and production rate of

Uikopleura dioica (Fol) (Tunicata: Appendicularia) in a temperate eutrophic inlet. *Journal of Experimental Marine Biology and Ecology,* 189, 1-11.

Yildirim, Ö., Korkut A.Y. (2004). Su Ürünleri Yemlerinin Çevreye Etkisi. *E.Ü. Su Ürünleri dergisi, E.Ü. Journal of Fisheries and Aquatic Sciences,* 21, 167-172.

Young, C.M., Sewell, M.A., Rice, M.E. (2006). Atlas of Marine Invertebrate Larvae. Elsevier, Barcelona. ISBN-10 0123736080

Research Article

PROCESSING OCEANOGRAPHIC DATA BY PYTHON LIBRARIES NUMPY, SCIPY AND PANDAS

Polina Lemenkova

Ocean University of China, College of Marine Geo-Sciences, 238 Songling Road, Laoshan, 266100, Qingdao, Shandong Province, People's Republic of China

ORCID IDs of the author(s):
P.L. 0000-0002-5759-1089

Correspondence:
Polina LEMENKOVA
E-mail:
lemenkovapolina@stu.ouc.edu.cn

ABSTRACT

The study area is located in western Pacific Ocean, Mariana Trench. The aim of the data analysis is to analyze the potential influence of how various geological and tectonic factors may affect the geomorphological shape of the Mariana Trench. Statistical analysis of the data set in marine geology and oceanography requires an adequate strategy on big data processing. In this context, current research proposes a combination of the Python-based methodology that couples GIS geospatial data analysis. The Quantum GIS part of the methodology produces an optimized representative sampling dataset consisting of 25 cross-section profiles having in total 12,590 bathymetric observation points. The sampling of the geospatial dataset are located across the Mariana Trench. The second part of the methodology consists of statistical data processing by means of high-level programming language Python. Current research uses libraries Pandas, NumPy and SciPy. The data processing also involves the subsampling of two auxiliary masked data frames from the initial large data set that only consists of the target variables: sediment thickness, slope angle degrees and bathymetric observation points across four tectonic plates: Pacific, Philippine, Mariana, and Caroline. Finally, the data were analyzed by several approaches: 1) Kernel Density Estimation (KDE) for analysis of the probability of data distribution; 2) stacked area chart for visualization of the data range across various segments of the trench; 3) spacial series of radar charts; 4) stacked bar plots showing the data distribution by tectonic plates; 5) stacked bar charts for correlation of sediment thickness by profiles, versus distance from the igneous volcanic areas; 6) circular pie plots visualizing data distribution by 25 profiles; 7) scatterplot matrices for correlation analysis between marine geologic variables. The results presented a distinct correlation between the geologic, tectonic and oceanographic variables. Six Python codes are provided in full for repeatability of this research.

Keywords: Mariana Trench, Pacific Ocean, Python, Programming language, SciPy, NumPy, Pandas, Statistics, Data analysis

Introduction

There are various geodynamic processes that influence tectonic rift dynamics and structure as well as and rifted margin geomorphology. Currently, the interest towards the geodynamics, the drivers and consequences of these processes was implemented as key target goals of the oceanographic research in China (Cui et al., 2014; Cui & Wu, 2018). Knowing and proper understanding of the driving factors affecting the ocean ecosystems gives an understanding of the possible dynamics, accumulation, and location of the target ocean resources that are crucial for economic development.

Understanding the bathymetry of the ocean is crucial for the marina geological research. As noted by Dierssen & Theberge (2014), the distribution of elevations on the Earth or hypsography is highly uneven. Thus, the majority of the depths is occupied by deep basins (4–6.5 km) covered with abyssal plains and hills, while seafloor with ranges 2- 4 km depth mostly consists of oceanic ridges and in total cover about 30% of the total ocean seafloor. Finally, the shallow areas and continental margins with 2 km depth and shallower cover only the least amount of area, that is 15% of the seafloor (Litvin, V. M., 1987). Finally, the valley, seamounts and submarine canyons are only the minor features of the seafloor. Given the importance of the hadal areas, the study of the ocean trenches geomorphology and distribution of its features with regards to the bathymetry seems to be obvious.

There are many attempts undertaken to understand, to what extent and how do the geophysical movements in the subduction zones affect the trench geomorphology, deformation and migration (e.g. Doglioni, 2009; Fernandez & Marques, 2018; Gorbatov et al., 2001; Hubble et al., 2016; Lemoine et al., 2002). General concepts and understanding of the functioning and current problems in research directions of the marine hadal observations were implied in the current research. Active sedimentation on the bottom of the seafloor leads to the accumulated amount at rifted margins, particularly at the deltas of the large rivers. Sediments outflowing further to the ocean provide important geological bodies and resources. Besides, the natural hazards taking place in the ocean, strongly correlate with submarine earthquakes and volcanic eruptions during active rifting (Brune, 2016). Moreover, there is a certain correlation between the high oceanic features and thickness of the subduction channels and earthquake rupture segments, as shown with a case study of the trenches in the eastern Pacific Ocean by Contreras-Reyes and Carrizo. (2011). Ocean hadal trenches result from the complex geodynamic processes that continuously shape the surface of the seafloor (Bogolepov & Chikov, 1976). Nowadays, the ocean seafloor demonstrates 'footprints' of the many continuous steps of the seafloor evolution.
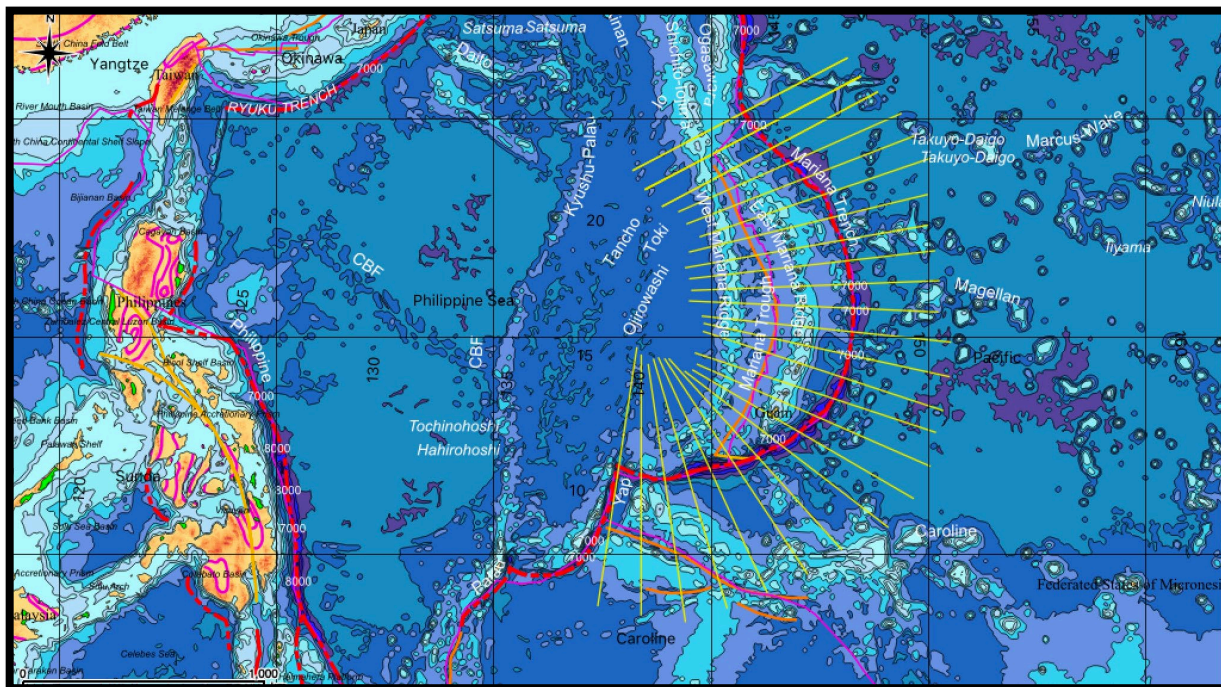
Figure 1. Study area visualizing 25 cross-section bathymetric profiles (yellow): QGIS map

Traditional methods of the marine geological modelling include using GIS based processing of the remote sensing images, such as for instance aerial photos, SPOT3, SPOT4 and ENVISAT data, or producing digital maps based on the data capture in the field (e.g., Bogdanov et al, 2011). On the contrary, the current paper makes an accent on using high-level programming language Python and its libraries Pandas, NumPy and SciPy for the processing of the large data frames imported from GIS. The effectiveness of the data computing and visualization by Python was the key factor for applying its functionality in this research. Some approaches of the scientific visualization and methods of the data analytics discussed previously by (Crameri, 2018) were considered in this research.

The actuality of the studies of marine natural hazards, such as submarine earthquakes and tsunamis cannot be underestimated. Recent progress in modelling earthquakes in Pacific ocean were proposed by (Kong et al., 2017). Using the global dataset of broadband and long-period seismograms, recorded as a time series ranging 2006-2014, from the Incorporated Research Institutions for Seismology (IRIS), it has been detected that there is a clearly descendance in the morphology of the Pacific plate, which becomes flatten at the base of the upper mantle and further goes westward towards a northern-central China (Dokht et al, 2016). Application of the geodynamic studies related to the tsunami, its possible reasons and consequences, are presented recently reporting that the shallowest reaches of plate boundary subductions host substantial slips that generate large and destructive tsunamis (Ikari et al. 2015). Attempts towards studies of the ocean geomorphology, dynamics, and intercorrelation between various factors affecting its functioning are given by various research (e.g. Mao et al., 2016; Masson, 1991; Luo et al., 2018; Loher et al., 2018).

Nevertheless, the problem of the proper understanding of the hadal areas in the ocean lies in its unreachable location. As justly noted by Jamieson (2018), understanding marine ecosystems for proper management and use of marine resources has a certain paradox, since there is a need to evaluate and protect the marine life and ocean ecosystems. However, the current knowledge on ocean functioning is relatively scarce. At the same time, modeling ocean and marine environment is a critical for the sustainable development of ocean resource usage. Recent studies only stress the strong correlation of the research with increasing ocean depths. However, the majority of the recent methods of ocean observations have overlooked

the Python programming approach for statistical analysis where the large data sets are being processed by a set of the embedded mathematical algorithms. Here, the paper presents improvements on the oceanographic data processing and interpretation methods by applying Python 3.2.7 languages and using its most essential libraries: NumPy, SciPy, Pandas and Matplotlib for data visualization and analysis.

Material and Methods

NumPy for Processing Arrays

Using Python modules and libraries enables processing of the large oceanographic data more effective and significantly improves the computation algorithms. The general functioning of the Python followed the existing references and manuals (e.g., Oliphant, 2007; Pedregosa et al., 2011; Perez et al., 2007). Using libraries enable to create namespaces while working with modules. Python's modules contain packed classes, objects, functions and constants used in the work. The installation of the libraries was done using pip upon the installing NumPy and SciPy, its dependancies:

$ python3 -m pip install numpy

$ python3 -m pip install scipy

The sorting and selecting of read in data from the tables was performed using NumPy. NumPy creates a multidimensional array object from a given 'table.csv'. Using Python's syntax and semantics, it operates with matrices using logical, bitwise, functional operations with elements, and performs a series of routines for fast operations on arrays (NumPy community, 2019). Finally, NumPy enables various object-oriented approach, mathematical and logical manipulations with table using ndarray. The scripts, modules and codes were written using reference semantics and built-in functions of NumPy and Python. The saved script included the written codes that parse command lines and perform graphs plotting by executing functions and modules. The namespaces of NumPy were imported from numpy.core and numpy.lib by calling:

>>> import numpy as np

The depending libraries have been installed as well. These include Jinja2, NumPy, Pillow, PyYAML, Six, Tornado. Manipulating with tabular data stored in csv files has been implemented in suitable Python library Pandas optimized for the high-level processing of tabular data. The Matplotlib library was installed as well and imported to customize plots.
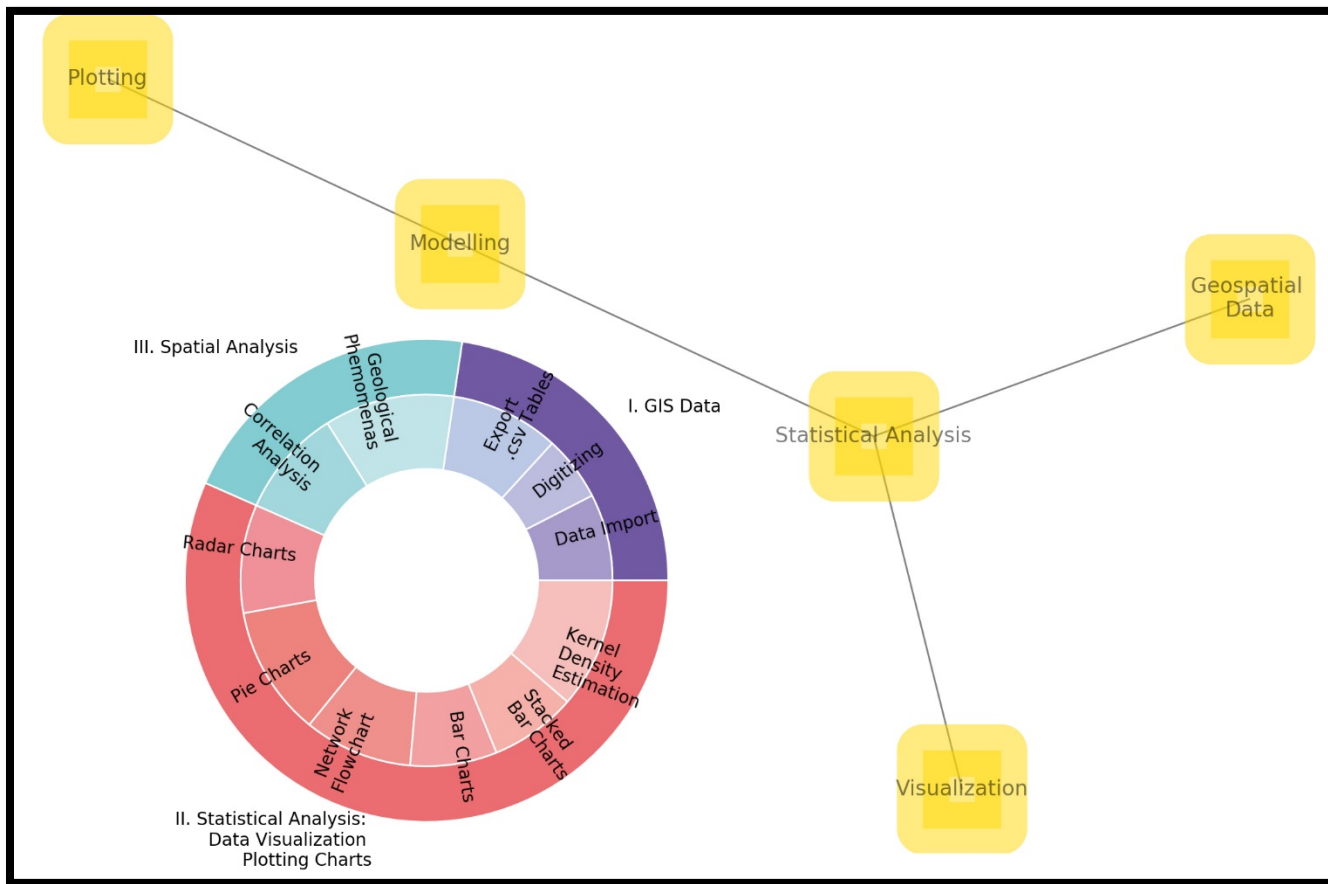
Figure 2. Methodological network

Various mathematical algorithms used in this work were applied from the statistical functionality provided by Python language (Beazley, 2009). The SciPy, an extension of NumPy, is another Python based package that was loaded for mathematical computations. The specific questions of usage SciPy were supported by large explanations of the SciPy principles and its usage in the statistical analysis (Jones et al., 2014).

Methodological Network

The methodological flowchart includes three main stages (Figure 2) visualized as the logical parts of this research: first, GIS part using Quantum GIS (QGIS), second, statistical analysis on Python language; third, spacial analysis of the data similarities on R language.

First block consisted in processing oceanographic data using QGIS software: data import, digitizing profiles, data export into .csv tables for further processing in Python and R. The cross-section profiles were digitized and the attribute tables were created (Figure 1). The tables contained numerical in-

formation on geology, tectonics, oceanography and bathymetry by observation points along each profile. In total there was 25 profiles, each containing 518 observation points. Hence, the total data intakes consisted in pool of 12,590 points.

Second block contained in data interpretation and statistical analysis. The steps include following approaches of the statistical data analysis: 1) Kernel Density Estimation (KDE) for analysis of the probability of data distribution; 2) stacked area chart for visualization of the data range across various segments of the trench; 3) spacial series of radar charts; 4) stacked bar plots showing the percentage of data distribution by tectonic plates; 5) stacked bar charts for correlation of sediment thickness by profiles, versus distance from the igneous volcanic areas; 6) circular pie plots visualizing data distribution by 25 profiles.

Third block presents the geospatial analysis of the data correlation. This implies correlation analysis of the scatterplot matrices by visualizing geological and tectonic interplay be-

tween the phenomenas. The scatterplot matrices for correlation analysis between marine geologic variables were performed using R language.

Probability of the Depths Distribution by Kernel Density Estimation Plots

In this part of the work, an implementation of the fundamental frequency estimation is presented. The algorithm of Kernel Density Estimation (KDE) is based on a frequency-domain approach (Figure 3). It was applied to visualize probability of the depth ranges and bathymetric patterns in various segments of the Mariana Trench. The method was implemented using the following code (Code 1):

Code (1), Python: Kernel Density Estimation, example for the subplot on Figure 3 (F).

```python
# step-1. Loading libraries
import seaborn as sns
from matplotlib import pyplot as plt
import pandas as pd
import os
os.chdir('/Users/pauline/Documents/Python')
df = pd.read_csv("Tab-Morph.csv")
sns.set_style('darkgrid')
# step-2. plotting 4 variables
ax=sns.kdeplot(df['Min'], shade=True, color="r")
ax=sns.kdeplot(df['Mean'], shade=True, color="#ffd900")
ax=sns.kdeplot(df['Max'], shade=True, color="b")
ax=sns.kdeplot(df['1stQ'], shade=True, color="#65318e")
ax=sns.kdeplot(df['3rdQ'], shade=True, color="#00a3af")
# step-3. Adding aesthetics and annotations
ax.set(xlabel='Depths, m', ylabel='KDE')
plt.title("Kernel Density Estimation: \nprobability of the statistical depth ranges, profiles 1-25")
ax.annotate('F', xy=(0.03, .90), xycoords="axes fraction", fontsize=18,
            bbox=dict(boxstyle='round, pad=0.3', fc='w', edgecolor='grey', linewidth=1, alpha=0.9))
plt.show()
```

Python libraries Pandas, Matplotlib, Seaborn and OS were used to process data by an embedded algorithms to obtain probability frequency. An open source Python code used for this plot is provided above (Code 1).

Visualizing Bathymetric Pattern by Stacked Area Charts

In marine geologic data sets, plotting stacked area charts is one of the key approaches to visualize the range of the bathymetric depths. In other words, we can answer the question of to what extent are the depths may reach in this or that particular segment of the trench? Apart from the visual clearance of the plot (Figure 4), showing the maximal abrupt depth by profiles 20 and 21 (that is, south-west of the Mariana Trench), there are other interesting particularities in this approach. Thus, on can investigate different phenomena of the oceanographic data sets by adding color ranges for stepwise visualization of the plot, sub-divided by statistical steps: minimal depths, third quartiles, mean depths, median values of the depths, first quartile, and finally, the shallowest parts of the geomorphology that is the minimal depths. In this way, one can understand the variability of the geo-morphic patters by the segments that could reveal new insights into how the bathymetric data variability affects the complex geomorphology of the profile.

Code (2) of Python: stacked area charts.

```python
# Step-1. Loading libraries
import pandas as pd
import numpy as np
import seaborn as sns
import matplotlib as mpl
import matplotlib.pyplot as plt
import matplotlib.ticker as ticker
import os
# Step-2. Importing data
os.chdir('/Users/pauline/Documents/Python')
df = pd.read_csv("Tab-Morph.csv")
df.head(5)
# Step-3. Plotting the dataset
fig = plt.figure(figsize=(8, 6))
df = pd.DataFrame(data=df, columns=['Min', '1stQ', 'Median', 'Mean', '1stQ','Max'])
ax = df.plot.area(stacked=False, alpha=0.8, colormap='PuBu_r')
# Step-4. Adding aesthetics and annotations
plt.legend(bbox_to_anchor=(1.05, 1), loc=2, borderaxespad=0.)
plt.title('Stacked area chart for the Mariana Trench bathymetry: \ndepths by 25 cross-section profiles', font-size=12, fontfamily='serif')
ax.set_xlabel('Bathymetric profiles')
ax.set_ylabel('Depths, m')
plt.xticks(np.arange(1, 26, step=1), rotation=30)
plt.show()
```

The following Python libraries were used to plot stacked area charts: Pandas, NumPy, Matplotlib, Seaborn and OS. An open source code is provided above (Code 2).
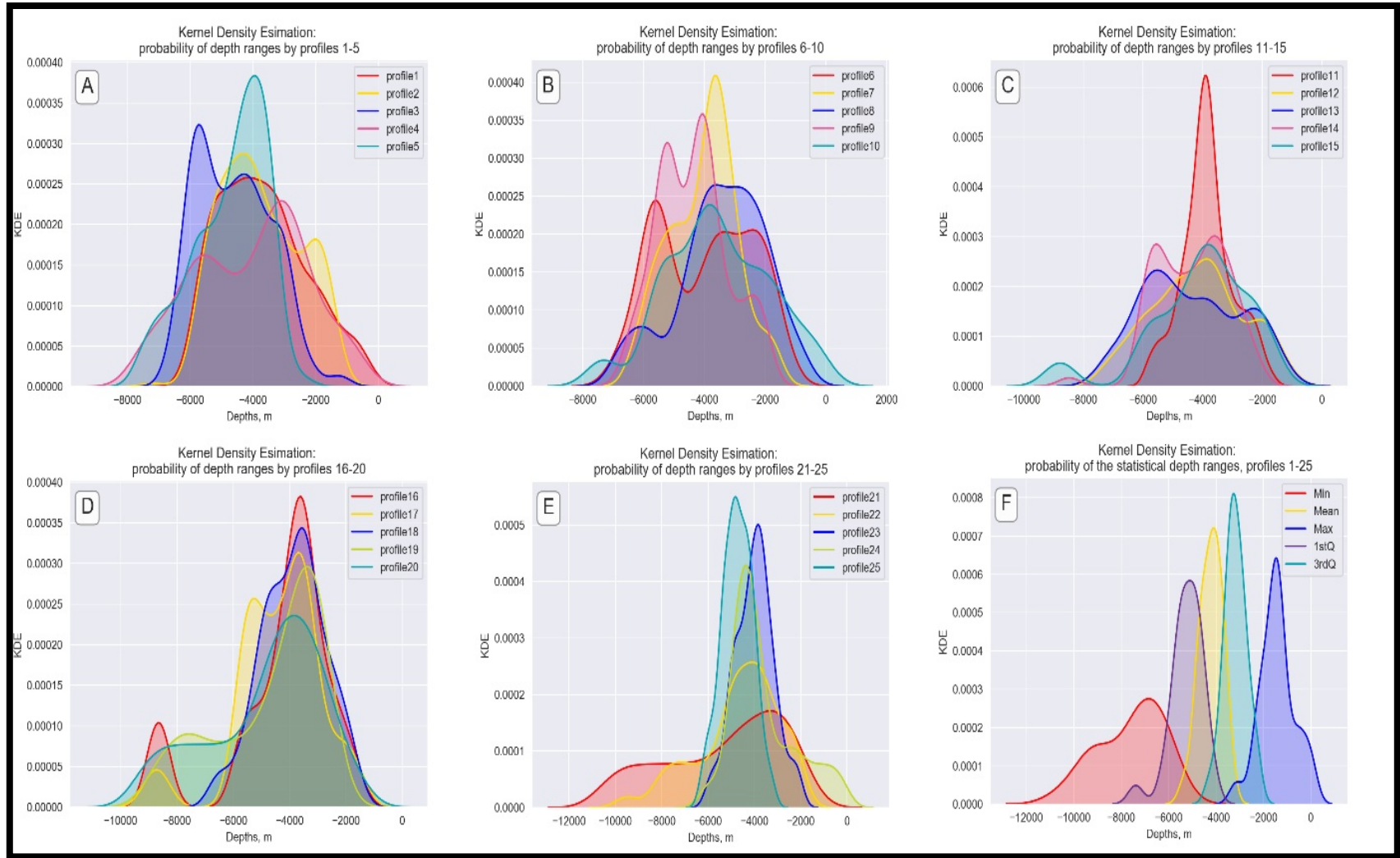
Figure 3. Kernel Density Estimation (KDE) for the bathymetry, profiles 1:25
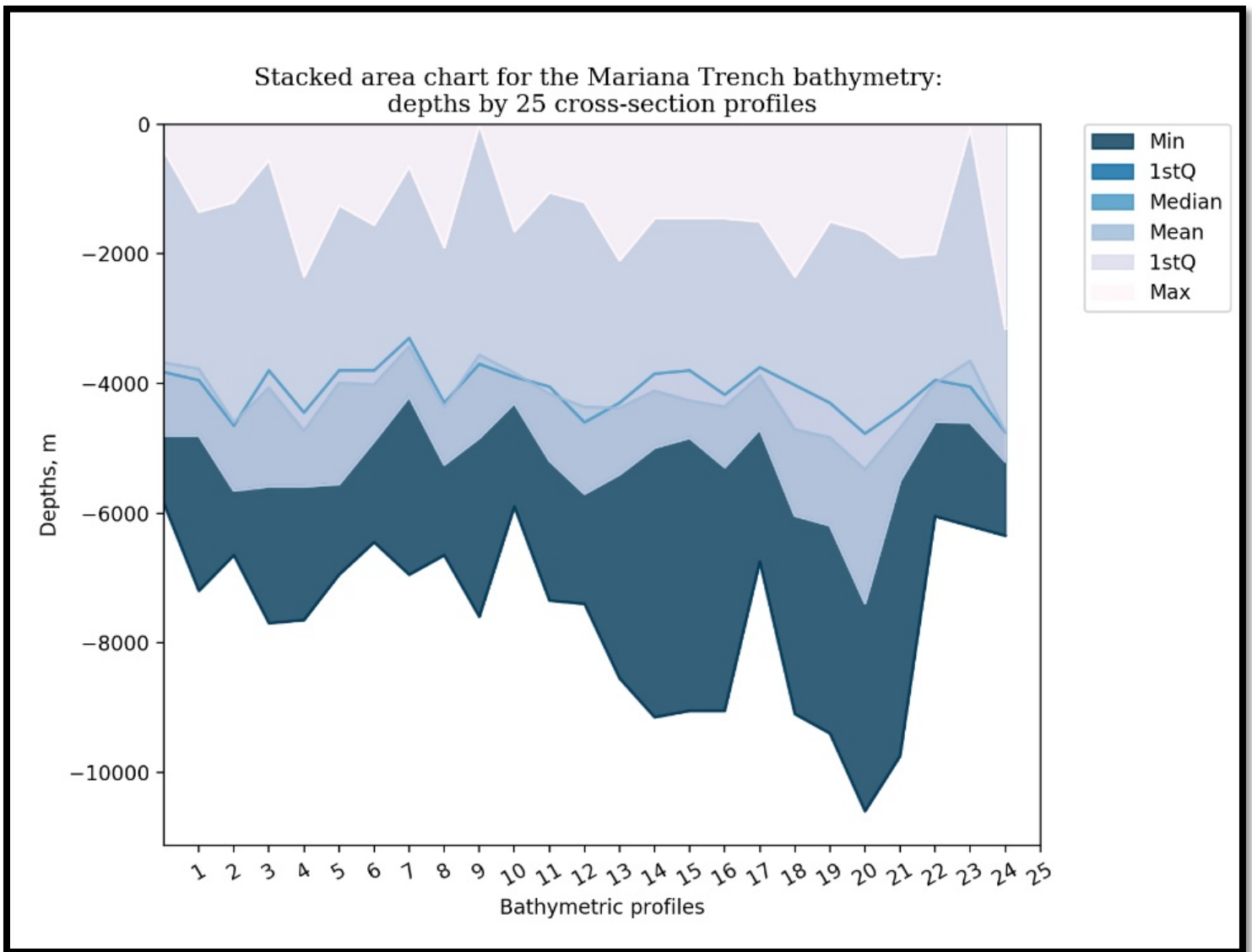
Figure 4. Mariana Trench: bathymetric patterns visualized by stacked area charts

Statistical Distribution of the Bathymetric Values by Radar Charts

Of particular interest is the case of radar charts. Recently, radar charts turned into a very interesting visualizing method in the data analysis. A radar chart is a graphical method of displaying multivariate data in the form of a two-dimensional circular chart of six quantitative variables represented on axes bathymetric depths and on the circular axes bathymetric values: maximal, 3rd quartile, median, mean 3rd quartile and minimal values.

The reason to choose the radar charts is that there are various statistical values that can be visualized by profiles, which requires a certain visualization technique for the facetted multi-plots (Figure 5). The series of the radar charts were plotted by libraries Math, Pandas, NumPy, Matplotlib, Seaborn and OS. An open source code is provided below (Code 3).

The algorithm for the radar charts was taken from the Matplotlib library of Python, well referenced by (Hunter, 2007).

Code (3) of Python, for Radar charts in 4 steps (a case study for profile Nr. 1):

Step-1. Loading libraries and data

```python
import matplotlib.pyplot as plt
import pandas as pd
from math import pi
import seaborn as sns
import numpy as np
import os
os.chdir('/Users/pauline/Documents/Python')
df = pd.read_csv("Tab-Morph.csv")
#df.head(5)
# Step-2.  Show 6 different variables on our radar chart, so take them out and set as a np.array.
labels=np.array(['Median', 'Max', '1stQ', '3rdQ', 'Min', 'Mean'])
stats=df.loc[1, labels].values
# Step-3. close the plot
angles=np.linspace(0, 2*np.pi, len(labels), endpoint=False)
stats=np.concatenate((stats,[stats[0]]))
angles=np.concatenate((angles,[angles[0]]))
# Step-4
fig = plt.figure()
ax = fig.add_subplot(111, polar=True)
ax.plot(angles, stats, 'o-', linewidth=2)
ax.fill(angles, stats, c='g',alpha=0.2)
ax.set_thetagrids(angles * 180/np.pi, labels)
plt.setp(ax.get_xticklabels(), fontsize=10)
plt.setp(ax.get_yticklabels(), fontsize=8)
plt.title('Radar chart for the Mariana Trench \nStatistics on bathymetric profile (nr.1)',
          fontsize=12, fontfamily='sans-serif')
ax.grid(True)
ax.annotate('(A)', fontsize=18, xy=(1.02, .90), xycoords="axes fraction")
plt.show()
```
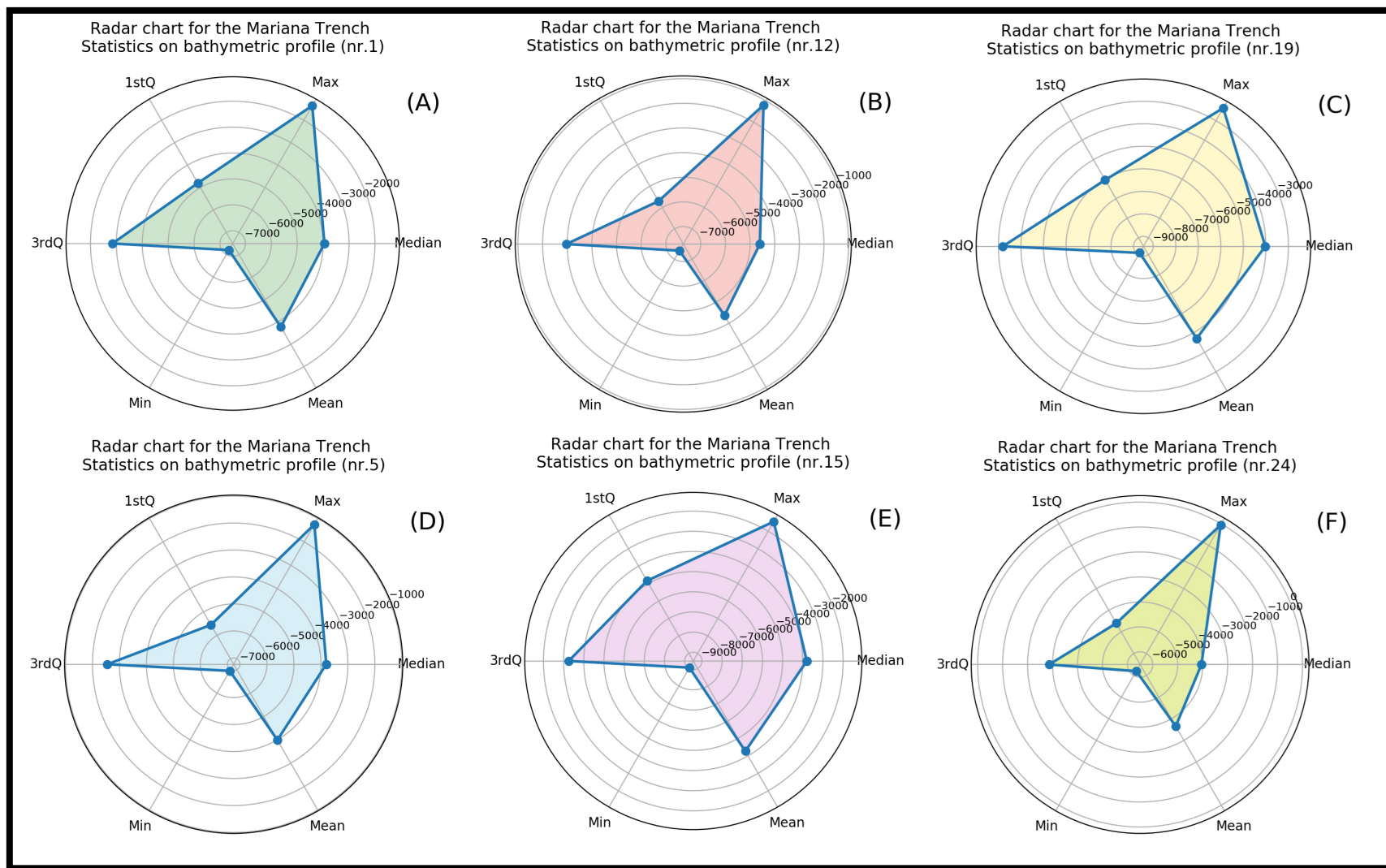
Figure 5. Series of the radar charts showing variation on the bathymetry by selected profiles

Variation in the Distribution of the Bathymetric Data by Stacked Bar Plots

Figure 6 shows the variation in the distribution of the bathymetric data by stacked bar plots

The following Python libraries were used to plot stacked area charts: NumPy, Pandas, Matplotlib and OS. An open source code is provided above (Code 4).

Code (4) of Python, for distribution of the bathymetric data by stacked bar plots:

```python
# Step-1. Loading libraries
import numpy as np
import matplotlib.pyplot as plt
from matplotlib import rc
import pandas as pd
import os
# Step-2. Importing data
os.chdir('/Users/pauline/Documents/Python')
df = pd.read_csv("Tab-Morph.csv")
# Step-3. Setting up values of each group
bars1 = df.plate_phill
bars2 = df.plate_pacif
bars3 = df.plate_maria
bars4 = df.plate_carol
# Step-4. Defining positions
profiles = df.profile
# Step-5. Selecting the names of the group
names = ["profile1", "profile2", "profile3", "profile4", "profile5",
        "profile6", "profile7","profile8", "profile9", "profile10",
        "profile11", "profile12", "profile13", "profile14", "profile15",
        "profile16", "profile17", "profile18", "profile19", "profile20",
        "profile21", "profile22", "profile23", "profile24", "profile25"]
barWidth = 1
# Step-6.Creating bars
ax = plt.subplot(111)
plt.bar(profiles, bars1, color='#dbd0e6', edgecolor='white', width=barWidth, label='Philippine Plate')
plt.bar(profiles, bars2, bottom=(bars1), color='#a0d8ef', edgecolor='white', width=barWidth,
        label='Pacific Plate')
plt.bar(profiles, bars3, bottom=(bars1 + bars2), color='#eebbcb', edgecolor='white', width=barWidth,
        label='Mariana Plate')
plt.bar(profiles, bars4, bottom=(bars1 + bars2 + bars3), color='#c1d8ac', edgecolor='white', width=barWidth,
        label='Caroline Plate')
# Step-7. Adding aesthetics
plt.xticks(profiles, names, fontweight='normal', fontsize=7, rotation=30)
plt.legend()
ax.legend(loc='upper center', bbox_to_anchor=(0.5, -0.10), shadow=True,
        markerscale=2, ncol=4, fontsize=6, title=False)
plt.title('Mariana Trench: Stacked barplots for the distribution \nof the bathymetric observations across tectonic
plates',
        fontsize=10, fontfamily='sans-serif')
plt.show()
```
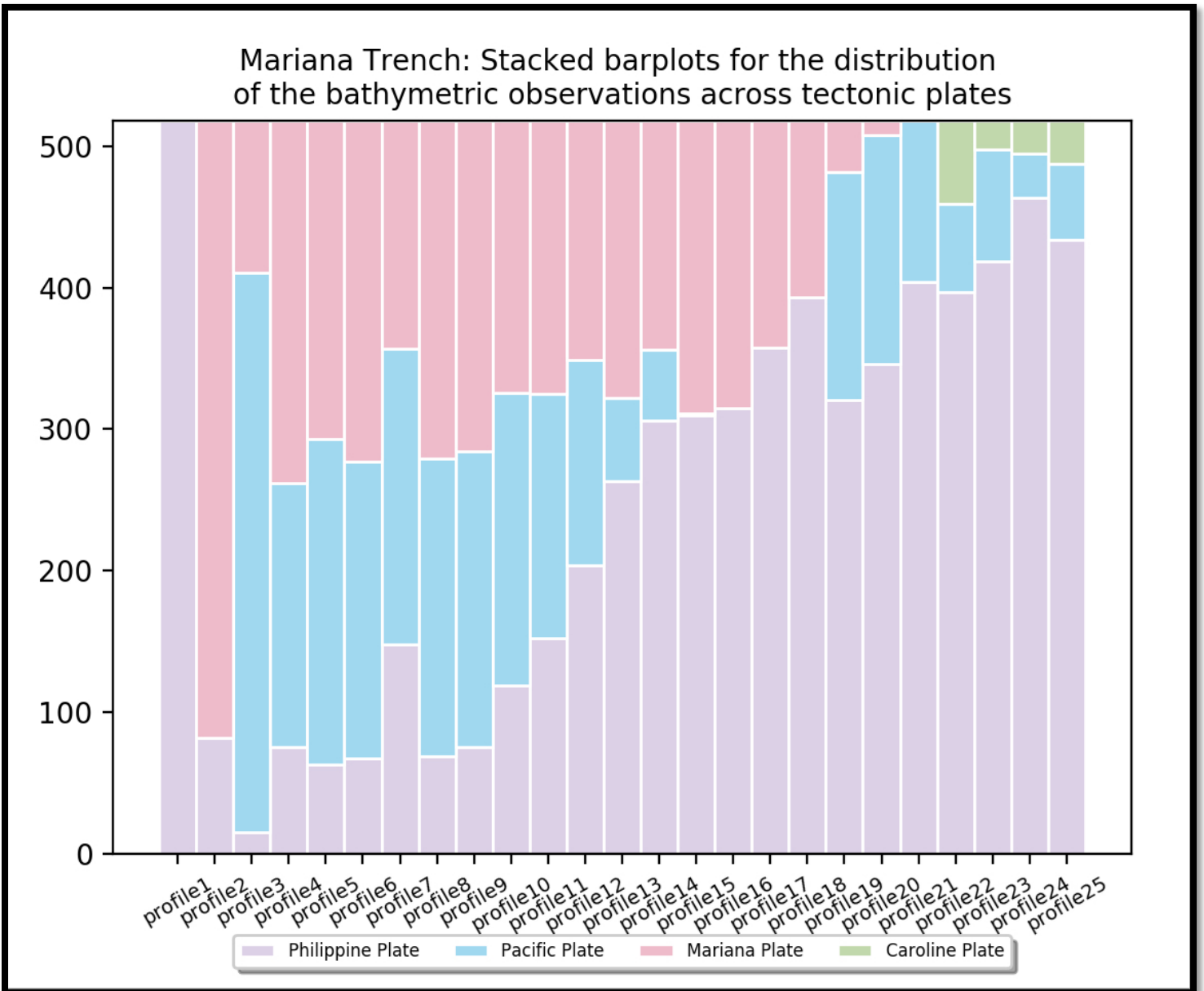
Figure 6. Stacked bar plots showing variation in the distribution of the bathymetric observations by the profiles, Mariana Trench

Analyzing Distribution of the Sediment Thickness by Stacked Bar Charts

Analysis of the distribution of the sediment thickness is visualized by the by stacked bar charts (Figure 7). The Python Code (5) in 7 steps provides an approach to visualize the sediment thickness by profiles and its correlation with closeness of the igneous volcanic areas as by distance. The code was written using calling following Python libraries: NumPy, Matplotlib, Pandas and OS.
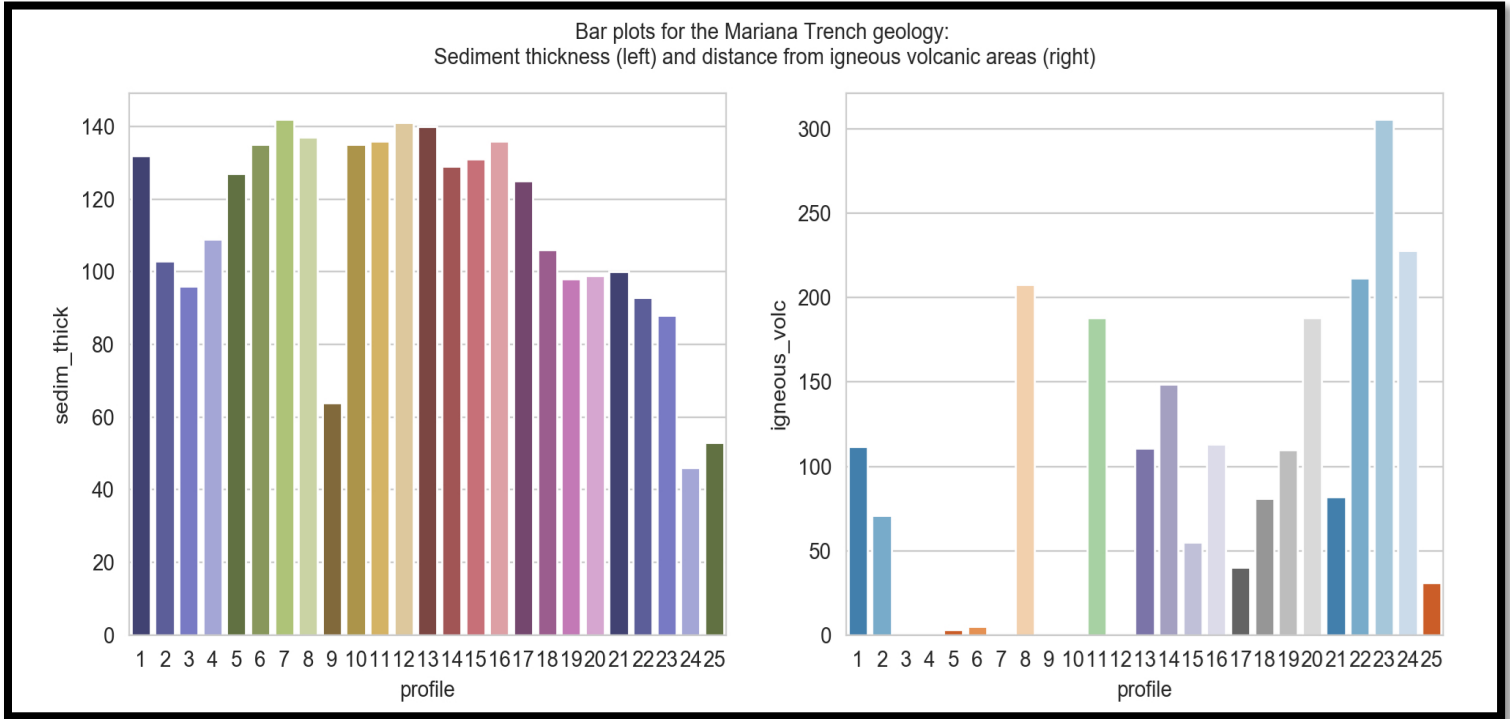
Figure 7.   Stacked bar charts showing distribution of values of sediment thickness by profiles (left), versus distance from the igneous volcanic areas (right), Mariana Trench.

Code (5) of Python, for analysis of sediment thickness distribution, stacked bar charts:

```python
# Step-1. Loading libraries
import numpy as np

import matplotlib.pyplot as plt

from matplotlib import rc

import pandas as pd

import os

# Step-2. Importing aata

os.chdir('/Users/pauline/Documents/Python')

df = pd.read_csv("Tab-Morph.csv")

# Step-3. Defining values for each group

bars1 = df.plate_phill

bars2 = df.plate_pacif

bars3 = df.plate_maria

bars4 = df.plate_carol
```

```
# Step-4. Setting up position of the bars on the x-axis
profiles = df.profile
# Step-5. Selecting the names of the groups and bar width
names = ["profile1", "profile2", "profile3", "profile4", "profile5",
        "profile6", "profile7","profile8", "profile9", "profile10",
        "profile11", "profile12", "profile13", "profile14", "profile15",
        "profile16", "profile17", "profile18", "profile19", "profile20",
        "profile21", "profile22", "profile23", "profile24", "profile25"]
barWidth = 1
# Step-6. Plotting bars
ax = plt.subplot(111)
plt.bar(profiles, bars1, color='#dbd0e6', edgecolor='white', width=barWidth, label='Philippine Plate')
plt.bar(profiles, bars2, bottom=(bars1), color='#a0d8ef', edgecolor='white', width=barWidth,
        label='Pacific Plate')
plt.bar(profiles, bars3, bottom=(bars1 + bars2), color='#eebbcb', edgecolor='white', width=barWidth,
        label='Mariana Plate')
plt.bar(profiles, bars4, bottom=(bars1 + bars2 + bars3), color='#c1d8ac', edgecolor='white', width=barWidth,
        label='Caroline Plate')
# Step-7. Customizing aesthetics
plt.xticks(profiles, names, fontweight='normal', fontsize=7, rotation=30)
plt.legend()
ax.legend(loc='upper center', bbox_to_anchor=(0.5, -0.10), shadow=True,
          markerscale=2, ncol=4, fontsize=6, title=False)
plt.title('Mariana Trench: Stacked barplots for the distribution \nof the bathymetric observations across tectonic
plates',
          fontsize=10, fontfamily='sans-serif')
plt.show()
```

Circular Visualization of the Bathymetry Versus Tectonic Plates by Pie Charts

Regarding the categorial distribution methods, a pie chart plotting is based on the analysis of the bathymetric distribution of the values by four tectonic plates (Figure 8). Circular visualization of the bathymetry showing the relationship between tectonic plates and distribution of bathymetric data by pie charts was performed by Code (6) in 3 steps. It used the following Python libraries: Pandas, NumPy, Matplotlib and OS.

Code (6) of Python, for visualizing bathymetry versus tectonic plates by pie charts:

```
# Step-1. Loading libraries
import pandas as pd
import numpy as np
from matplotlib import pyplot as plt
import os
os.chdir('/Users/pauline/Documents/Python')
dfM = pd.read_csv("Tab-Morph.csv")
# Step-2. Importing dataset
```

```
df = pd.DataFrame({'Pacific Plate':dfM.plate_pacif,
                   'Philippine Plate':dfM.plate_phill,
                   'Mariana Plate':dfM.plate_maria,
                   'Caroline Plate':dfM.plate_carol},
                 index=dfM.profile)
# Step-3. Plotting chart
df.plot(kind='pie', subplots=True, figsize=(10, 10),  legend=False, table=False,
        fontsize=8, sort_columns=True, layout=(2, 2), colormap='tab20b',
        title='Mariana Trench: Pie Charts for the \nBathymetry distribution by tectonic plates')
plt.show()
```


Figure 8. Circular visualization of the data distribution: bathymetric observation points by tectonic plates. Visualization method: pie charts

Figure 9. Scatterplot matrices showing correlation between environmental factors

Scatterplot Matrices of the Data Correlation: Geomorphology of the Mariana Trench

In general, the algorithms of the plotting scatterplot matrices consist of taking the values of the variables to show correlation of their values with others across the range of the data set. It is expected to show similarity at diagonal view, with increasing dissimilarity as the differences in the geologic and tectonic values increases. Scatterplot matrices have the following correlation characteristic (Figure 9): the correlation function shows similarities between the characteristics of the four tectonic plates: Philippine, Mariana, Caroline and Pacific. When the time bathymetric values increases (Figure 9, right center), the correlation with sediment thickness increases to a maximum (Figure 9, right low).

As the observation points change their position from plates by 518 observation points, the correlation again increases back to a maximum, because the characteristics of the geology change by geographic location.

The colors stand for the following variables: green for Philippine Plate, purple triangle – for Mariana Plate, red square for Caroline Plate, and orange – for Pacific Plate. The notable peak in the correlation between the magmatism of the close igneous volcanic areas and slope angle degree indicates the dependencies between the geomorphology and tectonic properties. The method of the scatterplot matrices shows appropriate visualization for the large data set overstepping thousands of the observation points. The scatterplot matrices were plotted using functionality of R language (R Core Team, 2014).

Visualized Concept of the Mariana Trench Project

Fundamental principle of the usage of Python libraries in oceanography is still a novel topic There are many approaches to analyze big data sets in marine science, and many of them are based on the use of GIS in various contexts: e.g. marine biology, bathymetric mapping, navigation, marine geology for exploration, etc. The difficulty of the current research lies in the attempt to perform a multidisciplinary approach that combine Python coding using its various libraries with traditionally geoscience domain of marine geology. Moreover, most of the current GIS tools do not include the power functionality of Python for the statistical analysis of the large data sets in full. Certain plugins do not able to perform a Python-level data analysis with the same effectiveness and visualization.

In addition, Python powerful libraries, such as NumPy, SciPy, as well as their dependencies such as Matplotlib, developed for a particular application in the IT domain, such as computer data analysis or data science 'pure', can effectively

be applied in the domain of the marine geology. An example of a programming tool in open source code provided in this research has a main focus of the analysis of the submarine geomorphology and factors affecting its structure and variability across various segments of the hadal trench, rather than the analysis of the marine ecosystems. However, in view of the multidisciplinarity of the Python algorithms, the methods and codes demonstrated with a case study of the given data frame can effectively be applied in other aspects of the oceanographic data, including those focused on the marine biological analysis of the data taken from the cruise R/V observations.

The schematic view of the combination of various methods and key words, concepts and tools, are visualized as a word cloud (Figure 10).

Figure 10. Word cloud on the 'Mariana Trench' project.

Results and Discussion

This paper, has presented a new approach for processing oceanographic data in big data sets on marine geology. The Python language and its libraries adequately perform statistical analysis and represent visualized graphs. The research implemented the proposed statistical approach using SciPy, NumPy and Pandas libraries of Python and embedded algorithms. Applied methods of Python programming defines the variability in the local geomorphological structure of the Mariana Trench, Pacific Ocean. Spatial correlation between certain environmental variables, such as sediment thickness, slope angle degree of the profiles and the geospatial location of the segments of the trench were detected.

Moreover, using Python language in the marina geology domain provides an appropriate base for the geospatial analysis of the environmental factors that may affect the morphology of the trench in its distinct parts across the crescent: southwest, central and north-west. Finally, processing a large set of data consisting of 518 observation points in 25 profiles, respectively, gives a set of 12,590 bathymetric points with variable numeric values: geomorphic, geologic and tectonic, as well as geometric values (degree of angle slope steepness by profiles).

Conclusions

The novelty and perspectives of the proposed approach lies in its repeatability using provided codes. The proposed research methodology can guide similar research focused on the understanding marine geologic variables in other trenches, in the context of oceanographic studies and marine geologic spatial analysis. Six Python codes supported this research are provided in full in for repeatability of the methods in other case studies of the oceanography.

The Python scripts provided in this research are freely available for others and may be repeated in similar research for plotting graphs: e.g. KDE curves, radar charts, stacked area and bar plots, circular plots. All graphs in this research were made using Python, a free open source programming language, distributed from the official web site: **https://www.python.org/** A map on Figure 1 is done using open source software Quantum GIS: **https://www.qgis.org**.

Compliance with Ethical Standard

Conflict of interests: The authors declare that for this article they have no actual, potential or perceived conflict of interests.

References

Beazley, D.M. (2009). *Python essential reference*. Addison-Wesley Professional. Available at ***www.python.org*** (accessed 18.03.2019)

Bogdanov, I., Huaman, D., Thovert, J.-F, Pierre, G., Adler, P.M. (2011). Tectonic stresses seaward of an aseismic ridge Trench collision zone. A remote sensing approach on the Loyalty Islands, SW Pacific. *Tectonophysics,* 499, 77-91.

Hunter, J.D. (2007). Matplotlib: A 2D graphics environment. *Computing in Science & Engineering,* 9(3), 90-95.

Bogolepov, K. V., Chikov, B. M. *Geologiya dna okeanov (Geology of the ocean floor)*. Russian. Ed. by Saks, V. N., Fotiadi, E. E. Moscow: Nauka, 1976, 246.

Brune, S. (2016). *Plate Boundaries and Natural Hazards*. AGU Geophysical Monograph 219. ed. by Duarte, J. C. & Schellart, W. P. Sydney, Australia: AGU. Chap. Rifts and rifted margins: A review of geodynamic processes and natural hazards, 1-21.

Jones, E., Oliphant, T., Peterson, P. (2014). *SciPy: open source scientific tools for Python*. Available at www.scipy.org (accessed 23.03.2019)

NumPy community (2019). *NumPy Reference. Release 1.16.1*. 1372 p.

Contreras-Reyes, E., Carrizo, D. (2011). Control of high oceanic features and subduction channel on earthquake ruptures along the Chile-Peru subduction zone. *Physics of the Earth and Planetary Interiors* 186, 49-58.

Crameri, F. (2018). Geodynamic diagnostics, scientific visualisation and StagLab 3.0. Geoscientific Model Development, 11, 2541-2562.

Cui, W., Hu, Y., Guo, W., Pan, B., Wang, F. Reprint of a preliminary design of a movable laboratory for hadal trenches. *Methods in Oceanography,* 10(2014), 178-193.

Cui, W., X., Wu (2018). A Chinese strategy to construct a comprehensive investigation system for hadal trenches. *Deep-Sea Research Part II* 155, 27–33.

Dierssen, H.M., Theberge, A.E.J. (2014). Encyclopedia of Natural Resources. Taylor & Francis. Chap. Bathymetry: Features and Hypsography, 1–7. https://doi.org/10.1081/E-ENRW-120048589

Doglioni, C. (2009). Comment on 'The potential influence of subduction zone polarity on overriding plate deformation, trench migration and slab dip angle' by W.P. Schellart. *Tectonophysics,* 463, 208-213.

Dokht, R.M.H., Gu, Y.J., Sacchi, M.D. (2016). Waveform inversion of SS precursors: An investigation of the northwestern Pacific subduction zones and intraplate volcanoes in China. *Gondwana Research,* 40, 77-90.

Fernandez, M.O., Marques, A.C. (2018). Combining bathymetry, latitude, and phylogeny to understand the distribution of deep Atlantic hydroids (Cnidaria). *Deep-Sea Research Part I,* 133, 39-48.

Gorbatov, A., Fukao, Y., Widiyantoro, S., Gordeev, E. (2001). Seismic evidence for a mantle plume oceanwards of the Kamchatka Aleutian trench junction. *Geophysical Journal International,* 146, 282-288.

Hubble, T., Webster, J., Yu, P., Fletcher, M., Airey, D., Clarke, S., Mitchell, D., Voelker, D., Puga-Bernabeu, A., Howard, F., Gallagher, S., Martin, T. (2016). Submarine Mass Movements and their Consequences. Advances in Natural and Technological Hazards Research. ed. by G. Lamarche. Switzerland: Springer International Publishing. Chap. Chapter 12. Submarine Landslides and Incised Canyons of the Southeast Queensland Continental Margin, 125-134. https://doi.org/10. 1007/978-3-319-20979-1_12

Ikari, M.J., Kameda, J., Saffer, D.M., Kopf, A.J. (2015). Strength characteristics of Japan Trench borehole samples in the high-slip region of the 2011 Tohoku-Oki earthquake. *Earth and Planetary Science Letters,* 412, 35-41.

Jamieson, A.J. (2018). A contemporary perspective on hadal science. *Deep-Sea Research Part II,* 155, 4-10.

Kong, X., Li, S., Wang, Y., Suo, Y., Dai, L., Géli, L., Zhang, Y., Guo, L., Wang, P. (2017). Causes of earthquake spatial distribution beneath the Izu-Bonin-Mariana Arc. *Journal of Asian Earth Sciences*, 151, 90-100.

Lemoine, A., Madariaga, R., Campos, J. (2002). Slab-pull and slab-push earthquakes in the Mexican, Chilean and Peruvian subduction zones. *Physics of the Earth and Planetary Interiors,* 132, 157-175.

Litvin, V.M. (1987). *Morfostruktura dna okeanov (Morphostructure of the ocean floor)*. In Russian. Ed. by A. N. Lastochkin. Leningrad: Nedra. 275.

Loher, M., Marcon, Y., Pape, T., Römer, M., Wintersteller, P., Santos Ferreira, C. dos, Praeg, D., Torres, M., Sahling, H., Bohrmann, G. (2018). Seafloor sealing, doming, and collapse associated with gas seeps and authigenic carbonate structures at Venere mud volcano, Central Mediterranean. *Deep-Sea Research Part I,* 137, 76-96.

Luo, M., Algeo, T.J., Tong, H., Gieskes, J., Chen, L., Shi, X., Chen, D. (2018). More reducing bottom-water redox conditions during the Last Glacial Maximum in the southern Challenger Deep (Mariana Trench, western Pacific) driven by enhanced productivity. *DeepSea Research Part II,* 155, 70-82.

Mao, X., Zhang, B., Deng, H., Zou, Y., Chen, J. (2016). Three-dimensional morphological analysis method for geologic bodies and its parallel implementation. *Computers & Geosciences,* 96, 11-22.

Masson, D.G. (1991). Fault Patterns at Outer Trench Walls. *Marine Geophysical Researches,* 13, 209-225.

Oliphant, T.E. (2007). Python for scientific computing. *Computing in Science & Engineering* 9(3), 10-20.

Pedregosa, F., Varoquaux, G., Gramfort, A., Michel, V., Thirion, B., Grisel, O., Blondel, M., Prettenhofer, P., Weiss, R., Dubourg, V., Vanderplas, J., Passos, A., Cournapeau, D., Brucher, M., Perrot, M., Duchesnay, E. (2011). Scikit-Learn: machine learning in Python. *The Journal of Machine Learning Research,* 12, 2825-2830.

Perez, F., Granger, B.E. (2007). IPython: a system for interactive scientific computing. *Computing in Science & Engineering* 9(3), 21-29.

R Core Team. (2014). R: a language and environment for statistical computing. Vienna. Available at http://www.R-project.org (accessed 14.12.2018)

Review Article

MODELLING THE PROGRESS AND EFFECTS OF EUTROPHICATION IN INLAND AND COASTAL WATERS

Ali Ertürk

Istanbul University Faculty of Aquatic Sciences, Ordu Caddesi No:8 Laleli Fatih, Istanbul-Turkey

ORCID IDs of the authors:

A.E. 0000-0002-3532-2961

Correspondence:

Ali ERTÜRK

E-mail: erturkali@istanbul.edu.tr

ABSTRACT

The aim of this paper is to give a detailed overview on the predictive-model building/coding techniques for simulating the progress and effects of eutrophication based on differently detailed model structures. First; historical development of predictive eutrophication modelling is reviewed. Then, a generic transport model that can be coupled with any eutrophication kinetics is described. In the following sections, ecological sub models based on eutrophication kinetics and food-web are described along with the bottom-up approach based linkage of nutrient kinetics, primary production and transfer of food to higher trophic levels are demonstrated together with an example case study based on previous studies. Finally, the paper is supported by two comprehensive appendices, one that guides the interested readers how to develop a simple eutrophication modelling tool from starch and another to that summarizes an example hydrodynamic model development for forcing the flow fields in the transport model described in this paper.

Keywords: Eutrophication, Model building, Ecological modelling, Water quality

Introduction

Mathematical models are theoretical constructs, together with assignment of numerical values to model parameters, incorporating some prior observation and data from field and/or laboratory and relating external inputs and forcing functions to system variable responses. Models can be defined as idealized formulations that represent the response of a physical system to external forcing. The cause-effect relationship between loading and concentration depends on the physical, chemical, and biological characteristics of the receiving water. In environmental science, ecological models are used to evaluate the potential impacts of external forcing factors and to understand the functioning of the system (Thomann and Mueller, 1987; Chapra, 1997; Arhonditsis and Brett, 2004). They are useful tools to get a holistic picture of ecosystems, fill in the gaps in field data or forecast the systems responses to different external forcings. Models can produce many instantaneous pictures of the ecosystem by spatially and temporally interpolation between monitoring data points, allow testing of hypotheses on how the ecosystem is functioning, forecast the ecosystem behaviour and give relatively fast answers to scientists, engineers and managers

Predictive Eutrophication Analysis Models

Historically, aquatic ecological modelling studies were initiated with simple models of nutrient cycles in fresh water ecosystem in late 1960s and early 1970s, when the focus on dissolved oxygen deficiency as the main environmental problem in aquatic ecosystems was shifted to the problems caused by excess nutrient inputs into aquatic ecosystems. The first models were relatively simple consisting only of simple nutrient balances (such as the ones shown in Equation 1) with assumptions such as completely mixed system, steady state conditions, representing a seasonal or annual average prevail, limiting nutrient being phosphorus only where total phosphorus is used as a measure of trophic status. An example of such models is given in Equation 1 and Equation 2,

$$V\frac{dP}{dt} = W - v_S A_S P - Q_{OUT}P$$

(Equation 1)

where V is volume $[L^3]$, P is the total phosphorus concentration $[M \cdot L^{-3}]$ Q_{OUT} is the outflow $[L^3 \cdot T^{-1}]$, A_S is the surface area $[L^{-2}]$, v_S is the settling velocity $[L \cdot T^{-1}]$ and W is the external sources for phosphorus $[M \cdot T^{-1}]$. Most of the analyses were done for steady state; hence, equations such as Equation 2 were used instead of Equation 1

$$P = \frac{W}{Q_{OUT} + v_S A_S}$$

(Equation 2)

Another type of simple models used in those years were empirical models that were derived by various researchers using curve fitting techniques, such as the ones listed below (N : Total nitrogen $[\mu g.l^{-1}]$, P : Total phosphorus $[\mu g \cdot L^{-1}]$, chl-A : Chlorophyll-A $[\mu g \cdot L^{-1}]$):

- Dillon and Rigler (1974)

$$\log(\text{chl - A}) = 1.449\log(P) - 1.136$$

(Equation 3)

- Bartsch and Gakstatter (1978)

$$\log(\text{chl - A}) = 0.807\log(P) - 0.194$$

(Equation 4)

- Rast and Lee (1978)

$$\log(\text{chl - A}) = 0.76\log(P) - 0.259$$

(Equation 5)

- Smith and Shapiro (1981)

$$\log(\text{chl - A}) = 1.55\log(P) - \log_{10}\left[\frac{6.404}{0.0204(N/P) + 0.334}\right]$$

(Equation 6)

where log and log10 are the natural and general algorithms respectively.

The trend considering the eutrophication environmental problem based on as lasted until 1980's. Therefore, extensive research was initiated on nutrients in aquatic ecosystems (O'Connor et al., 1968; Bloesch et al., 1977; Edmonson, 1979). Incorporation of nutrient cycles into water quality models necessitated introduction of new state variables such as Org-N, NH_4^+-N, NO_3^--N, Org-P, $PO4^{3-}$-P, phytoplankton biomass, etc. and chemical/biochemical processes. In other words, more complex models than were needed. Developments in the computer technology enabled scientists and engineers to design and develop these models. Models developed and used by Di Toro et al. (1971); Thomann et al. (1975) and Di Toro and Connolly (1980) are examples of such models. These models did not consider the aquatic ecosystem as fully mixed anymore. They were the first examples of box models and are considered as predecessors of modern nutrient dynamics modelling tools described in the following paragraphs.

WQRRS (Water Quality for River and Reservoir Systems)**,** is a one dimensional dynamic model which calculates the temporal variations of state variables in vertical dimension (z). WQRRS was developed by the United States Army Corps of Engineers (USACE), Hydraulic Engineering Centre (HEC, 1978). The model is designed to simulate nutrient dynamics in river and reservoir systems however state variables covered in the WQRRS make it also useful for ecological modelling in other aquatic ecosystems. Nutrients, phytoplankton, zooplankton, fish, and benthic organisms can be simulated by the model. CE-QUAL-R1 (Environmental Laboratory, 1995) is derived from this model can also simulate the sulphur cycle, iron and manganese under aerobic and anaerobic conditions.

Water Quality Analysis Simulation Program (WASP) (Di Toro et al., 1983; Ambrose et al., 1993; Wool et al., 2001) was developed by United States Environmental Protection Agency (USEPA). WASP covers transportation dynamics of advection-dispersion and suspended sediment transport. The model describes six transport fields; water column, water in sediment blanks, user defined settling and resuspension velocities in water for three sediment groups, and transportation due to precipitation and evaporation. WASP is a box model it is possible to generate 0, 1, 2, and 3 dimensional model networks depending on the number and topology of the boxes. Several hydrodynamic modelling software such as DYNHYD5, RIVMOD (Hosseinipour et al., 1990), SED3D (Sheng et al, 1991), and EFDC (Hamrick, 1996) can produce outputs, which can be used by WASP through external hydrodynamic linkage.

CE-QUAL-W2 (Cole and Wells, 2006) is a two-dimensional model which does both hydrodynamic and water quality simulations in longitudinal and vertical dimensions (x, z). State variables constituted in the model are temperature, salinity, dissolved oxygen, CBOD, organic material composed of carbon, nitrogen, and phosphorus (dissolved and labile, dissolved and refractory, particulate and labile, particulate and refractory), ammonia nitrogen, nitrate nitrogen, phosphorus, dissolved and particulate silica, and unlimited number of phytoplankton, zooplankton, epiphyte and rooted aquatic macrophyte groups.

CE-QUAL-ICM (Cerco and Cole, 1994; Cerco and Cole, 1995) is capable of simulating sediment processes in detail. However, it only includes water quality codes and to run the model output codes of CH3D hydrodynamic model, which is also developed by USACE, is necessary. Together with the

CH3D, CE-QUAL-ICM can make water quality simulations in three spatial dimensions. This model is also known as the Chesapeake Bay model. Chesapeake Bay (United States of America) was modelled intensively from 80's up today. Many ecological modelling studies conducted for the Chesapeake Bay (Di Toro and Fitzpatrick, 1993; USACE, 2000; Schaffner, et al., 2002; Xu, 2005; Galgeos et al., 2006) contributed to the ecological modelling science and the literature. These models did not only consider pelagic nutrient cycles and primary production but also benthic fluxes, zooplankton and filtrating organisms.

COHERENCE (Luyten et al., 1999) is a three dimensional hydrodynamic ecological model which was developed by the Management Unit of the Mathematical Models of the North Sea (MUMM) to use it in North Sea. ERSEM (European Regional Seas Ecosystem Model) (Paetsch, 2001) is developed by European Union for applications in North Sea. It is an advanced model including detailed description of pelagic and benthic dynamics.

In mid 70's another branch of ecological modelling was initiated. First examples of food web models that are designed to mimicking the trophic networks (Jansson, 1974; Jansson, et al., 1982; Polovina, 1984a; Polovina, 1984b) were used for research purposes. Unlike the most of the biogeochemical or nutrient dynamics models, which consider the nutrient cycles and primary production more detailed, trophic network models use relatively simplified approaches to consider them, or they accept them as model input rather than state variables. Trophic network models are equipped with algorithms for dealing with higher trophic levels and balancing the energy and matter in a user defined trophic network. Organisms in higher trophic levels such as fishes and macro invertebrates are good environmental indicators to track environmental health and ecological changes as adaptive response to stress, especially in estuaries and lagoons (USEPA, 2000; Villanueva, et al. 2006) and therefore food network models that can simulate these organisms are valuable tools for ecological assessment of those ecosystems. These models have been applied to transitional aquatic ecosystem such as coastal lagoons (Hull, et al., 2000; Gamito and Erzini, 2005; Villanueva, et al. 2006).

Coupling the nutrient dynamics and trophic network models provides the opportunity to benefit from the advantages of both frameworks. This topic was discussed by Mergey, et al.

(2001) and the Royal Comission on Environmental Pollution (2004). Tillmann et al. (2006) coupled CE-QUAL-ICM (Cerco and Cole, 1994) with EwE (Christensen, et al. 2005) and applied the coupled models to the Cheasepeake Bay.

Development of these models took years of study and research efforts. Appendix-A gives an insight to the reader by illustrating how a simple eutrophication model could be developed from scratch.

Modelling of Transport for Inland and Coastal Waterbodies

Some aquatic ecosystems are either too large in lateral dimensions or too deep so that they should not be considered as completely mixed. If this is the case, a model, which assumes that the ecosystem is completely mixed (such as the simple eutrophication model discusses in the previous section) should not be applied directly. For partly mixed aquatic ecosystem, the advection-dispersion-reaction equation given below should be applied.

$$\frac{\partial C}{\partial t} = -u \cdot \frac{\partial C}{\partial x} + D_x \cdot \frac{\partial^2 C}{\partial x^2} - v \cdot \frac{\partial C}{\partial y} + D_y \cdot \frac{\partial^2 C}{\partial y^2} - w \cdot \frac{\partial C}{\partial z} + D_z \cdot \frac{\partial^2 C}{\partial z^2}$$
$$+ \sum k \cdot C - \upsilon_{sedimentation} \cdot \frac{\partial C}{\partial z} \pm \text{external sources and sinks}$$

(Equation 7)

The terms used in Equation 7 are given below

x, y, z : Spatial coordinates [L]

u, v, w : Flow velocities in x, y, z directions respectively [$L \cdot T^{-1}$]

Dx, Dy, Dz : Dispersion coefficients in x, y, z directions respectively [$L^2 \cdot T^{-1}$]

C : Concentration [$M \cdot L^{-3}$]

$\sum k \cdot C$: Reaction kinetics partial derivative [$M \cdot L^{-3} \cdot T^{-1}$]

Figure 1 provides a detailed description of the advection-dispersion-reaction equation. The reaction kinetics partial derivative corresponds to the content of the kinetic function in the example model described in the next section. All the biogeochemical and ecological interactions to be modelled are written into this partial derivative. Some model variables such as phytoplankton or detritus can settle. This is handled by the

partial derivative of settling. External sources and sinks are important to represent the effect of point and non-point sources of loads. The velocities u, v and w can be calculated using a hydrodynamic model. An example hydrodynamic model is given in Appendix B.
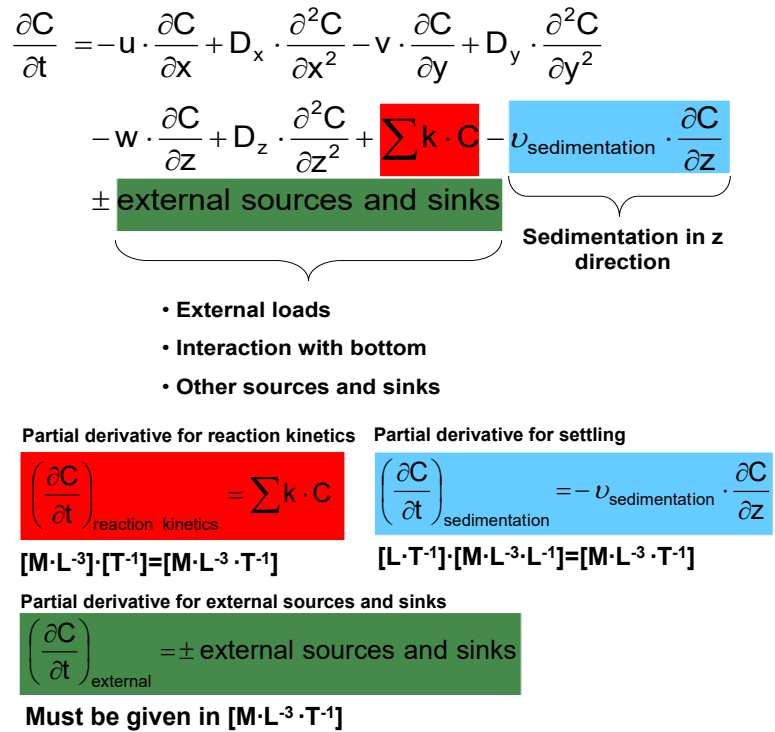
Figure 1. The advection-dispersion-reaction equation

Ecological Sub-Models for Prediction of the Progress and Effects of Eutrophication

Eutrophication is a complicated process that includes many ecological components and processes in addition to nutrients and primary production. A model designed for detailed and realistic eutrophication analysis should contain those components and processes. The model developed in Appendix A would be too simplified for such eutrophication analyses. Spatial variability and more advanced representation of transport processes should be incorporated into such a model as well. This section aims to instruct the reader how to construct this type of eutrophication models.

Development of Biogeochemical Cycle Sub-Models for Eutrophication Analyses

Biogeochemical cycle sub-models simulate processes that run among the biotic and abiotic components of the ecosystem.

These sub-models could be as simple incorporating free nutrients (N, P compounds), organic matter and nutrients bound to it and a single group of phytoplankton or as complicated as incorporating more detailed representation of nutrients (N, P, Si compounds) other inorganic compounds (S, Fe, Mn with different ionic states), detailed representation of detritus, multiple groups of phytoplankton, multiple groups of zooplankton and fish, benthic organisms, sediment diagenesis, macrophytes, bacteria, etc. In this section, a biogeochemical submodel that is moderately complicated will be described. The model includes 22 state variables namely; NH4 and NO3 Nitrogen, PO4 Phosphorus, Available Silicon, Inorganic Carbon, Dissolved Oxygen, Diatoms, Cyanobacteria and Other Planktonic Algae Carbon, Zooplankton Carbon, External Labile Dissolved Org Carbon, External Labile Particulate Detritus Carbon, External Refractory Dissolved Organic Carbon, External Refractory Particulate Detritus Carbon, Diatoms based Dissolved Organic Carbon, Diatoms based Particulate Detritus Carbon, Other Planktonic Algae based Dissolved Organic Carbon, Other Planktonic Algae based Particulate Detritus Carbon, Cyanobacteria based Dissolved Organic Carbon, Cyanobacteria based Particulate Detritus Carbon, Zooplankton based Dissolved Organic Carbon and Zooplankton based Particulate Detritus Carbon.

A model with these state variables is classified as an NPZD (Nutrients Phytoplankton Zooplankton Detritus) model. The state variables and processes letting them interact with each other are illustrated in Figures 2 to 7. As seen in Figure 2, nitrogen is assumed to be in three main pools by the example NPZD model. The first of them is ammonia nitrogen, the second is the nitrate nitrogen and the third is nitrogen bound to molecules found in living (phytoplankton and zooplankton) and dead organic matter. Phosphorus is assumed to be in two main pools. The first of them is phosphate phosphorus and the second is phosphorus bound to molecules found in living (phytoplankton and zooplankton) and dead organic matter similar to nitrogen. Silicon is assumed to be in two main pools. The first of them is available silica silicon (dissolved inorganic silicon) and the second is silicon found with living (diatoms and zooplankton feeding on diatoms) and dead (diatoms and zooplankton based organic carbon and detritus) organic matter. As seen in Figure 3, Dissolved oxygen is dissolved oxygen is interacting with most of the other state variables in the example NPZD model. Carbon cycle is modelled extensively by the example NPZD model. External labile dissolved organic

carbon, external labile particulate detritus carbon, external refractory dissolved organic carbon and external refractory particulate detritus carbon are used to model the allochtonous organic carbon and detritus carbon. The autochthonous detritus carbon is simulated using other planktonic algae based dissolved organic carbon, other planktonic algae based particulate detritus, diatoms based dissolved organic carbon, diatoms based particulate detritus, cyanobacteria based dissolved organic carbon, cyanobacteria based particulate detritus, zooplankton based dissolved organic carbon and zooplankton based particulate detritus. Representation of inorganic carbon cycle is illustrated in Figure 2. Three phytoplankton groups (diatoms, cyanobacteria and other planktonic algae) and one zooplankton group (resembling total zooplankton) are simulated by the NPZD model. The equations and other details of the NPZD model would be too space consuming to give here. The reader is referred to Erturk (2008) and Erturk et al (2015) for more detailed information and complete set of equations. As seen in Figures 2 to 7, the example NPZD model is designed to keep track from the inorganic nutrients up to the zooplankton biomass and back to inorganic nutrients via detritus and its decomposition. Organically bound nutrients are coupled within the detritus cycle so that they are no separate state variables representing them. The model can be used to identify the contribution of each plankton group to autochthonous organic matter hence analyse the eutrophication process in detail.

Development of Foodweb Sub-Models

Trophic network is defined as a set of interconnected food chains, by which energy is materials circulate within an ecosystem. The classical food web can be divided into two broad categories: the grazing web, which starts with primary producers and ends at top predators and the detrital web which starts with detritus, continues over decomposers (bacteria, fungi, etc.) and detrivores and ends at their predators. Unlike the biogeochemical sub-models, the foodweb sub-models are usually more specific to the system for which they are developed. This is because, each system has a different combination of complex behaving organisms on the higher levels of the trophic network. Depending on the aim of model development, a group of organisms, a particular species or a development stage within a species can be state variables of a food web model. To construct a food-web model, two components are needed: The basic knowledge about the food-web of the

ecosystem for which the model is developed and the modelling tools. There are many tools for developing foodweb models.
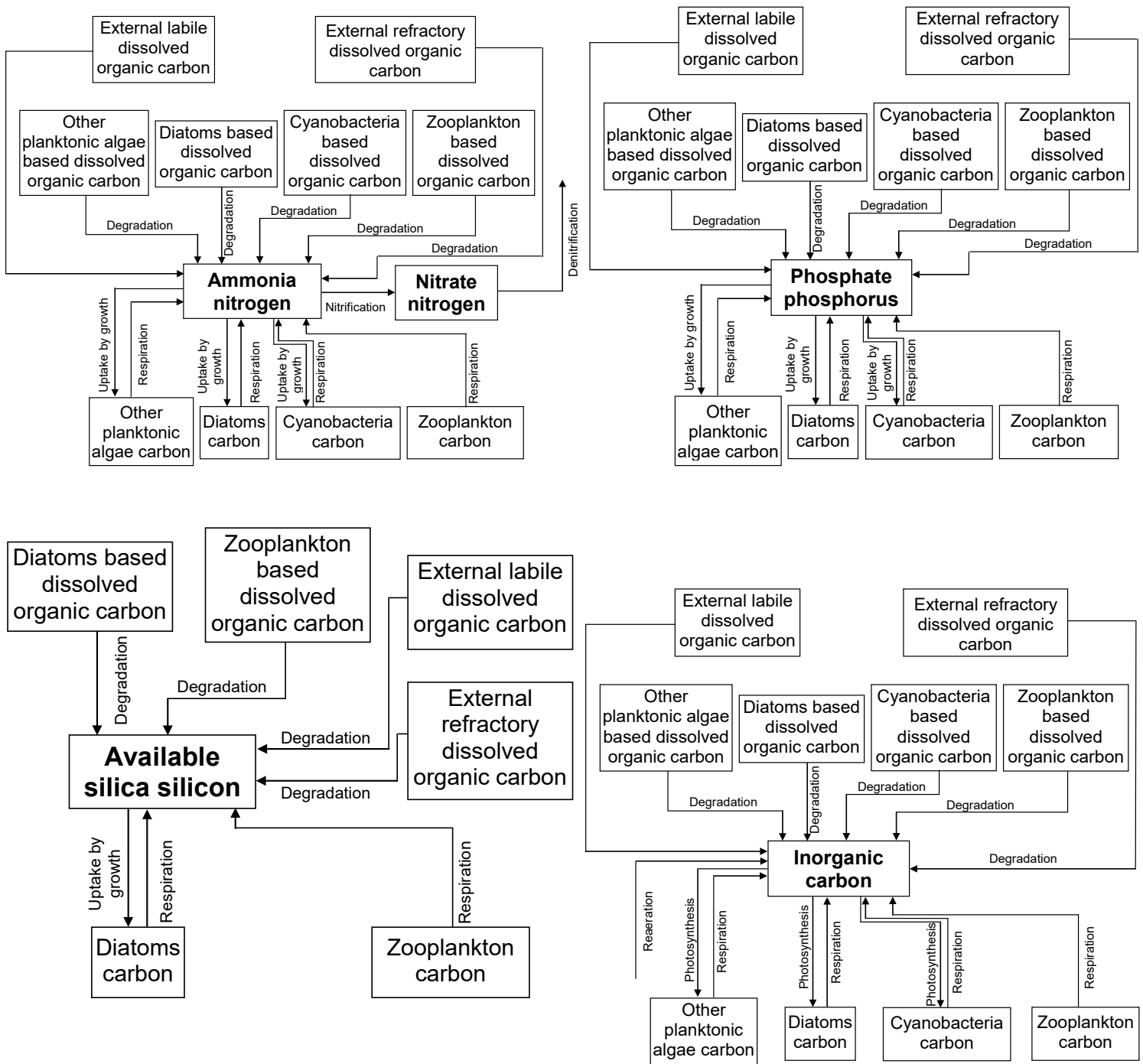
Figure 2. Nutrient cycles in the NPZD model
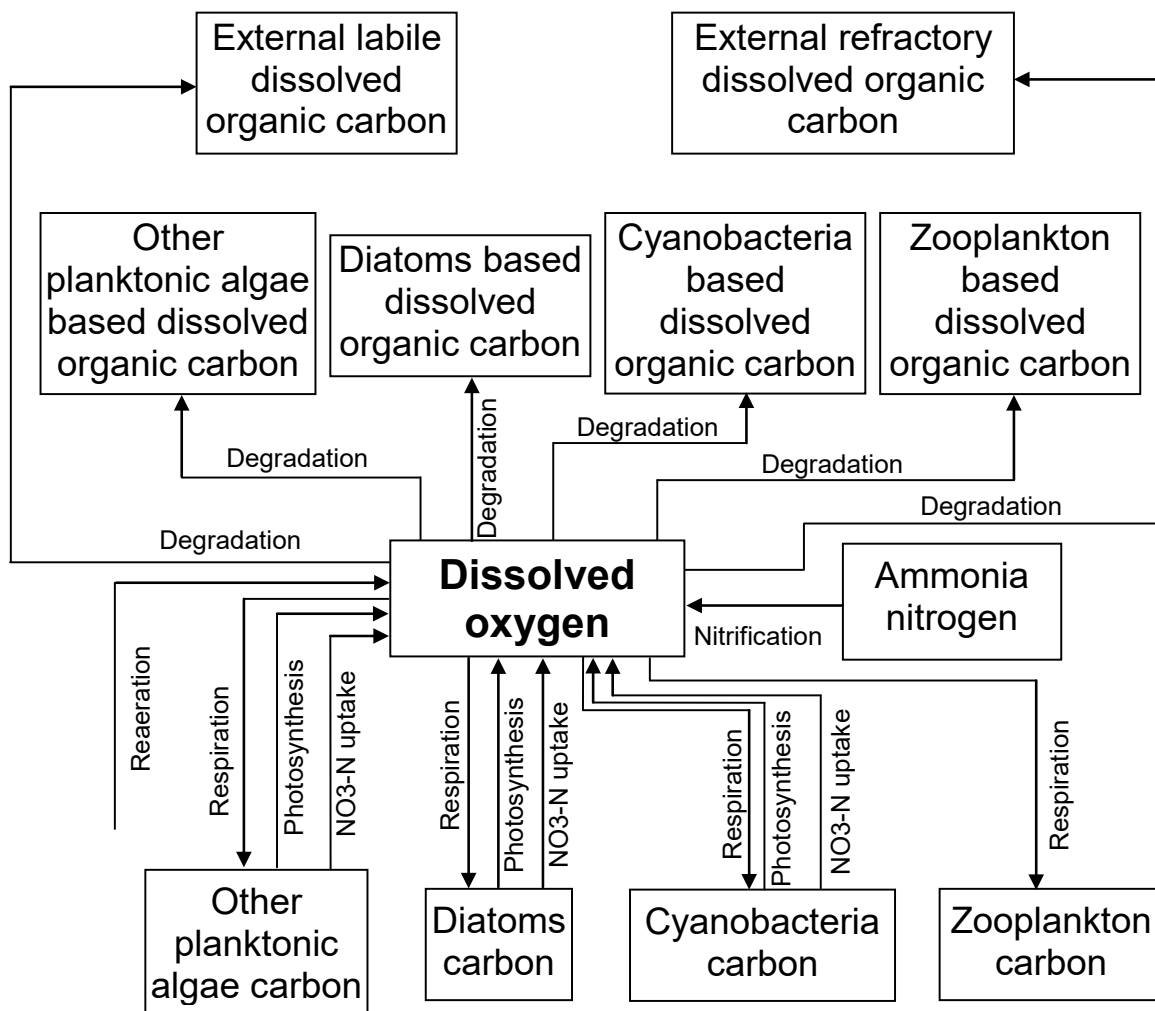
Figure 3. Dissolved oxygen cycle
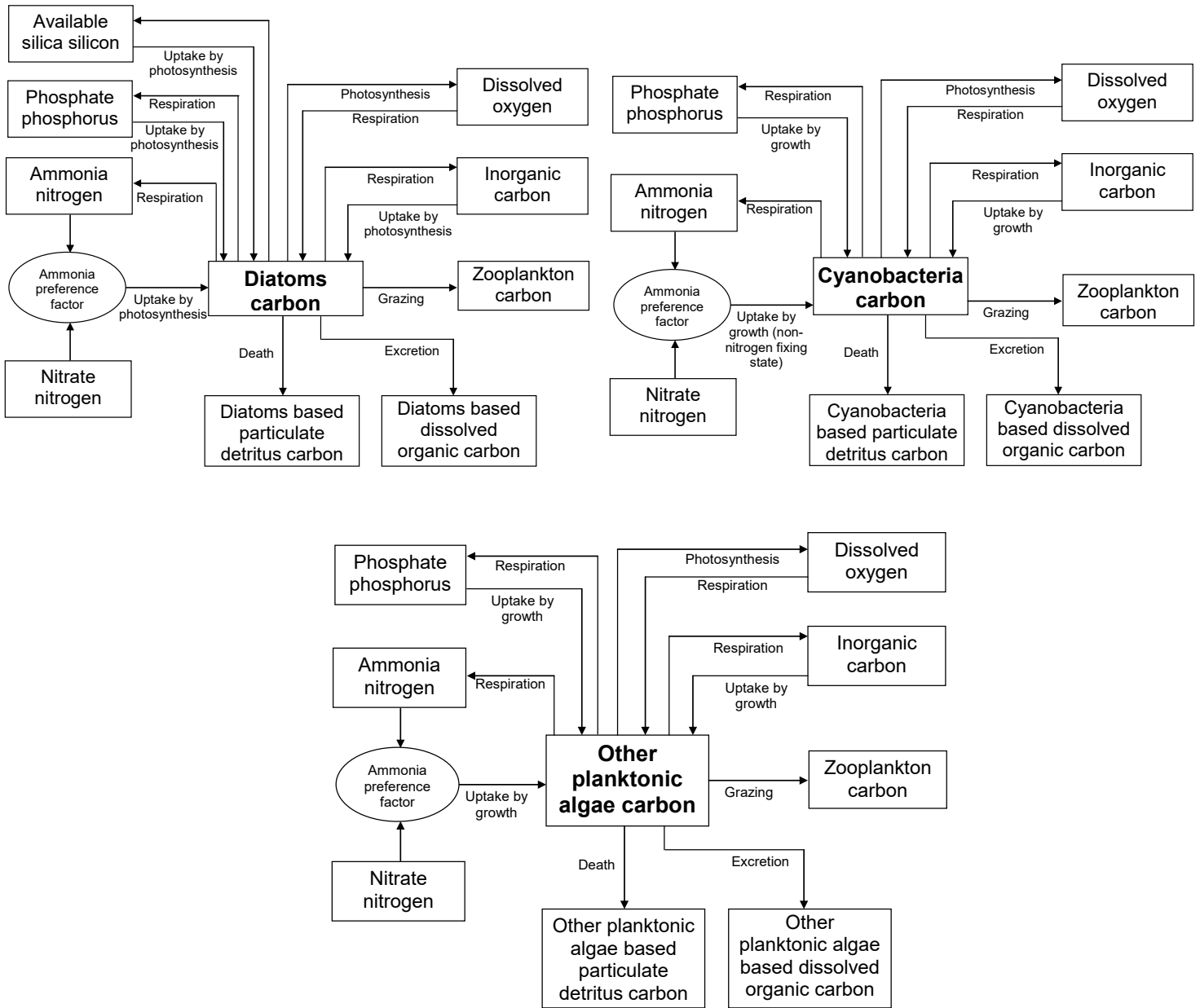
Figure 4. Phytoplankton in the NPZD model
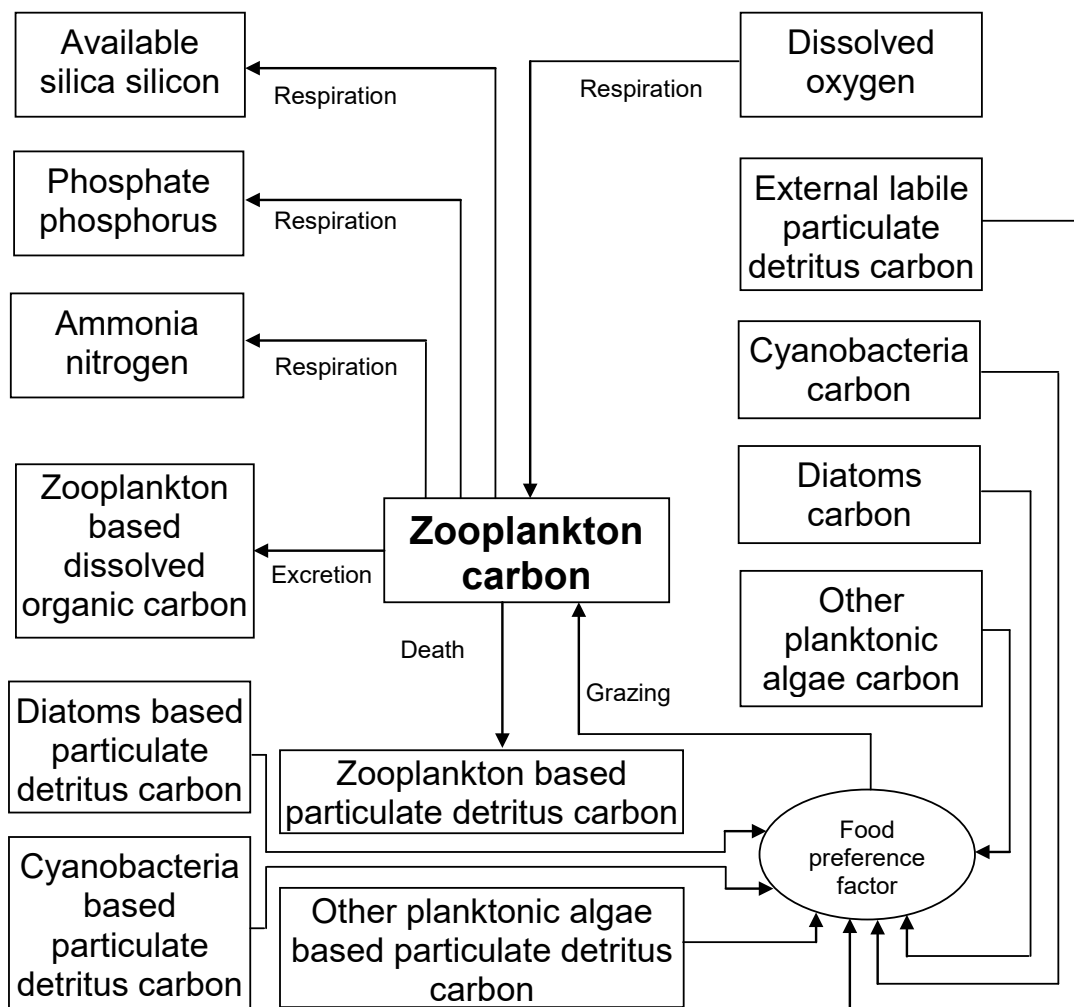
Figure 5. Zooplankton in the NPZD model

Figure 6. Authocthounus organic matter cycle in the NPZD model
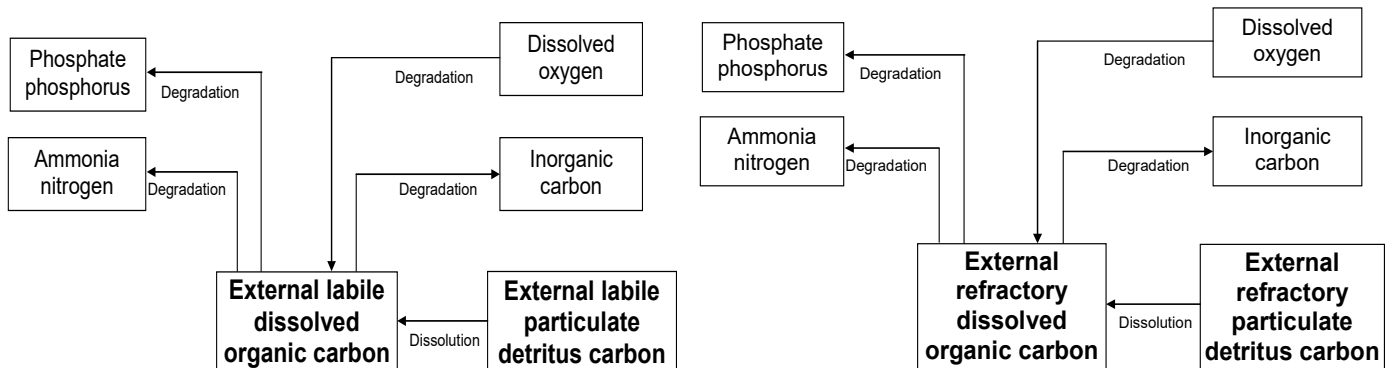
Figure 7. Allochtonous organic carbon and detritus cycles in the NPZD model

Ecopath with Ecosim that is optimized for aqutic ecosystems will be described in this section as an example. Ecopath with Ecosim is designed for straightforward construction, parameterization and analysis of mass-balance trophic models for various ecosystems. The core of Ecopath is derived from ECOPATH program developed by Polovnia and Ow (1983). However, Ecopath does not work under the steady state assumption any more. Instead, it is bases the parameterization on an assumption of mass balance of an arbitrary period (Chiristensen et al., 2005). This period is usually one year, but modelling an ecosystem seasonally is also possible. Ecopath allows the user to develop a generic model for any ecosystem, which can contain any number of state variables. In Ecopath terminology, a state variable is called as group or box. A box (group) in an Ecopath model can be a group of ecologically related species, a single species, or a single size/age group of given species. Since the original ECOPATH from early 1980s, Ecopath has undergone a long development process for both; the theory, ideas and as well as the software itself. The system has been optimized for direct use in fisheries assessment as well as for addressing other more general environmental questions through the inclusion of the temporal dynamic model Ecosim and spatial dynamic model Ecospace. Furthermore, tools such as Ecoranger (tool for addressing uncertainty), Ecoempire (tool for calculation of empirical relationships of production over biomass ratios), Flow diagram (tool for plotting the defined trophic network) or Ecowrite (reporting tool) ease and enhance the model development (Christensen et al., 2005). Different versions of Ecopath with Ecosim are used for various studies with topics such as analyses of trophic interactions (Opiz, 1996; Okey and Pauly, 1999; Harvey et al. 2003), trophic modelling for aquatic ecosystems (Aydin et al., 2003; Mohamed et al, 2005), fisheries management and fish stock assessment (Pauly, 1998; Fayram 2005) in different aquatic ecosystems. Being applied to different aquatic ecosystems from the tropics up to Arctics, Ecopath with Ecosim is proven to be reliable. Detailed information related to methods used in,

Ecopath, Ecosim and Ecospace as well as capabilities and limitations of these models is given by Walters et al. (1999), Walters et al. (2000), Pauly et al. (2000), Christensen and Walters (2004), Kavanagah et al. (2004) and Christensen et al., (2005). Ecopath has two master equations. The first equation describes the production and second equation describes the energy balance for each modelled group the energy balance via consumption. The first master equation of Ecopath (Equation 8) describes how the production term for each group modelled can be split into components.

In mathematical terms, the first master equation is written as in Equation 9, where i is the index for the relevant group, P_i is the total production rate of group i, Y_i is the total fishery catch rate of group i, $M2_i$ is the total predation rate for group i, B_i the biomass of the group i, E_i the net migration rate (emigration – immigration), BA_i is the biomass accumulation rate for group i, while $M0_i = P_i(1-EE_i)$ is the 'other mortality' rate for group i and EE_i is the ecotrophic efficiency of group i. Equation 9 can be rearranged as Equation 10 and rewritten as Equation 11.

In Equation 11; j is the index for prey, P/B_i is the production/biomass ratio, Q/B_i is the consumption/biomass ratio and $DC_{j,i}$ is the fraction of prey j in the average diet of predator i (diet composition). A system of n linear equations (Equation 12) is obtained from Equation 12 for a trophic system with n groups.

Ecopath includes algorithms to solve this system of linear equation for one of following variables for each group: biomass (B), production/biomass ratio (P/B), consumption/biomass ratio (Q/B) or ecotrophic efficiency (EE). The energy input and output of all living groups must be balanced in a model. When balancing the energy for a living group additional terms, which do not exist in the first master equation, are needed and with their incorporation, the second master equation of Ecopath (Equation 13) is formed.

$$\text{Production} = \text{catches} + \text{mortality by predation} + \text{biomass accumulation} +$$
$$\text{net migration} + \text{other mortality}$$

(Equation 8)

$$P_i = Y_i + B_i M2_i + E_i + BA_i + P_i(1 - EE_i)$$

(Equation 9)

$$B_i\left(\frac{P}{B}\right)_i - \left(\sum_{j=1}^{n}\left(B_j\left(\frac{Q}{B}\right)_j\right)DC_{j,i}\right) - B_i\left(\frac{P}{B}\right)_i P_i(1-EE_i) - Y_i - E_i - BA_i = 0$$

(Equation 10)

$$B_i\left(\frac{P}{B}\right)_i EE_i - \left(\sum_{j=1}^{n}\left(B_j\left(\frac{Q}{B}\right)_j\right)DC_{j,i}\right) - Y_i - E_i - BA_i = 0$$

(Equation 11)

$$B_1\left(\frac{P}{B}\right)_1 EE_1 - B_1\left(\frac{Q}{B}\right)_1 DC_{1,1} - B_2\left(\frac{Q}{B}\right)_2 DC_{2,1} - \cdots - B_n\left(\frac{Q}{B}\right)_n DC_{n,1} - Y_1 - E_1 - BA_1 = 0$$

$$B_2\left(\frac{P}{B}\right)_2 EE_2 - B_1\left(\frac{Q}{B}\right)_1 DC_{1,2} - B_2\left(\frac{Q}{B}\right)_2 DC_{2,2} - \cdots - B_n\left(\frac{Q}{B}\right)_n DC_{n,2} - Y_2 - E_2 - BA_2 = 0$$

$$\vdots$$

$$B_n\left(\frac{P}{B}\right)_n EE_n - B_1\left(\frac{Q}{B}\right)_1 DC_{1,n} - B_2\left(\frac{Q}{B}\right)_2 DC_{2,n} - \cdots - B_n\left(\frac{Q}{B}\right)_n DC_{n,n} - Y_n - E_n - BA_n = 0$$

(Equation 12)

$$\text{Consumption} = \text{production} + \text{respiration} + \text{unassimilated food}$$

(Equation 13)

As stated previously, at least three of biomass (B), production/biomass ratio (P/B), consumption/biomass ratio (Q/B) and ecotrophic efficiency (EE) must be given as the basic input. Additionally; diet compositions as well as immigration and emigration rates must be given.

Fooweb models are usually presented as diagrams where the predators are put on the upper trophic levels of their preys. A line connecting two state variables means that the one in the lower trophic level is a food source for the one in the upper level. Figure 10 is an example food web model, developed for a coastal lagoon at the Baltic Sea using Ecopath. Food web models are good tools for simulating organism in the upper levels of the trophic network, however they sometimes lack the components to simulate the nutrients and phytoplankton as accurately as the biogeochemical models. A new emerging approach is to link (one way from the biogeochemical model to the foodweb model) or couple (two ways that both models send feedback to each other) them together. Figure 9 illustrates how the NPZD model described by Figures 2 to 7 could be linked with the food web model described in Figure 8. Figure 9 illustrates the linkage on state variable level. However,

according to Equations 10-13 the foodweb model needs more information such as Production over Biomass and diet composition for the linked state variables of the NPZD model. This kind of information can only be extracted from the process rates internally calculated by the NPZD model.

Linking/Coupling of Ecological Models with Transport Models

As stated previously, some ecosystems are either too large in lateral dimensions or too deep so that they should not be considered as completely mixed. If this is the case, then the system must be spatially discretized into different compartments. There are several methods for spatial discretization; such as the finite difference method, finite element method or box modelling approach. In any case the biogeochemical and/or foodweb sub-models equations should be solved for each spatial compartment and the exchanges of material between these compartments should be considered. For this purpose, advection dispersion equation is extended with a reaction term, which includes the ecological sub-models (Figure 10).
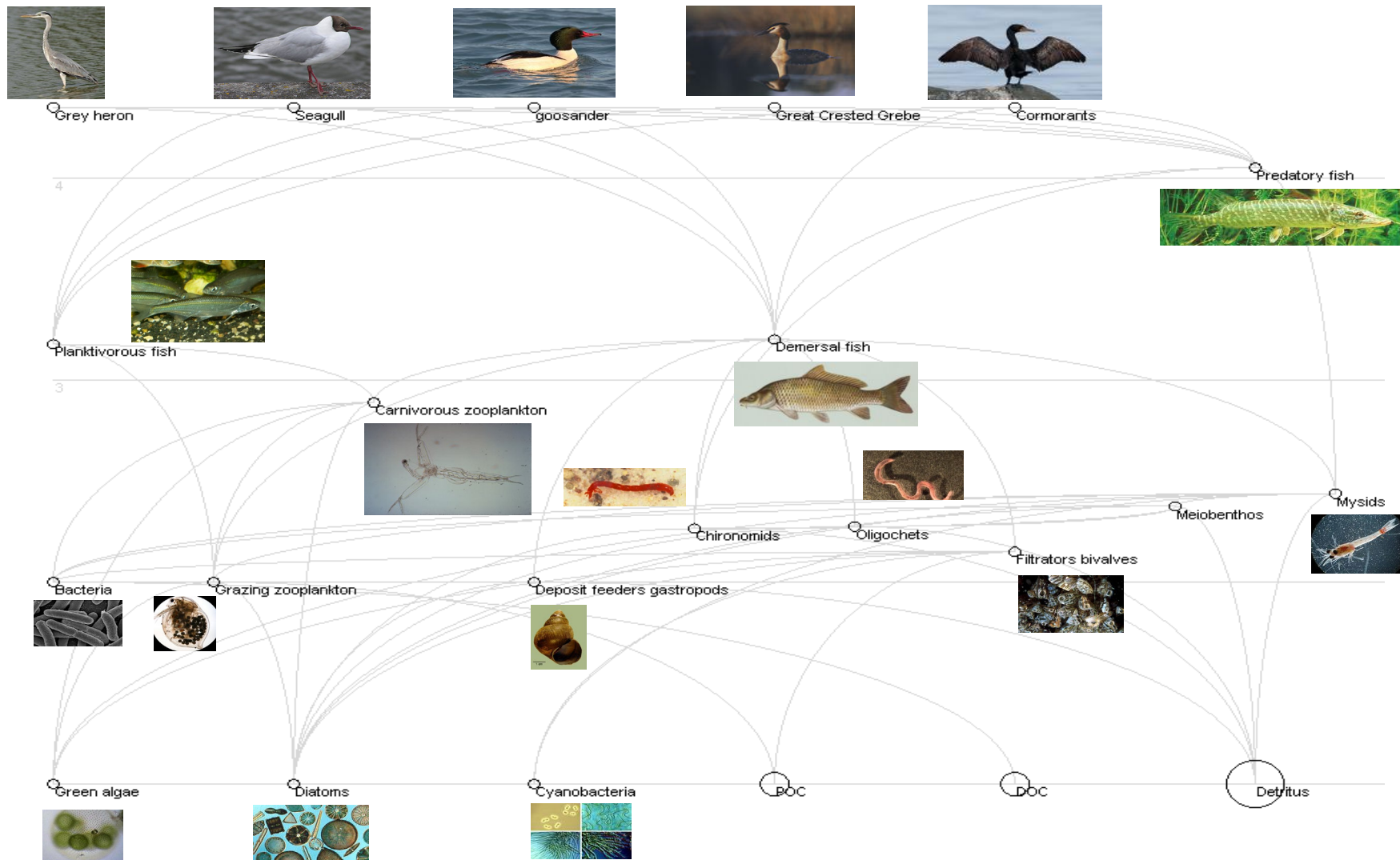
Figure 8. An example foodweb model
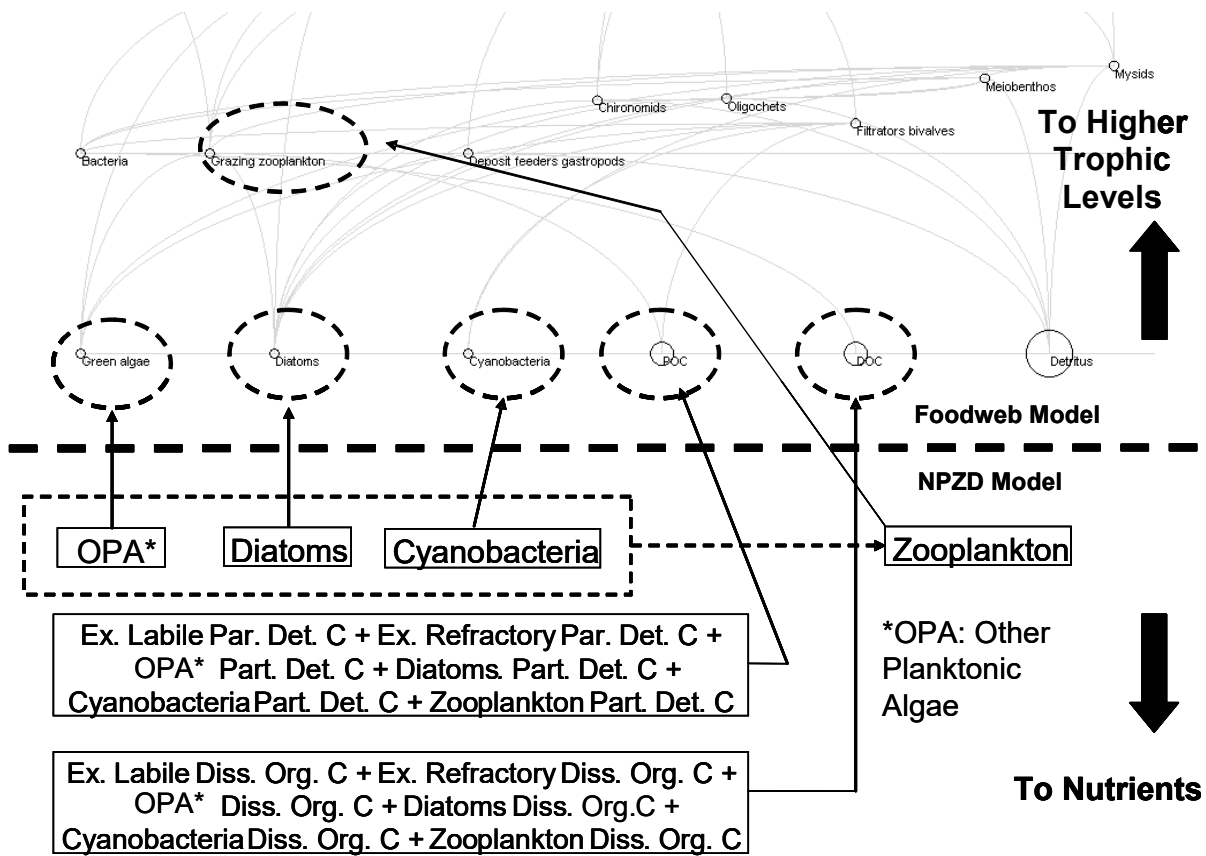
Figure 9. Linking an NPZD model with a foodweb model

Figure 10. Advection dispersion equation extended with ecological sub-model

This equation can be solved using different spatial discretization schemes such as the finite differences (Figure 11a), finite elements (Figure 11b) and box discretization (Figure 12). Finite elements are more difficult to handle mathematically than the finite differences, but provide the advantage of spatially variable resolution of discretization. A third commonly used spatial discretization method is the box modelling approach that is similar to finite differences. It is unstructured grid so that the exchanges between the model boxes have to be defined one by one. The advantage is that the boxes can be organized in one, two or three dimensional model domains easily and with a small number of computational elements. The advection diffusion equation extended with ecological sub-model can be rewritten as Equation 14 for a box model.

(a) (b)
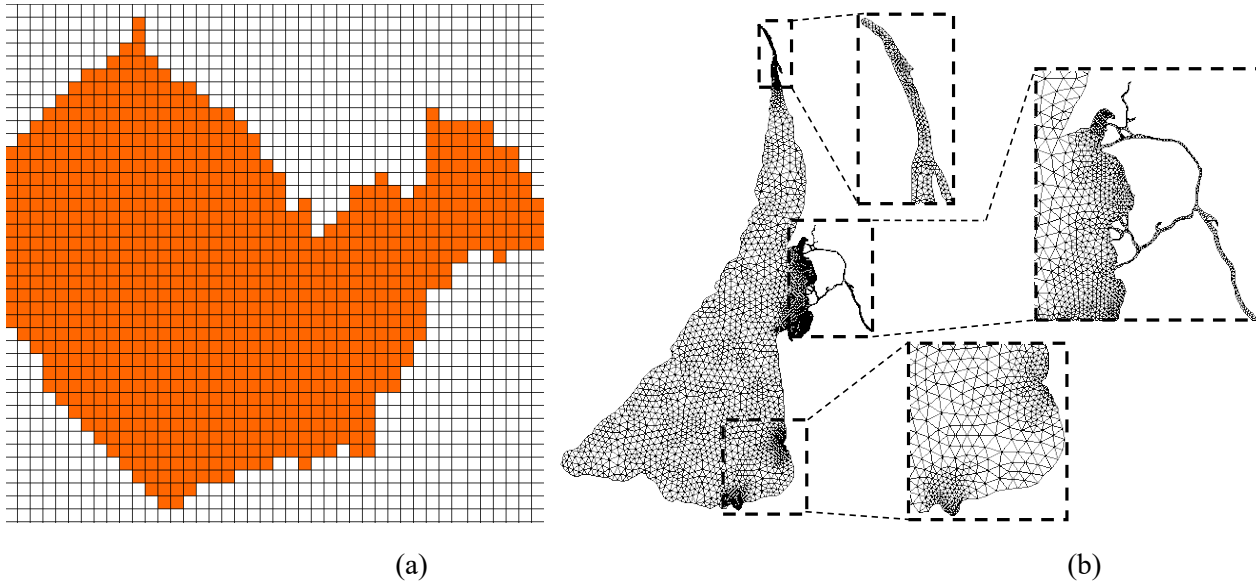
Figure 11. Finite differences (a) and finite elements (b)
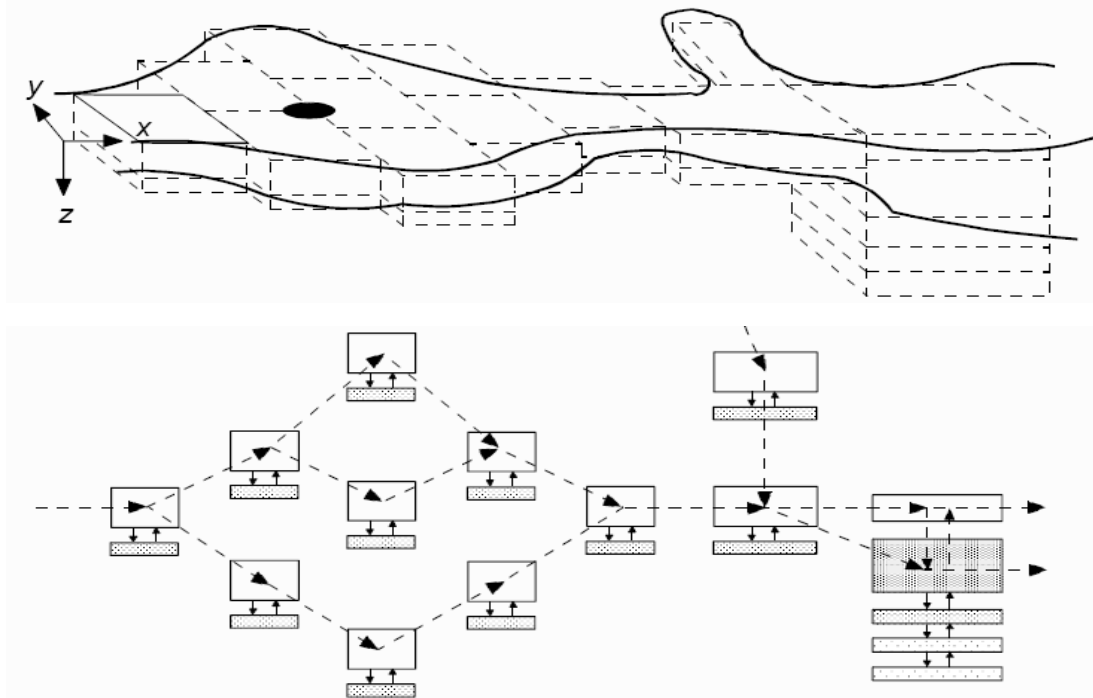
Figure 12. Discretization by box modelling approach

$$\frac{d}{dt}C_1^1 = \sum_{j=1}^{\substack{\text{number of}\\\text{inflows for}\\\text{box 1}}} \frac{Q_{j,1}}{V_1}\cdot C_j^1 - \sum_{j=1}^{\substack{\text{number of}\\\text{outflows for}\\\text{box 1}}} \frac{Q_{1,j}}{V_1}\cdot C_j^1 + \sum_{j=1}^{\substack{\text{number of}\\\text{dispersive}\\\text{exchanges}\\\text{for box 1}}} \frac{A_{1,j}\cdot D_{1,j}}{\ell_{1,j}\cdot V_1}\cdot\left(C_j^1 - C_1^1\right) + \sum_{m=1}^{\substack{\text{number of}\\\text{sources and}\\\text{sinks for box 1}\\\text{state variable 1}}} S_{1,m}^1 + \sum_{k=1}^{\substack{\text{number of}\\\text{kinetic reaction}\\\text{processes for box 1}\\\text{state variable 1}}} R_{1,k}^1$$

$$\vdots$$

$$\frac{d}{dt}C_i^1 = \sum_{j=1}^{\substack{\text{number of}\\\text{inflows for}\\\text{box i}}} \frac{Q_{j,i}}{V_i}\cdot C_j^1 - \sum_{j=1}^{\substack{\text{number of}\\\text{outflows for}\\\text{box i}}} \frac{Q_{i,j}}{V_{i1}}\cdot C_j^1 + \sum_{j=1}^{\substack{\text{number of}\\\text{dispersive}\\\text{exchanges}\\\text{for box i}}} \frac{A_{i,j}\cdot D_{i,j}}{\ell_{i,j}\cdot V_i}\cdot\left(C_j^1 - C_i^1\right) + \sum_{m=1}^{\substack{\text{number of}\\\text{sources and}\\\text{sinks for box i}\\\text{state variable 1}}} S_{i,m}^1 + \sum_{k=1}^{\substack{\text{number of}\\\text{kinetic reaction}\\\text{processes for box i}\\\text{state variable 1}}} R_{i,k}^1$$

$$\frac{d}{dt}C_i^2 = \sum_{j=1}^{\substack{\text{number of}\\\text{inflows for}\\\text{box i}}} \frac{Q_{j,i}}{V_i}\cdot C_j^2 - \sum_{j=1}^{\substack{\text{number of}\\\text{outflows for}\\\text{box i}}} \frac{Q_{i,j}}{V_{i1}}\cdot C_j^2 + \sum_{j=1}^{\substack{\text{number of}\\\text{dispersive}\\\text{exchanges}\\\text{for box i}}} \frac{A_{i,j}\cdot D_{i,j}}{\ell_{i,j}\cdot V_i}\cdot\left(C_j^2 - C_i^2\right) + \sum_{m=1}^{\substack{\text{number of}\\\text{sources and}\\\text{sinks for box i}\\\text{state variable 2}}} S_{i,m}^2 + \sum_{k=1}^{\substack{\text{number of}\\\text{kinetic reaction}\\\text{processes for box i}\\\text{state variable 2}}} R_{i,k}^2$$

$$\vdots$$

$$\frac{d}{dt}C_i^{ns} = \sum_{j=1}^{\substack{\text{number of}\\\text{inflows for}\\\text{box i}}} \frac{Q_{j,i}}{V_i}\cdot C_j^{ns} - \sum_{j=1}^{\substack{\text{number of}\\\text{outflows for}\\\text{box i}}} \frac{Q_{i,j}}{V_{i1}}\cdot C_j^{ns} + \sum_{j=1}^{\substack{\text{number of}\\\text{dispersive}\\\text{exchanges}\\\text{for box i}}} \frac{A_{i,j}\cdot D_{i,j}}{\ell_{i,j}\cdot V_i}\cdot\left(C_j^{ns} - C_i^{ns}\right) + \sum_{m=1}^{\substack{\text{number of}\\\text{sources and}\\\text{sinks for box i}\\\text{state variable ns}}} S_{i,m}^{ns} + \sum_{k=1}^{\substack{\text{number of}\\\text{kinetic reaction}\\\text{processes for box i}\\\text{state variable ns}}} R_{i,k}^{ns}$$

$$\vdots$$

$$\frac{d}{dt}C_{nb}^{ns} = \sum_{j=1}^{\substack{\text{number of}\\\text{inflows for}\\\text{box nb}}} \frac{Q_{j,nb}}{V_{nb}}\cdot C_j^{ns} - \sum_{j=1}^{\substack{\text{number of}\\\text{outflows for}\\\text{box nb}}} \frac{Q_{nb,j}}{V_{nb}}\cdot C_j^{ns} + \sum_{j=1}^{\substack{\text{number of}\\\text{dispersive}\\\text{exchanges}\\\text{for box nb}}} \frac{A_{nb,j}\cdot D_{i,j}}{\ell_{nb,j}\cdot V_{nb}}\cdot\left(C_j^{ns} - C_{nb}^{ns}\right) + \sum_{m=1}^{\substack{\text{number of}\\\text{sources and}\\\text{sinks for box nb}\\\text{state variable ns}}} S_{nb,m}^{ns} + \sum_{k=1}^{\substack{\text{number of}\\\text{kinetic reaction}\\\text{processes for box nb}\\\text{state variable ns}}} R_{nb,k}^{ns}$$

<div align="right">(Equation 14)</div>

In Equation 14; nb is the number of boxes, ns is the number of state variables, index i corresponds to the actual box, index j corresponds to any neighbouring box, $Q_{i,}$ is the flow rate between boxes i and j [$L^3\cdot T^{-1}$], $D_{i,j}$ is the dispersion coefficient between boxes i and j [$L^2\cdot T^{-1}$], $\ell_{i,j}$ is the mixing length between boxes i and j [L], $A_{i,j}$ the interface area between boxes i and j [L^2], V_i the volume of box i [L^2], $S_{i,m}^s$ the external source m related to state variable s for box i [$M\cdot L^{-3}\cdot T^{-1}$] and the $R_{i,k}^s$ is Kinetic reaction rate k for state variable s in for box i [$M\cdot L^{-3}\cdot T^{-1}$]. The water exchanges between boxes can be calculated using a hydrodynamic model such as the one given in Appendix B.

A Case Study

The model described in "Development of Biogeochemical Cycle Sub-Models for Eutrophication Analyses" Section was applied to Curonian Lagoon (Figure 13), which is a shallow estuarine lagoon located in Lithuania at the south-eastern coast of the Baltic Sea. Curonian lagoon is a eutrophic estuarine lagoon downstream the Nemunas River. During cyanobacterial blooms, chlorophyll-a concentrations exceeding 200 mg·m⁻³ were measured on monitoring studies. Peak total organic carbon concentrations exceeding 30 g·m⁻³ are common.

The lagoon was previously modelled by Erturk (2008) and Erturk et al (2015) using the NPZD model described in "Development of biogeochemical cycle sub-models for eutrophication analyses" Sub-section incorporated into Equation 14. The model then was successfully linked to a foodweb model as illustrated in "Development of foodweb sub-models" Sub-section and used for nutrient management scenarios in Nemunas River Basin. The water exchanges between boxes are calculated using the finite element hydrodynamic model SHYFEM. The model setup and linkage is illustrated in Figure 14.

The model was used to simulate the effects of possible warming of the Curonian Lagoon due to climate change. The scenarios here are fictive just to test the behaviour of the model at increased lagoon water temperature. Forcing factors except the temperatures were not changed. The spatially and temporally (yearly) averaged results are summarized in Figure 15 and Figure 16.

As seen from the figures, the total phytoplankton biomass increases first with temperature, but then decreases. This is because of the temperature stress effects considered by the model where the death rate constant is increasing with the temperature. Dead organic carbon is increasing with increasing temperature indicating that the total primary production is increasing, however with decreased net primary production so that dead organic matter is accumulating in the system even though the total phytoplankton concentration is decreasing af-

ter an increase of 4ºC in water temperature. Figure 15b illustrates the response of production over biomass ratio to the increase in temperature. Basically, diatoms that prefer coder water are not affected by temperature increase since they dominate the phytoplankton community on the colder seasons and do not peak in warmer seasons. Therefore, their yearly average biomass does not change considerably. Consequently, the main competition is between the cyanobacteria and the greens. As seen in figure 15b, production over biomass ratio is increasing by cyanobacteria and decreasing by other planktonic algae. Since cyanobacteria are less available as food source, the ecotrophic efficiency of the Curonian Lagoon can be expected to decrease if the temperature increases, because there would be less of available phytoplankton biomass to upper levels of the food web. This effect is reproduced by the model as well by the continually decrease of zooplankton when the temperature increases (Figure 16).
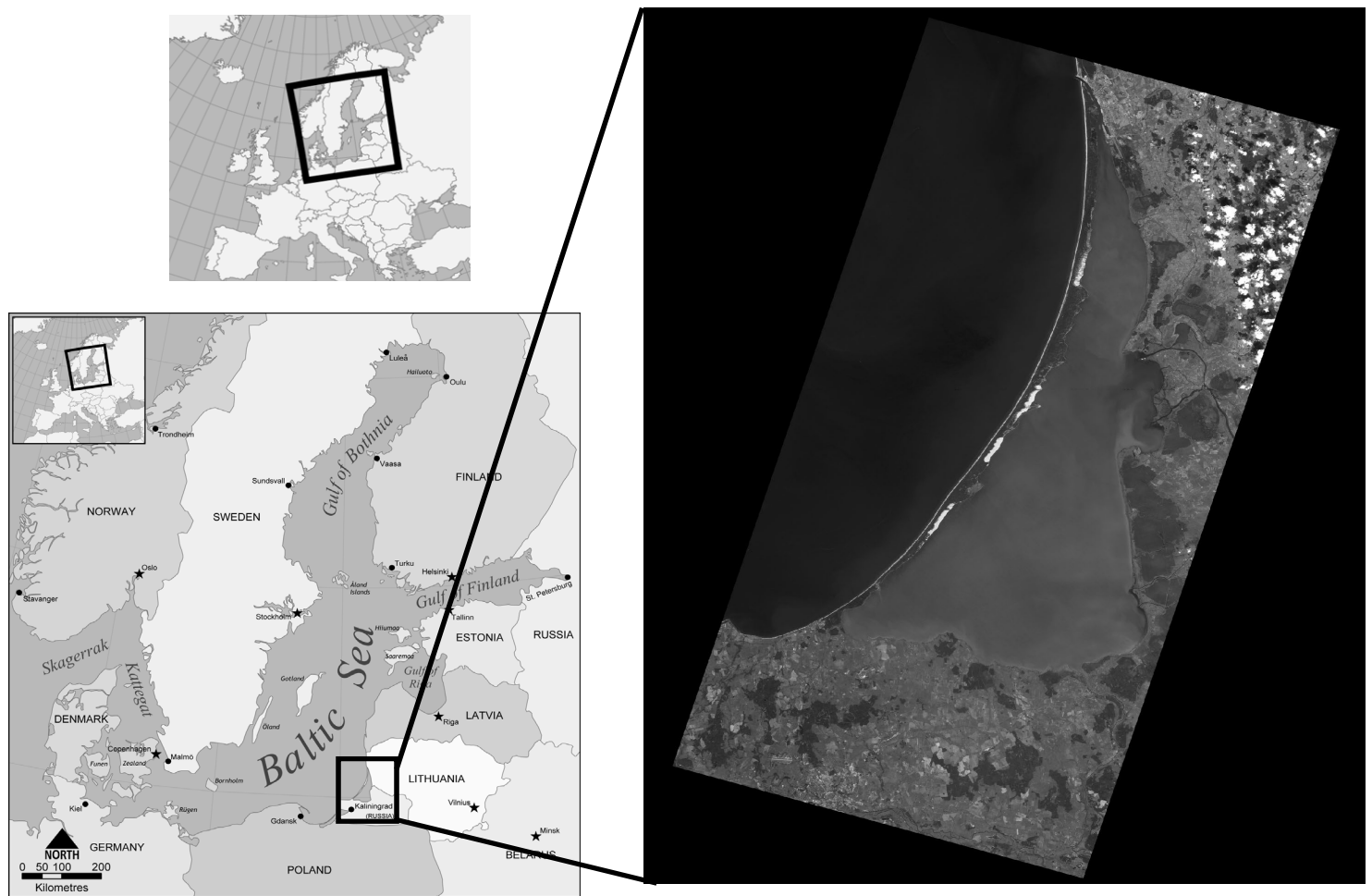
Figure 13. The Curonian Lagoon

(a) Sketch of model boxes
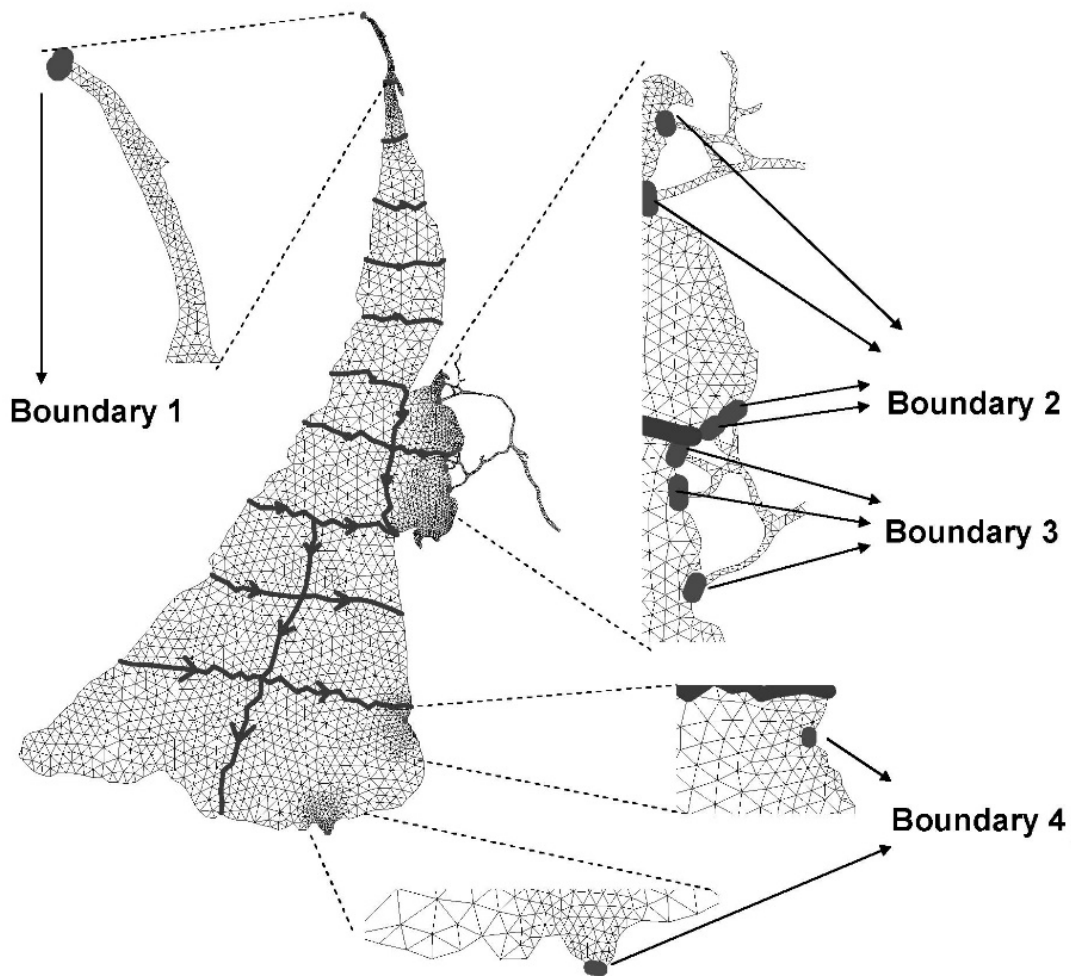
(b) Linking model boxes with hydrodynamic model elements and boundaries

Figure 14. Model setup (Erturk, 2008; Erturk et al., 2015)
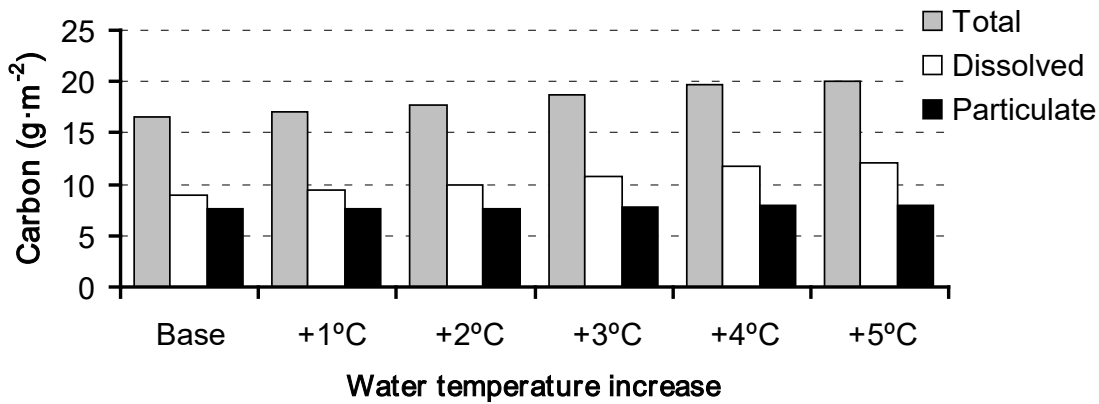
(a) Yearly Averaged Results for Organic Carbon
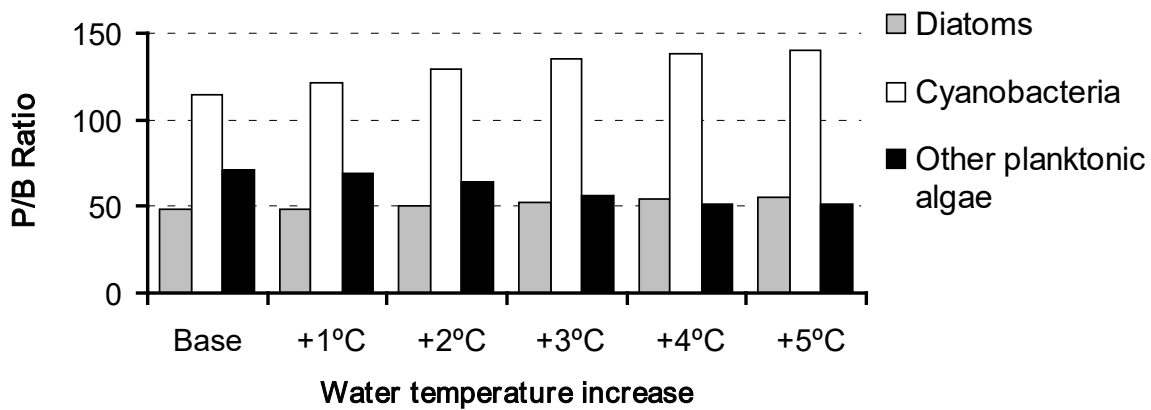
(b) Yearly Production over Biomass Results for Organic Carbon

Figure 15. Simulation results related to organic matter and primary production (Erturk et al., 2015)
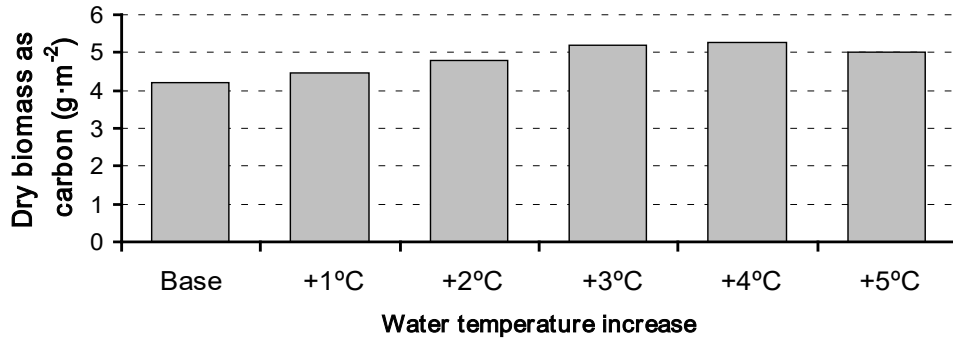
(a) **Yearly Averaged Results for Total Phytoplankton Biomass**
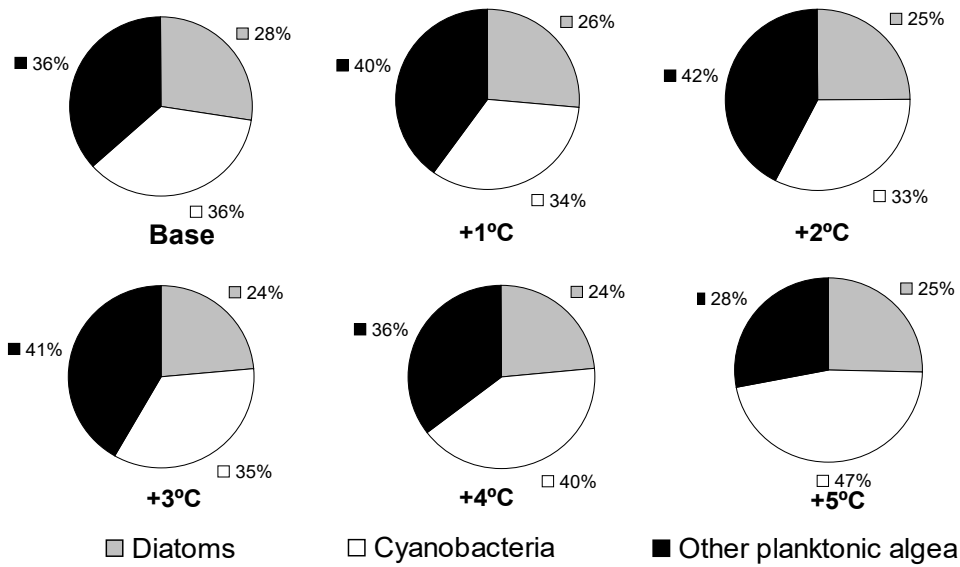
(b) **Yearly Averaged Results for Phytoplankton Composition**
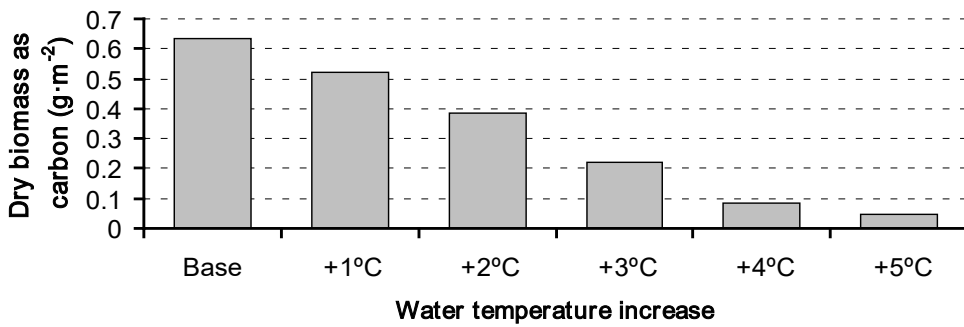
(c) **Yearly Averaged Results for Total Zooplankton Biomass**

Figure 16. Simulation results related to phytoplankton and zooplankton (Erturk et al., 2015)

Conclusions

Eutrophication is a complicated process and its predictive modelling may involve many tools applied in an interdisciplinary manner. Such a modelling effort could seem overwhelming for many researchers new to the topic. This paper however shows that building such models even from scratch is really not "rocket science" and most of the aquatic scientists already have the necessary mathematical background.

Once a simple model such as the one illustrated in Appendix A, it is quite easy to extend it into more comprehensive frameworks, such as a combined ecological model linked to higher trophic compartments as described in "Ecological Sub-Models for Prediction of the Progress and Effects of Eutrophication" Section.

Mathematical models are not only useful to predict the progress of eutrophication but they are also valuable tools for system identification. The model presented in "Development of Foodweb Sub-Models" Section is such an example, where in internals such as ecotrophic efficiency of the foodweb is estimated rather than the biomasses of individual trophic compartments.

Compliance with Ethical Standard

Conflict of interests: The authors declare that for this article they have no actual, potential or perceived conflict of interests.

References

Ambrose, B, Jr., Wool, T.A. Martin, J.L. (1993). *The Water Quality Analysis Simulation Program, WASP5; Part A: Model Documentation*, U.S. Environmental Protection Agency, Center for Exposure Assessment Modeling, Athens, GA.,

Arhonditsis, G. B., Brett, M. T. (2004). Evaluation of the current state of mechanistic aquatic biogeochemical modelling. *Marine Ecology Progress Series,* 271, 13-26.

Aydin, K.Y., McFarlane, G.A., King, J.R., Megrey, B.A. (2003). *The BASS/MODEL Report on Trophic Models of the Subarctic Pacific Basin Ecosystems*, PICES Scientific Report No. 25, https://www.pices.int/publications/scientific_reports/Report25/default.aspx, (accessed 8.4.2019).

Bartsch, A.F., Gakstatter, J.H. (1978). *Management Decision for Lake Systems on a Survey of Trophic Status, Limiting Nutrients, and Nutrient Loadings*, American-Soviet Symposium on Use of Mathematical Models to Optimize Water Quality Management, 1975, U.S. Environmental Protection Agency Office of Research and Development, Environmental Research Laboratory, Gulf Breeze, FL, pp 372-394, EPA-600/9-78-024

Bloesch, J, Stadelmann, P., Bührer, H. (1977). Primary production, mineralization and sedimentation in the euphotic zone of two swiss lakes. *Limnology and Oceanography*, 22(3), 511-526.

Cerco, C.F., Cole, T. (1994). *Three Dimensional Eutrophication Model of Chesapeake Bay; Volume 1, Main Report*, Technical Report EL 94-4, U.S. Army Corps of Engineers Waterways Experiment Station, Vicksburg, MS.

Cerco, C.F., Cole, T. (1995). *User's Guide to the CE-QUAL-ICM Three Dimensional Eutrophicaiton Model, Release Version 1.0.* Technical Report EL-95-15, US Army Corps of Engineers Waterways Experiment Station, Vicksburg, MS.

Chapra, S.C. (1997). *Surface Water-Quality Modeling*, WCB McGraw-Hill Publisher, ISBN 0-07-024186-4

Christensen, V., Walters, C.J. (2004). Ecopath with ecosim: methods capabilities and limitations. *Ecological Modelling*, 172, 109-139.

Christensen, V., Walters, C.J., Pauly, D. (2005). *Ecopath with Ecosim: A User's Guide*, Fisheries Centre University of British Columbia Vancouver, Canada.

Cole, T.M., Wells, S.A. (2006). *CE-QUAL-W2 A Two dimensional, Laterally Averaged Hydrodynamic and Water Quality Model, Version 3.5*, Instruction Report EL-2006-1, U.S. Army Engineering and Research Development Center, Vicksburg, MS.

Dillon, P.J., Rigler, F.H. (1974). The phosphorus-chlorophyll relationship for lakes. *Limnology and Oceanograpgy*, 19, 767-773.

Di Toro, D.M., O'Connor, D.L., Thomann, R.V. (1971). *A Dynamic Model of the Phytoplankton Population in the Sacramento-San Joaquin Delta*. Advances in Chemistry Series 106, Nonequilibrium Systems in Natural Water Chemistry, 131.

Di Toro, D.M., Connolly, J.P. (1980). *Mathematical Models of Large Lakes, Part 2. Ontario Lake*. National Environmental Research Center, Office of Research and Development, U.S. Environmental Protection Agency, Ecological Research Series, EPA-600/3-80-065.

Di Toro, D.M., Fitzpatrick, J.J., Thomann, R.V. (1983). *Water Quality Analysis Simulation Program (WASP) and Model Verification Program (MVP) – Documentation*. Contract No 68-01-3872, Hydroscience, Inc., USA.

Di Toro, D.M., Fitzpatrick, J.J. (1993). *Chesapeake Bay Sediment Flux Model*. Contract Report EL-93-2, Environmental Laboratory U.S. Army Engineer Waterways Experiment Station.

Edmonson, W.T. (1979). Phosphorus, nitrogen and algae in lake washington after diversion of sewage. *Science*, 169, 690-691.

Environmental Laboratory, (1995). CE-QUAL-R1: *A Numerical One Dimensional Model of Reservoir Water Quality; User's Manual*. Instruction Report E-82-1, Rev. Ed., US Army Engineer Waterways Experiment Station, Vicksburg MS.

Erturk, A. (2008). *Modelling the Response of an Estuarine Lagoon to External Nutrient Inputs*. Dissertation, Klaipeda University.

Erturk, A., Razinkovas-Baziukas, A., Zemlys, P., Umgiesser, G. (2015). Linking carbon-nitrogen-phosphorus cycle and foodweb models of an estuarine lagoon ecosystem. *Computational Science and Tecniques*, 3(1), 350-412.

Fayram, A.H. (2005). *Walleye Stocking in Wisconsin Lakes: Species Interactions, Changes in Angler Effort, Optimal Stocking Rates and Effects on Community Maturity,* Dissertation in Biological Sciences at the University of Wisconsin, Milwaukee, USA.

Gamito, S., Erzini, K. (2005). Trophic food web and ecosystem attributes of a water reservoir of the Ria Formosa (south portugal), *Ecological Modelling*, 181, 509-520.

Hamrick, J.M. (1996). *User's Manual for the Environmental Fluid Dynamics Computer Code*, Special Report No. 331 in Applied Marine Science and Ocean Engineering Virginia Institute of Marine Science School of Marine Science, The College of William and Mary Gloucester Point, VA 23062.

Harvey, C.J., Cox, S.P., Essington, T.E., Hansson, S, Kitchell, J.F. (2003). An ecosystem model of food web and fisheries interactions in the Baltic Sea. *ICES Journal of Marine Science*, 60, 939-950.

HEC (1978). *Generalized Computer Program, Water Quality for River-Reservoir Systems*, The Hydrologic Engineering Center, United States Army Corps of Engineers.

Hossenipour, E.Z., Martin J.L. (1990). T*he One-Dimensional Riverline Hydrodynamic Model*, RIVMOD-H Model Documentation and User's Manual, Environmental Laboratory Office of Research and Development USEPA Athens, Georgia 30605-2700.

Hull, V., Mocenni, C., Falcucci, M., Marchettini, N. (2000). A trophodynamic model for the lagoon of Fogliano (Italy) with ecological dependent modifying parameters. *Ecological Modelling*, 134, 153-167.

Kavanagah, P., Newlands, N., Christensen, V., Pauly, D. (2004). Automated parameter optimization for ecopath ecosystem models. *Ecological Modelling*, 172, 141-149.

Luyten, P.J., Jones, J.H., Proctor, R., Tabor, A., Tett, P., Wild-Allen, K. (1999). *COHERENS – A Coupled Hydrodynamical – Ecological Model for Regional and Shelf Seas: User Documentation*. MUMM Report, Management Unit of the Mathematical Models of the North Sea.

Megrey, B.A., Taft, B.A., Peterson, W.T. (Eds.) (2001). *PICES-GLOBEC International Program on Climate Change and Carrying Capacity*. Report of the 2000 BASS, MODEL, MONITOR and REX Workshops, and the 2001 BASS/MODEL Workshop. PICES Sci. Rep. No. 17.

Mohamed, K.S., Zacharia, P.U., Muthiah, C., Abdurahiman, K.P., Nayak, T.H. (2005). *A Trophic Model of the Arabian Sea Ecosystem off Karnataka and Simulation of Fishery Yields for its Multigear Marine Fisheries*. Research Centre of Central Marine Fisheries Research Institute, Karnataka, India.

O'Connor D. J., John, P. St., Di Toro, M. (1968). Water quality analyses of the Delaware River Estuary. *Journal of the Sanitary Engineering Division,* 94(SA6), 1225-1252.

Okey, T.A., Pauly, D.A. (1999). *Mass-Balanced Model of Trophic Flows in Prince William Sound: Decompartmentalizing Ecosystem Knowledge*. Ecosystem for Fisheries Management, Alaska Sea Grant College Program, AL-SG-99-01, pp 621-635.

Opiz, S. (1996). *Trophic Interactions in Caribbean Coral Reefs*, International Center for Living Aquatic Resources, Makati City, Philippines.

Pauly, D. (1998). *Use Ecopath with Ecosim to Evaluate Strategies for Sustainable Exploitation of Multi-Species Resources*: Proceedings of a Workshop held at the Fisheries Centre of University of British Columbia, Vancouver, B.C., Canada, edited by Pauly, D., Fisheries Centre Research Reports, Volume 6(2), ISSN 1198-6727

Pauly, D., Christensen, V., Walters, C. (2000). Ecopath ecosim and ecospace as tools for evaluating ecosystem impacts of fisheries. *ICES Journal of Marine Science*, 57, 1-10.

Polovina, J.J., Ow, M.D. (1983). *ECOPATH: A user's manual and program listings*, Administrative report, H-83-23, Sothwest Fisheries Center, Honolulu Laboratory, Honolulu, Hawaii, USA.

Rast, W., Lee, G.F. (1978). *Summary Analyses of the North American Project (US Portion) OECD Eutrophication Project: Nutrient Loading-Lake Response Relationships and Trophic State Indices*, USEPA Corvallis Environmental Research Laboratory, Corvallis, OR, EPA-600/3-78-008.

Royal Comission on Environmental Pollution, (2004)*. Turning the Tide: Addressing the Impact of Fisheries on the Marine Environment*, 25th Repot, Chairman: Tom Blundell, FMedSci.

Sheng, Y.G. Eliason, D.E., Chen, X.J., Choi, J.K. (1991). A *Three Dimensional Numerical Model of Hydrodynamics and Sediment Transport in Lakes and Estuaries: Theory, Model Development and Documentation*. USEPA Athens, GA, USA.

Smith, V.H., Shapiro, J. (1981). A *Retroperspective Look at the Effects of Phosphorus Removal in Lakes, in Restoration of Lakes and Inland Waters*. USEPA, Office of Water Regulations and Standards, Washington, DC. EPA-440/5-81-010.

Thomann, R.V. Di Toro, D.M., Winfield, R.P. O'Connor, D.O. (1975). *Mathematical Modeling of Phytoplankton in Lake Ontario, 1. Model Development and Verification*, National Environmental Research Center, Office of Research and Development, USEPA, Ecological Research Series, EPA-660/3-75-005.

Thomann, R.V., Mueller, J.A., (1987). *Principles of Surface Water Quality Modeling and Control*, Harper Collins Publishers Inc., USA.

Tillman, D.H., Cerco, C.F., Noel, M.R. (2006). *Conceptual Processes for Linking Eutrophication and Network Models*. ERDC TN-SWWRP-06-9, United States Army Corps of Engineers.

USEPA, (2000). *Estuarine and coastal marine waters: Bioassessment and biocriteria technical guidance*. USEPA Report EPA-822-B00-024, Washington, DC.

Villanueva, M.C. Laleyeb, P., Albaret J.J., Lae, R., de Moraise, L. Tito, Moreaua J. (2006). Comparative analysis of trophic structure and interactions of two tropical lagoons. *Ecological Modelling*, 197, 461-477.

Walters, C., Pauly, D., Christensen, V. (1999). Ecospace: prediction of mesoscale spatial patterns in trophic relationships of exploited ecosystems with emphasis on the impact of marine protected areas. *Ecosystems* (1999)2, 539-554.

Walters, C., Pauly, D., Christensen, V., Kitchell, J.F. (2000). Representing density dependent consequences of life history strategies in aquatic ecosystems: Ecosim II. *Ecosystems* (2000)3, pp 70-83.

Wool, T.A., Ambrose, R.B.Jr., Martin, J.L., Comer, E.A. 2001. *The Water Quality Analysis Simulation Program, WASP* USEPA, Centre for Exposure Assessment Modeling, Athens, GA.

APPENDIX A

Development and Implementation of Simplified Eutrophication Modelling Tools from Scratch

The aim of this section is to illustrate the reader how to develop own modelling tools that can simulate the progress of the eutrophication process on simple but complete examples. Before starting to read this section, be advised that the development of an eutrophication model from scratch is not a simple process and consists of several tasks listed below:

- Development of a conceptual model
- Writing the equations that form the mathematical construct of the model
- Development of solution schemes for the equations
- Implementation of the model as a tool
- Development of the supporting environment and tools for the model

A.1. Development of a conceptual model

Development of a conceptual model is the first and most important step for developing a complete modelling tool. The conceptual model is the first level of modelling and describes the simplified system (actually aquatic ecosystem since our aim is to develop a eutrophication model) as it will be assumed by our model based analysis. The conceptual model "glues" the models state variables (the variables that are calculated by the model to describe the state of the aquatic ecosystems in terms of eutrophication), the auxiliary variables needed by the model itself and the processes (here the ecological processes related to eutrophication within the framework of the model) together. The conceptual model for the example in this subsection is illustrated in Figure A.1 is used as the conceptual model.

The aquatic ecosystem that is assumed to be a lake in this example is considered as a fully mixed reactor. The three state variables are unavailable phosphorus that includes all the dead and organically bound phosphorus, dissolved reactive phosphorus that can be utilized as nutrient and the phytoplankton chlorophyll representing the primary produces. The loads shown in Figure 1 are examples of auxiliary variables. The conceptual model includes the processes listed below:

- Settling of unavailable phosphorus
- Release of unavailable phosphorus by phytoplankton death

- Conversion of unavailable phosphorus to dissolved reactive phosphorus by decomposition
- Uptake of soluble reactive phosphorus by photosynthesis
- Release of unavailable phosphorus by phytoplankton
- Death of phytoplankton
- Settling of phytoplankton
- Inflow and outflow of soluble reactive phosphorus
- Inflow and outflow of unavailable phosphorus
- Inflow and outflow of phytoplankton
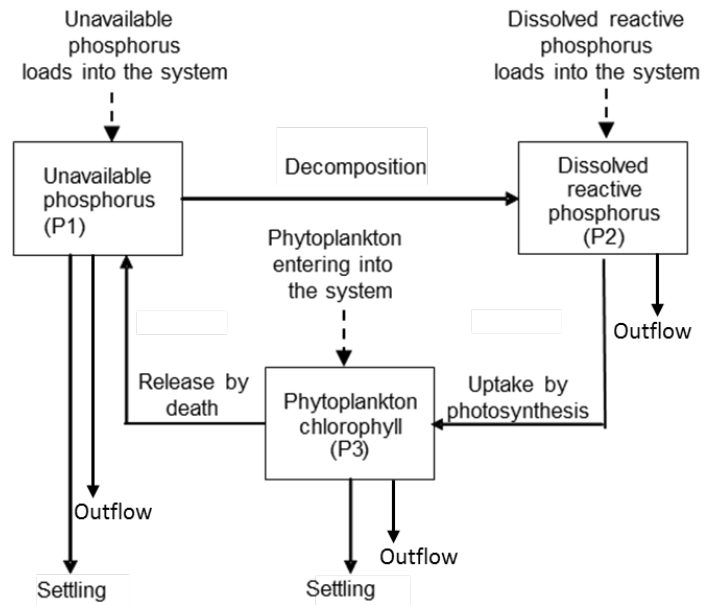
Figure A.1. A simple, process based nutrient cycle model

A.2. Writing the equations that form the mathematical construct of the model

The next step is the writing the equations that describe the lake ecosystem mathematically. Since the aim of the model in this example is to describe the progress of eutrophication, it must be a dynamic model, where time (t) is the independent variable, whereas the state variables (P1, P2 and P3) are dependent variables. The processes as well as loads force the values of state variables to change. The state variables are in concentration dimensions ($[M \cdot L^{-3}]$- mass over the third power of length or mass of volume), whereas the processes are in reaction rate dimensions ($[M \cdot L^{-3} \cdot T^{-1}]$-change of concentration per unit time). To put the state variables and processes on the same equation, state variables should be rewritten in reaction rate

dimensions as well, so mathematically divided by time. To describe the change in a moment (indefinitely small time) differential equations are needed. Since there are three state variables where the rate of change of a state variable depends on itself and on other state variables, we end up with system with three unknowns (the state variable) and three differential equations.

$$\frac{dP1}{dt} = \underbrace{\frac{W_{Chl\text{-}A}}{V}}_{\substack{\text{Incomming}\\\text{mass of}\\\text{unavailable}\\\text{phosphorus}}} - \underbrace{\frac{Q_{OUT}}{V} \cdot P1}_{\substack{\text{Outgoing}\\\text{mass of}\\\text{unavailable}\\\text{phosphorus}}} - \underbrace{\left(K_{12} \cdot \underbrace{\theta_{Decomp}^{\;TEMP-20}}_{\text{Temperature effect}} + \frac{v_{S,P1}}{H} \right) \cdot P1}_{\substack{\text{Settling rate of unavailable}\\\text{phosphorus plus its conversion}\\\text{rate to dissolved reavtive phosphorus}\\\text{by decomposition}}} + \underbrace{D_P \cdot a_P \cdot Chl\text{-}A}_{\substack{\text{Death rate}\\\text{of phytoplankton}}} \qquad \text{(Equation A.1)}$$

$$\frac{dP2}{dt} = \underbrace{\frac{W_{P2}}{V}}_{\substack{\text{Incomming}\\\text{mass of}\\\text{dissolved}\\\text{reactive}\\\text{phosphorus}}} - \underbrace{\frac{Q_{OUT}}{V} \cdot P2}_{\substack{\text{Outgoing}\\\text{mass of}\\\text{dissolved}\\\text{reactive}\\\text{phosphorus}}} + \underbrace{K_{12} \cdot \theta_{Decomp}^{\;TEMP-20} \cdot P1}_{\substack{\text{Conversion rate of}\\\text{unavailable}\\\text{phosphorus to dissolved}\\\text{reactive phosphorus by}\\\text{decomposition}}} - \underbrace{G_P \cdot a_P \cdot Chl\text{-}A}_{\substack{\text{Uptake rate of dissloved}\\\text{reactive phosphorus by}\\\text{phytoplankton}}} \qquad \text{(Equation A.2)}$$

$$\frac{dChl\text{-}A}{dt} = \underbrace{\frac{W_{Chl\text{-}A}}{V}}_{\substack{\text{Incomming}\\\text{mass of}\\\text{phytoplankton}}} - \underbrace{\frac{Q_{OUT}}{V} \cdot Chl\text{-}A}_{\substack{\text{Outgoing}\\\text{mass of}\\\text{phytoplankton}}} - \underbrace{\frac{v_{S,Phyto}}{H} \cdot Chl\text{-}A}_{\substack{\text{Settling rate of}\\\text{phytoplankton}}} + \underbrace{\left(G_P - D_P \right) \cdot Chl\text{-}A}_{\substack{\text{Net growth rate}\\\text{of phytoplankton}}} \qquad \text{(Equation A.3)}$$

where V is the volume of the lake $[L^3]$; P1, P2, Chl-A are unavailable (organically bound) phosphorus, available phosphorus and chlorophyll-a respectively $[M \cdot L^{-3}]$, Q_{OUT} is the outflow $[L^3 \cdot T^{-1}]$, H is the depth of the lake $[L]$, $v_{S,P1}$ is the settling velocity for unavailable phosphorus $[L \cdot T^{-1}]$, $v_{S,Chl\text{-}A}$ is the settling velocity for phytoplankton $[L \cdot T^{-1}]$; W_1, W_2, $W_{Chl\text{-}A}$ are the loads for unavailable phosphorus, available phosphorus and chlorophyll-a respectively $[M \cdot T^{-1}]$, K_{12} is the decomposition rate constant $[T^{-1}]$. G_P and D_P are the growth and death rate coefficients of phytoplankton respectively $[T^{-1}]$. As seen in below, these coefficients are calculated using three relatively long algebraic equations.

$$G_P = G_{MAX} \cdot \underbrace{\theta_{Phyto,G}^{\;TEMP-20}}_{\substack{\text{Limiting effect of}\\\text{temperature on}\\\text{phytoplankton}\\\text{growth}}} \cdot \min \left(\underbrace{\frac{P2}{P2 + K_{HS,Phyto,P2}}}_{\substack{\text{Limiting effect of}\\\text{dissolved reactive}\\\text{phosphorus on}\\\text{phytoplankton}\\\text{growth}}} , \underbrace{\frac{2.718 \cdot f_{day}}{K_e \cdot H} \cdot \left(\exp\left(-\frac{I_A}{I_S} \cdot \exp(-K_e \cdot H) \right) - \exp\left(-\frac{I_A}{I_S} \right) \right)}_{\substack{\text{Limiting effect of}\\\text{light on}\\\text{phytoplankton}\\\text{growth}}} \right) \qquad \text{(Equation A.4)}$$

$$K_e = K_{b,e} + 0.0088 \cdot Chl\text{-}A + 0.054 \cdot Chl\text{-}A^{\frac{2}{3}} \qquad \text{(Equation A.5)}$$

$$D_P = \underbrace{\mu_R \cdot \theta_{Phyto,D}^{TEMP-20}}_{\substack{\text{non-predatory death} \\ \text{of phytoplankton}}} + \underbrace{C_G \cdot a_{Chl} \cdot Z}_{\substack{\text{predatory death} \\ \text{of phytoplankton} \\ \text{by zooplankton} \\ \text{grazing}}}$$ (Equation A.6)

where TEMP is the temperature, K_e [L^{-1}] is the total light extinction coefficient, $K_{b,e}$ [L^{-1}] is the background light extinction coefficient, f_{day} is the fraction of time with day light, G_{max} is the growth rate constant for phytoplankton at optimum conditions, $K_{HS,Phyto,P2}$ is the half saturation concentration of dissolved reactive phosphorus for phytoplankton growth where a Monod-type relation is assumed [M·L^{-3}]; I_A and I_S are the available light intensity and saturating light intensity respectively, $\square_R$ is the death rate constant of phytoplankton, C_G is the grazing rate of zooplankton [T^{-1}]; $\theta_{Phyto,G}$ and $\theta_{Phyto,D}$ are the temperature coefficients for phytoplankton growth and non-predatory death respectively [T^{-1}] where both processes are assumed to accelerate with increasing temperature and Z is the zooplankton concentration [M·L^{-3}].

Equations A.1, A.2 and A.3 may seem like linear differential equations, however the term G_P contains non-linear terms making the entire system non-linear since this term is substituted into the differential equation system. Equation A.4 states that the primary production that is the key process for eutrophication is under the influence of two limiting factors: the nutrient availability and the light availability. Equation A.5 states that the more phytoplankton grow, the more light extinction will increase a process known as "algal self shading" so that the model prevents indefinite growth of phytoplankton even if unlimited amount of dissolved reactive phosphorus would be available.

The non-linear structure of Equations A.4 and A.5 make the analytical integration (exact solution) of the differential equation system formed by Equations A.1, A.2 and A.3 impossible. This is usually the case in ecological models. Therefore they have to be solved numerically and approximate solutions will be obtained instead of exact solutions. The next sub-section gives more details on these topics for the example eutrophication model. However, before starting to develop the solution let us classify the terms in equations as given in Table A.1.

The forcing factors and auxiliary variables are changing with time. The forcing factors are external variables that are given to the equations from outside. Auxiliary variables are computed using state variables, forcing factors and other auxiliary variables during the model calculations. Model constants are used during the model calibration and model validation process.

Table 1 Terms in the model equations

Term	Description	Type	Unit
P1	Unavailable (organically bound) phosphorus	State variable	$gP \cdot m^{-3}$
P2	Available (dissolved reactive) phosphorus	State variable	$gP \cdot m^{-3}$
Chl-A	Chlorophyll-a	State variable	$g\ Chl\text{-}A \cdot m^{-3}$
V	Volume	Auxiliary variable	m^3
H	Depth of the lake	Auxiliary variable	M
G_P	Growth rate of phytoplankton	Auxiliary variable	day^{-1}
D_P	Death rate of phytoplankton	Auxiliary variable	day^{-1}
K_e	Total light extinction coefficient	Auxiliary variable	m^{-1}
Q_{OUT}	Outflow rate	Forcing factor	$m^3\ day^{-1}$
$v_{S,P1}$	Settling velocity for unavailable phosphorus	Forcing factor	$m\ day^{-1}$
$v_{S,Chl\text{-}A}$	Settling velocity for phytoplankton	Forcing factor	$m\ day^{-1}$
W_1	Unavailable phosphorus load	Forcing factor	$kg\ day^{-1}$
W_2	Available phosphorus load	Forcing factor	$kg\ day^{-1}$
$W_{Chl\text{-}A}$	Chlorophyll-a load	Forcing factor	$kg\ day^{-1}$
I_A	Available light intensity	Forcing factor	$Watt \cdot m^{-2}$
TEMP	Temperature	Forcing factor	ºC
f_{day}	Fraction of sunlight hours	Forcing factor	Unitless
Z	Zooplankton concentration	Forcing factor	$g \cdot m^{-3}$
a_p	Phosphorus to chlorophyll-a ratio	Model constant	Unitless
a_{chl}	Chlorophyll a to zooplankton grazing ratio	Model constant	Unitless
$K_{b,e}$	Background light extinction coefficient	Model constant	m^{-1}
K_{12}	Decomposition rate constant	Model constant	day^{-1}
θ_{Decomp}	Temperature correction coefficient for decomposition	Model constant	Unitless
G_{max}	Maximum growth rate costant of phytoplankton	Model constant	day^{-1}
$K_{HS,Phyto,P2}$	Half saturation concentration of dissolved reactive phosphorus for phytoplankton growth	Model constant	$gP \cdot m^{-3}$
I_S	Saturation light intensity	Model constant	$Watt \cdot m^{-2}$
μ_R	Death rate constant of phytoplankton	Model constant	day^{-1}
C_G	Grazing rate constant of zooplankton	Model constant	day^{-1}
$\theta_{Phyto,G}$	Temperature correction coefficient for phytoplankton growth and non-predatory death	Model constant	Unitless
$\theta_{Phyto,D}$	Temperature correction coefficient for non-predatory phytoplankton death	Model constant	Unitless

A.3 Development of solution schemes for the equations

Numerical integration methods convert a system of differential equation into a system algebraic equation that can be solved easily. The differential terms will simply be converted to difference terms, so that the model will have limited number of points in time and/or space. This process is called discretization. There are many discretization algorithms each of which having its own advantages and disadvantages. There are many excellent numerical methods books that contain details related to discretization algorithms. In this example we will use the simplest discretization method, the explicit Euler algorithm. Since the lake is considered as completely mixed in our model, there is no discretization in space and we only need to discretize in time. In other words, time is the only independent variable. Using the Euler algorithm, Equation A.1 can be

transformed into Equation A.8. In these equations; Δt which is a small time interval, where everything is assumed to be constant is called the time step. The superscript t means that the value at time point t of the relevant variable *(not to be confused with the t-th power operation)* will be used and superscript $t+\Delta t$ means that the value at time point $t+\Delta t$ of the relevant variable will be used. In any case, one important assumption is made that within each time steps, some of the variables are assumed to be frozen on time point t and some on time point $t+\Delta t$. This will always lead to some errors, since we know that in the real world none of the eutrophication related variables are frozen in time. On the other hand, this is the only way to obtain solutions to the model equations. If we take Δt small enough, the errors will be small and we will end up with

an acceptably accurate approximate solution. If Δt is too small, then the calculations will take unnecessary long, if Δt is too large than the solutions will contain larger errors leading to inaccurate results which will diverge from the real case. Further increase of Δt may lead to physically unacceptable results such as negative concentrations and eventually to mathematical errors that may lead the calculation algorithm to destabilize and collapse. This situation is called numerical instability. Unfortunately, for non-linear systems there is no way to tell what could be an optimum value for Δt, but experience shows that for ecological models of completely mixed shallow lakes it is on the order of hours. After the temporal discretization and substation of all terms, and reorganization of terms, the model equations are as follows:

$$\frac{P1^{t+\Delta t} - P1^{t}}{\Delta t} = \frac{W_{P1}^{t}}{V^{t}} - \frac{Q_{OUT}^{t}}{V^{t}} \cdot P1^{t} - \left(K_{12}^{t} + \frac{v_{S,P1}^{t}}{H^{t}}\right) \cdot P1^{t} + D_{P}^{t} \cdot a_{P} \cdot Chl\text{-}A^{t} \qquad \text{(Equation A.7)}$$

$$P1^{t+\Delta t} = P1^{t} + \left(\frac{W_{P1}^{t}}{V^{t}} - \frac{Q_{OUT}^{t}}{V^{t}} \cdot P1^{t} - \left(K_{12}^{t} + \frac{v_{S,P1}^{t}}{H^{t}}\right) \cdot P1^{t} + D_{P}^{t} \cdot a_{P} \cdot Chl\text{-}A^{t}\right) \cdot \Delta t \qquad \text{(Equation A.8)}$$

$$P1^{t+\Delta t} = P1^{t} + \left(\underbrace{\frac{W_{P1}^{t}}{\overline{V}^{t}} - \left(\frac{Q_{OUT}^{t}}{\overline{V}} + \frac{v_{S,P1}^{t}}{\overline{H}}\right) \cdot P1^{t}}_{\text{Transport derivative}} + \underbrace{\left(\mu_{R} \cdot \theta_{Phyto,D}^{TEMP-20} + C_{G}^{t} \cdot Z^{t}\right) \cdot a_{P} \cdot Chl\text{-}A^{t} - K_{12} \cdot \theta_{Phyto,D}^{TEMP-20} \cdot P1^{t}}_{\text{Kinetic derivative}}\right) \cdot \Delta t \qquad \text{(Equation A.9)}$$

$$P2^{t+\Delta t} = P2^{t} + \left(\underbrace{\frac{W_{P2}^{t}}{\overline{V}} - \frac{Q_{OUT}^{t}}{\overline{V}} \cdot P2^{t}}_{\text{Transport derivative}} + \underbrace{K_{12}^{t} \cdot \theta_{Phyto,D}^{TEMP-20} P1^{t} - G_{P}^{t} \cdot a_{P} \cdot Chl\text{-}A^{t}}_{\text{Kinetic derivative}}\right) \cdot \Delta t \qquad \text{(Equation A.10)}$$

$$Chl\text{-}A^{t+\Delta t} = Chl\text{-}A^{t} + \left(\underbrace{\frac{W_{Chl\text{-}A}^{t}}{\overline{V}} - \left(\frac{Q_{OUT}^{t}}{\overline{V}} + \frac{v_{S,Phyto}^{t}}{\overline{H}}\right) \cdot Chl\text{-}A^{t}}_{\text{Transport derivative}} + \underbrace{\left(G_{P}^{t} - \mu_{R} \cdot \theta_{Phyto,D}^{TEMP-20} - C_{G}^{t} \cdot Z^{t}\right) \cdot Chl\text{-}A^{t}}_{\text{Kinetic derivative}}\right) \cdot \Delta t \qquad \text{(Equation A.11)}$$

$$G_{P}^{t} = G_{MAX} \cdot \theta_{Phyto,G}^{TEMP-20} \cdot \min\left(\frac{P2^{t}}{P2^{t} + K_{HS,Phyto,P2}}, \frac{2.718 \cdot f_{day}^{t}}{K_{e}^{t} \cdot \overline{H}} \cdot \left(\exp\left(-\frac{I_{A}^{t}}{I_{S}} \cdot \exp\left(-K_{e}^{t} \cdot \overline{H}\right)\right) - \exp\left(-\frac{I_{A}^{t}}{I_{S}}\right)\right)\right) \qquad \text{(Equation A.12)}$$

$$K_{e}^{t} = K_{b,e} + 0.0088 \cdot Chl - A^{t} + \left(0.054 \cdot \left(Chl - A^{t}\right)^{\frac{2}{3}}\right) \qquad \text{(Equation A.13)}$$

$$\overline{V} = \frac{V^{t} + V^{t+\Delta t}}{2} = \frac{V^{t}}{2} + \frac{V^{t} + \left(Q_{in}^{t} - Q_{out}^{t}\right) \cdot \Delta t}{2} = \frac{2 \cdot V^{t} + \left(Q_{in}^{t} - Q_{out}^{t}\right) \cdot \Delta t}{2} \qquad \text{(Equation A.14)}$$

$$\overline{H} = f\left(\overline{V}\right) \qquad \text{(Equation A.15)}$$

where the terms $\overline{V}$ and $\overline{H}$ represent the volume and spatially mean depth averaged over the time step. The spatially mean depth is assumed to be a function of volume. The derivative terms in equations A.9 to A.11 are divided into transport and kinetic derivatives. This is a good model development practice since transport equations do not change usually, but the kinetic relations may need to be changed if the model has to be extended to include different eutrophication mechanisms.

It is important to consider during the implementation of the model as a tool is that, any variable regardless a state variable, auxiliary variable, forcing factor with a temporal superscript (t+Δt or t) should change in time. The values of P1, P2 and Chl-A must be calculated for each time step from the values of all variables that are superscripted as t. In other words, if the time step is one hour and the model has to be run for a year, Equations A.9 to A.12 must be solved $24 \cdot 365 = 8760$ times ($8760 + 24 = 8784$ times in case of a leap year). From this figures it is clear that computers will be needed to implement the model developed in this section.

A.4. Implementation of the model as a tool

The implementation algorithm of the solution illustrated in Figure 2 is simple and straightforward, where n is the number of time steps for the entire simulation. However; the solution algorithm itself as implemented directly is not a complete modelling tool.

Referring to Section A.2, there are terms in equations that have to be updated every time step. The forcing factors are given to the model from outside so they have to be organized as time series. One option is to read one element for each time step. In the example model however, we will use daily time series for the sake of simplicity. The auxiliary variables should be updated every time step. Considering these necessities, the flowchart of all operations to be conducted by the model is as illustrated in Figure A.3.
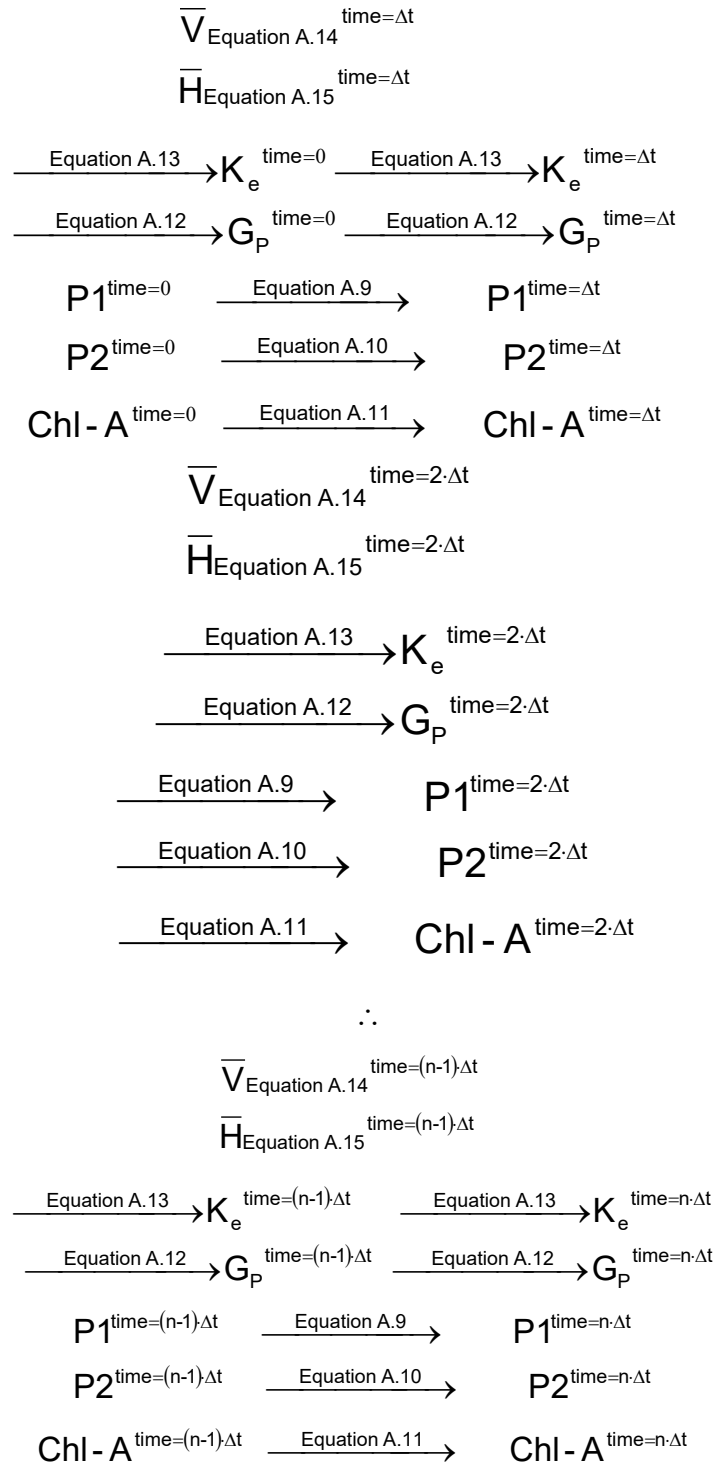
Figure A.2. The implementation algorithm of the model
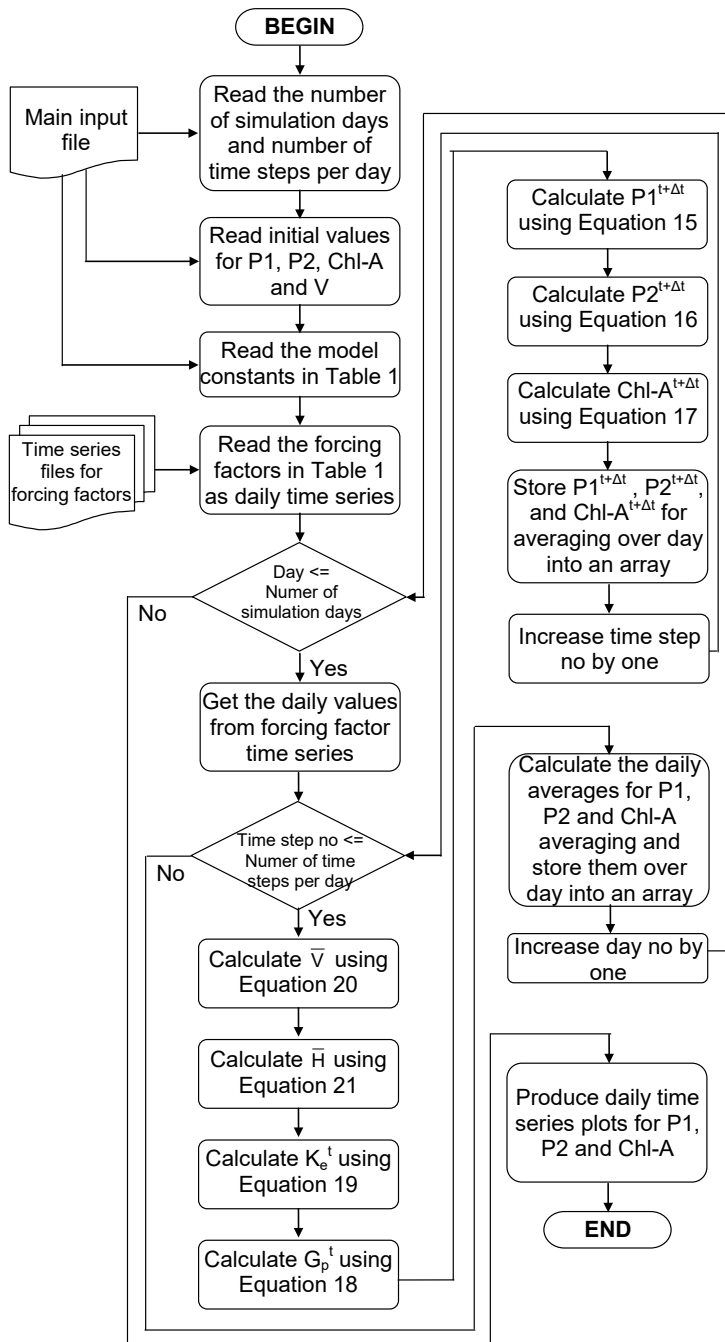
Figure A.3. Flowchart of the operations to be conducted by the model

The flowchart given in Figure A.3. can be coded in any programming language. For this model, we will use MATLAB because

- MATLAB is easy to program
- MATLAB gives a good post processing environment
- MATLAB has many tools that ease to develop a supporting environment for the model

The source code of the model is given below. The program consists of four MATLAB functions listed below:

- Phos_ChlA_Model.m: It is the main function that forms the body of the model following the algorithm that is given in flowchart illustrated in Figure 3.

- TRANSPORT.m: It handles the transport related terms in Equations A.9, A.10 and A.11. If the effects of additional inputs or outflows of nutrients and phytoplankton such as new inflowing or out flowing rivers, then this function will be changed by the user.

- KINETICS.m: It handles the kinetics related terms in Equations A.9, A.10 and A.11. New processes have to be added to the model, then this function will be changed by the user.

- GET_SPATIALLY_AVERAGED_DEPTH.m: It calculates the depth from the volume. According to the source code given in Appendix A, it is designed to calculate the depth of a rectangular prismatic basin with a surface area of 166 km^2. However; it can be extended to handle a variety of situations with the capabilities provided by MATLAB.

The reader should know the basics of MATLAB before starting to explore and modify the code. To keep the example code simple, advanced numerical integration techniques available in MATLAB were not used.

A.5. Development of the supporting environment and tools for the model

Many advanced eutrophication models such as WASP, AQUATOX, EFDC, Delft3D-DELWAQ, MOHID and MIKE have their own graphical model input editors, post processors and even data exchange capabilities with geographical information systems. The example eutrophication model here reads text files or csv files created/edited with text editors or spreadsheet programs and it produces a simple time series plot as output, so one can say that the model has no supporting environment that would ease the modelling process. However, MATLAB itself can be considered as supporting environment for the model developed in this example:

- The main body of the model (function Phos_ChlA_Model) is designed to produce a matrix output for daily results with time index. MATLAB has very powerful functions to process such matrices. For example, one can easily do statistical analysis of the columns. MATLAB has also many options for plotting so that within few commands it would be possible to write powerful graphs. All this commands could be written as scripts each of them not exceeding ten lines of code.

- MATLAB has powerful tools that are useful for general modelling steps such as autocalibration, optimization or more advanced modelling steps such as uncertainty analysis or parameter identification.

Source code of the simple eutrophication model

Phos_ChlA_Model.m

```matlab
function [DAILY_P1, DAILY_P2, DAILY_CHLA] = Phos_ChlA_Model()
    %Read the main input file
    MAIN_INPUT_DATA        = load('MAIN_INPUT.inp');
    NUM_DAYS               = MAIN_INPUT_DATA(1);
    NUM_TIME_STEPS_PER_DAY = MAIN_INPUT_DATA(2);

    %Read the initial conditions
    INITIAL_CONDIITONS     = load('INITIAL_CONDITIONS.inp');
    V_T                    = INITIAL_CONDIITONS(4);

    %Read the model constants file
    MODEL_CONSTANTS        = load('MODEL_CONSTANTS.inp');

    %Read the forcing factors as the daily time series files
    Q_IN_TS                = load('Q_IN.inp');
    Q_OUT_TS               = load('Q_OUT.inp');
    VS_P1_TS               = load('VS_P1.inp');
    VS_CHLA_TS             = load('VS_CHLA.inp');
    W_P1_TS                = load('W_P1.inp');
    W_P2_TS                = load('W_P2.inp');
    W_CHLA_TS              = load('W_CHLA.inp');
    I_A_TS                 = load('I_A.inp');
    TEMP_TS                = load('TEMP.inp');
    FDAY_TS                = load('FDAY.inp');
    Z_TS                   = load('Z.inp');

    STATE_VARIABLES(1)     = INITIAL_CONDIITONS(1);
    STATE_VARIABLES(2)     = INITIAL_CONDIITONS(2);
    STATE_VARIABLES(3)     = INITIAL_CONDIITONS(3);
    DAILY_P1   = zeros(NUM_DAYS);
    DAILY_P2   = zeros(NUM_DAYS);
    DAILY_CHLA = zeros(NUM_DAYS);

    for DAY = 1:NUM_DAYS
        %Get daily values from forcing time series
        FORCING_FACTORS = ...
            [interp1(Q_IN_TS    (:,1), Q_IN_TS    (:,2), DAY_NO + 0.5), ...
             interp1(Q_OUT_TS   (:,1), Q_OUT_TS   (:,2), DAY_NO + 0.5), ...
             interp1(VS_P1_TS   (:,1), VS_P1_TS   (:,2), DAY_NO + 0.5), ...
             interp1(VS_CHLA_TS(:,1), VS_CHLA_TS(:,2), DAY_NO + 0.5), ...
             interp1(W_P1_TS    (:,1), W_P1_TS    (:,2), DAY_NO + 0.5), ...
             interp1(W_P2_TS    (:,1), W_P2_TS    (:,2), DAY_NO + 0.5), ...
             interp1(W_CHLA_TS (:,1), W_CHLA_TS (:,2), DAY_NO + 0.5), ...
             interp1(I_A_TS     (:,1), I_A_TS     (:,2), DAY_NO + 0.5), ...
             interp1(TEMP_TS    (:,1), TEMP_TS    (:,2), DAY_NO + 0.5), ...
             interp1(FDAY_TS    (:,1), FDAY_TS    (:,2), DAY_NO + 0.5), ...
             interp1(Z_TS       (:,1), Z_TS       (:,2), DAY_NO + 0.5)];

        P1_ARRAY   = zeros(NUM_TIME_STEPS_PER_DAY);
        P2_ARRAY   = zeros(NUM_TIME_STEPS_PER_DAY);
        CHLA_ARRAY = zeros(NUM_TIME_STEPS_PER_DAY);
```

```
        for TIME_STEP_NO = 1:NUM_TIME_STEPS_PER_DAY
            %Calculate V using Equation 20
            V = (2 * V_T + ((Q_IN_T - Q_OUT_T) * DT)) / 2;

            %Calculate H using Equation 21
            H = GET_SPATIALLY_AVERAGED_DEPTH(V);

            AUXILLARY_VARIABLES = [V, H];

            %Calculate the transport derivatives
            TRANSPORT_DERIVATIVES = ...
                KINETICS(STATE_VARIABLES, AUXILLARY_VARIABLES,FORCING_FACTORS);
            P1_TRANSPORT_DERIV   = TRANSPORT_DERIVATIVES(1);
            P2_TRANSPORT_DERIV   = TRANSPORT_DERIVATIVES(2);
            CHLA_TRANSPORT_DERIV = TRANSPORT_DERIVATIVES(3);

            %Calculate the kinetic derivatives
            KINETIC_DERIVATIVES = ...
                KINETICS(STATE_VARIABLES, AUXILLARY_VARIABLES, FORCING_FACTORS, MODEL_CONSTANTS);

            P1_KINETIC_DERIV   = KINETIC_DERIVATIVES(1);
            P2_KINETIC_DERIV   = KINETIC_DERIVATIVES(2);
            CHLA_KINETIC_DERIV = KINETIC_DERIVATIVES(3);
            P1_T               = STATE_VARIABLES(1);
            P2_T               = STATE_VARIABLES(2);
            CHLA_T             = STATE_VARIABLES(3);

            %Calculate P1_T_PLUS_DT using Equation 15
            P1_T_PLUS_DT   = P1_T + (P1_TRANSPORT_DERIV + P1_KINETIC_DERIV) * DELTA_T;

            %Calculate P2_T_PLUS_DT using Equation 16
            P2_T_PLUS_DT   = P2_T + (P2_TRANSPORT_DERIV + P2_KINETIC_DERIV) * DELTA_T;

            %Calculate CHLA_T_PLUS_DT using Equation 17
            CHLA_T_PLUS_DT = CHLA_T + (CHLA_TRANSPORT_DERIV + CHLA_KINETIC_DERIV) * DELTA_T;
            P1_ARRAY(TIME_STEP_NO)   = P1_PLUS_DT;
            P2_ARRAY(TIME_STEP_NO)   = P2_PLUS_DT;
            CHLA_ARRAY(TIME_STEP_NO) = CHLA_T_PLUS_DT;
            STATE_VARIABLES(1) = P1_T_PLUS_DT;
            STATE_VARIABLES(2) = P2_T_PLUS_DT;
            STATE_VARIABLES(3) = CHLA_T_PLUS_DT;
            V_T = V;
        end

        DAILY_P1(DAY_NO)   = mean(P1_ARRAY);
        DAILY_P2(DAY_NO)   = mean(P1_ARRAY);
        DAILY_CHLA(DAY_NO) = mean(P1_ARRAY);
    end

    DAYS = 1:NUM_DAYS;
    plot(DAYS, DAILY_P1(DAY_NO), DAYS, DAILY_P2(DAY_NO), DAYS, DAILY_CHLA(DAY_NO));
end
```

KINETICS.m

```
function [P1_KIN_DERIV, P2_KIN_DERIV, CHLA_KIN_DERIV] = KINETICS ...
        (STATE_VARIABLES, AUXILLARY_VARIABLES, FORCING_FACTORS, ...
         MODEL_CONSTANTS)
    P1             = STATE_VARIABLES(1);
    P2             = STATE_VARIABLES(2);
    CHLA           = STATE_VARIABLES(3);
    H              = AUXILLARY_VARIABLES(1);
    I_A_T          = FORCING_FACTORS(8);
    TEMP_T         = FORCING_FACTORS(9);
    FDAY_T         = FORCING_FACTORS(10);
    Z_T            = FORCING_FACTORS(11);
    A_P            = MODEL_CONSTANTS(1);
    K_B_E          = MODEL_CONSTANTS(2);
    K_12           = MODEL_CONSTANTS(3);
```

```matlab
    THETA_DECOMP   = MODEL_CONSTANTS(4);
    G_MAX          = MODEL_CONSTANTS(5);
    K_HS_PHYTO_P2  = MODEL_CONSTANTS(6);
    I_S            = MODEL_CONSTANTS(7);
    MU_R           = MODEL_CONSTANTS(8);
    C_G            = MODEL_CONSTANTS(9);
    THETA_PHYTO_G  = MODEL_CONSTANTS(10);
    THETA_PHYTO_D  = MODEL_CONSTANTS(11);

    %Calculate K_E_T using Equation 19
    K_E_T = K_B_E + (0.088 * CHLA) + (0.054 * (CHLA.^(2/3)));

    %Calculate G_P_T using Equation 18
    G_P_T = G_MAX * (THETA_PHYTO_G.^(TEMP - 20)) * ...
            min((P2 / (P2 + K_HS_PHYTO_P2)),(((2.718 * FDAY_T) / (K_E_T * H)) * ...
            (exp(-(I_A_T / I_S) * exp(-K_E_T * H)) - exp(-(I_A_T / I_S)))));

    %Calculate the kinetic derivative for P1
    P1_KIN_DERIV   = (MU_R * THETA_PHYTO_D.^(TEMP_T - 20)) * A_P * CHLA - ...
                     (K_12 * THETA_DECOMP.^(TEMP_T - 20)) * P1;

    %Calculate the kinetic derivative for P2
    P2_KIN_DERIV   = (K_12 * THETA_DECOMP.^(TEMP_T - 20)) * P1 - G_P_T * A_P * CHLA;

    %Calculate the kinetic derivative for CHLA
    CHLA_KIN_DERIV =  (G_P_T - MU_R * THETA_PHYTO_D.^(TEMP_T - 20) - C_G * Z_T) * A_P * CHLA;
end
```

TRANSPORT.m

```matlab
function [P1_TRANS_DERIV, P2_TRANS_DERIV, CHLA_TRANS_DERIV] = TRANSPORT ...
        (STATE_VARIABLES, AUXILLARY_VARIABLES, FORCING_FACTORS)
    P1         = STATE_VARIABLES(1);
    P2         = STATE_VARIABLES(2);
    CHLA       = STATE_VARIABLES(3);
    V          = AUXILLARY_VARIABLES(1);
    H          = AUXILLARY_VARIABLES(2);
    Q_OUT_T    = FORCING_FACTORS(2);
    VS_P1_T    = FORCING_FACTORS(3);
    VS_CHLA_T  = FORCING_FACTORS(4);
    W_P1_T     = FORCING_FACTORS(5);
    W_P2_T     = FORCING_FACTORS(6);
    W_CHLA_T   = FORCING_FACTORS(7);

    %Calculate the kinetic derivative for P1
    P1_TRANS_DERIV   = (W_P1_T / V) - ((Q_OUT_T / V) + (VS_P1_T / H)) * P1;

    %Calculate the kinetic derivative for P2
    P2_TRANS_DERIV   = (W_P2_T / V) - (Q_OUT_T / V) * P2;

    %Calculate the kinetic derivative for CHLA
    CHLA_TRANS_DERIV =  (W_CHLA_T / V) - .((Q_OUT / V) + (VS_CHLA_T / H)) * CHLA;
end
```

GET_SPATIALLY_AVERAGED_DEPTH.m

```matlab
function [DEPTH] = GET_SPATIALLY_AVERAGED_DEPTH(V)
    % A very simple representation of bathymetry. It is the users
    % to program this function to represent the bathymetry of his/her lake
    % realistically
    AREA  = 166000000;
    DEPTH = V / AREA;
end
```

APPENDIX B

Solving the Hydrodynamic Equations

Hydrodynamic equations are relatively more difficult to solve. The task becomes more challenging if they have to be solved in three dimensions. Here, the solution of simplified version of two dimensional hydrodynamic equations is shown. This type of hydrodynamic models can be applied to deep and narrow waterbodies that are well mixed laterally but not longitudinally or vertically.

There are two basic equations in hydrodynamics, the continuity equation and the momentum equation. The simplified versions of these equations for the so called x-z model are given below,

Continuity equation in longitudinal and vertical dimensions:

$$\frac{\partial V}{\partial t} + \frac{\partial U}{\partial x} = 0 \qquad \text{(Equation B.1)}$$

Momentum equation in longitudinal and vertical dimensions:

$$B \cdot \frac{\partial u}{\partial t} = -g \cdot B \cdot \frac{\partial \eta}{\partial x} + \frac{\partial}{\partial z}\left(A_z \cdot B \cdot \frac{\partial u}{\partial z}\right) - \text{friction terms}$$

$$\text{(Equation B.2)}$$

where, U is the velocity integrated over the depth therefore in volumetric flow rate dimensions [$L^3 \cdot T^{-1}$], V is the control volume over which the continuity equation is solved [L^3], B is the width the channel as a function of depth [L], g is the gravitational acceleration [$L \cdot T^{-2}$] u is the velocity in x direction [L], η is the water surface elevation [L] and A_z is the eddy viscosity. Equation B2 is derived from the Navier-Stokes equations, however it is simplified so that the non-linear advective inertia terms are neglected.

Even though the hydrodynamic equations are in simplified form, there is no direct analytical solution for them. Therefore, numerical solution schemes have to be applied. To apply a numerical solution scheme it is necessary to discretize the hydrodynamic equation on time and space.

There are many spatial discretization schemes for hydrodynamic equations. In this example, we will use the cell-link scheme. This scheme is efficient and easy to apply. If is more compatible with box models, if the results from the hydrodynamic model are to be imported into a box model described by Equation 14. In this discretization scheme, a waterbody is assumed to consist of basins that exchange water with each other through channels. An example model domain is given in Figure B.1. Each basin is represented with a cell and each channel is represented with a link. A link is between two cells. The flow directions are assumed to be from one cell (begin) to another (end). If the actual flow direction is opposite or the flow reveres during the simulation, then a simply a negative velocity will be returned by the model.

The surface area of a channel is calculated by Equation B.3

$$A_{surf} = \sum_{channel=1}^{\substack{\text{Number of} \\ \text{channels}}} \frac{\Delta x_{channel} \cdot B_{channel}}{2}$$

$$\text{(Equation B.3)}$$

Where A_{surf} is the surface area [L^2], $\Delta x_{channel}$ is the length of the channel that is connecting a cell with another cell [L]. If Equation B.1 is divided by the surface area, then Equation B.4 is obtained,

$$\frac{\partial \eta}{\partial t} + \frac{1}{A_{surf}} \cdot \frac{\partial U}{\partial x} = 0 \qquad \text{(Equation B.4)}$$

where the term $\dfrac{\partial \eta}{\partial t}$ would correspond to the change of depth over time. Since it is a derivative and chance of depth over time is the same as change of water surface elevation over time, we can use the term as change of water surface elevation over time. The latter definition is more convenient to solve the momentum equation. Discretizing Equation B.4 spatially according to cell, node scheme yields Equation B.5.

$$\frac{\partial \eta_{Cell}}{\partial t} = \frac{1}{A_{surf}} \cdot \left(\sum_{Inflow=1}^{\substack{\text{Number of} \\ \text{inflowing} \\ \text{channels}}} \sum_{k=1}^{\substack{\text{Number of} \\ \text{layers}}} u_{Inflow,k} \cdot h_k \cdot B_k - \sum_{Outflow=1}^{\substack{\text{Number of} \\ \text{outflowing} \\ \text{channels}}} \sum_{k=1}^{\substack{\text{Number of} \\ \text{layers}}} u_{Outflow} \cdot h_k \cdot B_k \right)$$

$$\text{(Equation B.5)}$$

where u is the velocity in a layer of a channel [$L \cdot T^{-1}$], h is the layer depth [L] and B is the layer width [L]. Discretizing Equation B.5 over time yields Equation B.6.
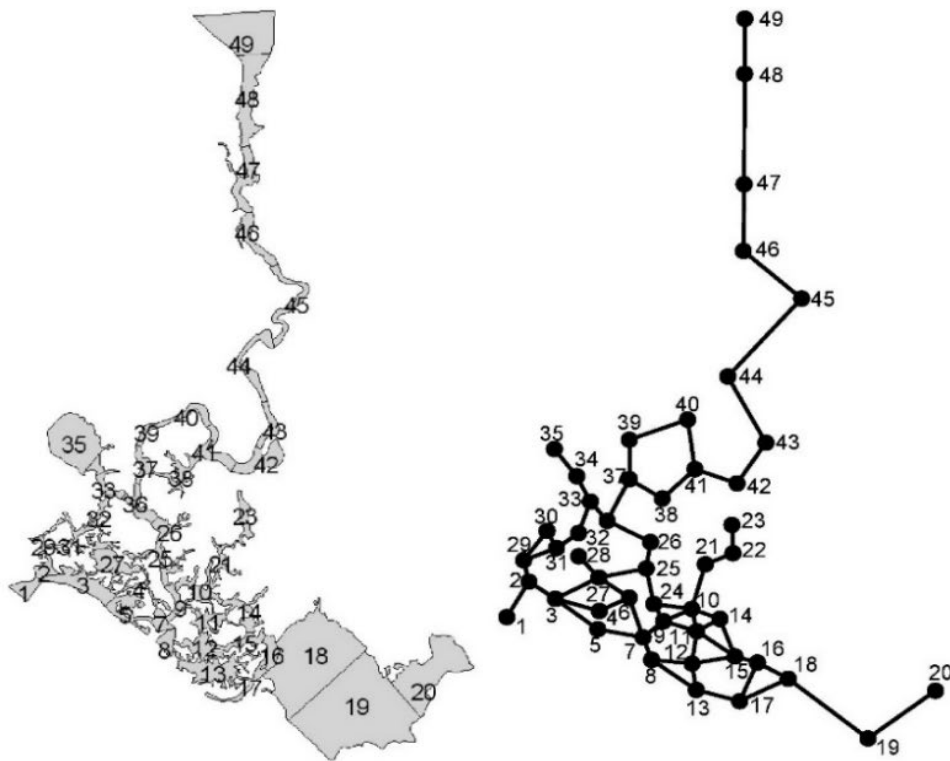
Figure B.1. The cell-node scheme discretization

Channel No	Cell 1	Cell 2
1	2	1
2	3	2
3	5	3
4	4	3
5	27	3
6	7	5
7	6	4
8	27	6
9	28	27
10	25	27
11	6	7
12	25	24
13	24	9
14	24	10
15	10	9
16	9	7
17	8	7
18	12	8
19	9	11
20	10	11
21	10	14

Channel No	Cell 1	Cell 2
22	14	15
23	11	12
24	14	15
25	11	15
26	15	12
27	12	13
28	13	8
29	17	13
30	15	16
31	16	17
32	16	18
33	18	17
34	19	18
35	20	19
36	21	10
37	22	21
38	23	22
39	29	2
40	30	29
41	31	29
42	31	30

Channel No	Cell 1	Cell 2
43	32	31
44	33	32
45	33	34
46	34	35
47	36	33
48	36	26
49	26	25
50	37	36
51	38	37
52	41	38
53	39	37
54	40	39
55	41	40
56	42	41
57	43	42
58	44	43
59	45	44
60	46	45
61	47	46
62	48	47
63	49	48

Channel No	Cell 1	Cell 2
64	Koycegiz Lake Boundary	49
65	1	Mediterranean Sea Boundary

The discretization of the momentum equation (Equation B.2) is more complicated. The momentum equation must be discretized horizontally on channels and vertically for each layer, where each layer is interacting with the layers above and below. The first layer is interacting with the atmosphere and the second layer and the lowest layer is interacting with its upper layer and the bottom. Each layer has an upper and lower interaction. The general form of discretized momentum equation for a channel is given in Equation B.7 to B.9.

$$\eta_{Cell}^{t+\Delta t} = \eta_{Cell}^{t} + \frac{\Delta t}{A_{surf}} \cdot \left(\underbrace{\sum_{Inflow=1}}_{\substack{\text{Number of} \\ \text{inflowing} \\ \text{channels}}} \underbrace{\sum_{k=1}}_{\substack{\text{Number of} \\ \text{layers}}} u_{Inflow,k} \cdot h_k \cdot B_k - \underbrace{\sum_{Outflow=1}}_{\substack{\text{Number of} \\ \text{outflowing} \\ \text{channels}}} \underbrace{\sum_{k=1}}_{\substack{\text{Number of} \\ \text{layers}}} u_{Outflow} \cdot h_k \cdot B_k \right)$$

(Equation B.6)

$$-B_k \cdot \Delta t \cdot C_{upper} \cdot u_{k-1}^{t+\Delta t} + \left(B_k \cdot h_k^{t+\Delta t} + B_k \cdot \Delta t \cdot C_{upper} + B_k \cdot \Delta t \cdot C_{lower} \right) \cdot u_k^{t+\Delta t} - B_k \cdot \Delta t \cdot C_{lower} \cdot u_{k+1}^{t+\Delta t} =$$

$$B_k \cdot h_k^t \cdot u_k^t - g \cdot h_k^{t+\Delta t} \cdot B_k \cdot \frac{\eta_{end}^{t+\Delta t} - \eta_{begin}^{t+\Delta t}}{\Delta x} \cdot \Delta t$$

(Equation B.7)

$$C_{upper} = \frac{2 \cdot A_z}{h_{k-1} + h_k}$$

(Equation B.8)

$$C_{lower} = \frac{2 \cdot A_z}{h_k + h_{k+1}}$$

(Equation B.9)

For the first layer, Equation B.10 and Equation B.11 are substituted into Equation B.7

$$C_{upper} = 0$$

(Equation B.10)

$$k=1$$

$$\left(B_1 \cdot h_1^{t+\Delta t} + B_1 \cdot \Delta t \cdot \frac{2 \cdot A_z}{h_1^{t+\Delta t} + h_2^{t+\Delta t}} \right) \cdot u_1^{t+\Delta t} - B_1 \cdot \Delta t \cdot \frac{2 \cdot A_z}{h_1^{t+\Delta t} + h_2^{t+\Delta t}} \cdot u_2^{t+\Delta t} = B_1 \cdot h_1^{t+\Delta t} \cdot \left(u_1^t - g \cdot \frac{\eta_{end}^{t+\Delta t} - \eta_{begin}^{t+\Delta t}}{\Delta x} \cdot \Delta t \right)$$

(Equation B.11)

Equation B.10 indicates that there is no interaction with the atmosphere. If the interaction with the atmosphere such as the effect of wind shear stress is important, then Equation B.10 should be modified accordingly. For an intermediate layer Equation B.8 and Equation B.9 are substituted into Equation B.7

$$-B_k \cdot \Delta t \cdot \frac{2 \cdot A_z}{h_{k-1}^{t+\Delta t} + h_k^{t+\Delta t}} \cdot u_{k-1}^{t+\Delta t} + \left(B_k \cdot \left(h_k^{t+\Delta t} + 2 \cdot A_z \cdot \Delta t \left(\frac{1}{h_{k-1}^{t+\Delta t} + h_k^{t+\Delta t}} + \frac{1}{h_k^{t+\Delta t} + h_{k+1}^{t+\Delta t}} \right) \right) \right) \cdot u_k^{t+\Delta t} -$$

$$B_k \cdot \Delta t \cdot \frac{2 \cdot A_z}{h_k^{t+\Delta t} + h_{k+1}^{t+\Delta t}} \cdot u_{k+1}^{t+\Delta t} = B_k \cdot h_k^{t+\Delta t} \cdot \left(u_k^t - g \cdot \frac{\eta_{end}^{t+\Delta t} - \eta_{begin}^{t+\Delta t}}{\Delta x} \cdot \Delta t \right)$$

(Equation B.12)

For the last layer Equations B.13 to Equation B.16 are substituted into Equation B.7

$$C_{upper} = \frac{2 \cdot A_z}{h_{k-1} + h_k}$$

(Equation B.13)

$$C_{lower} = C_D \cdot \left| u_L^t \right|$$ (Equation B.14)

$$u_{k+1}^{t+\Delta t} = 0$$ (Equation B.15)

k=L (Equation B.16)

where L is the number of layers

$$-B_k \cdot \Delta t \cdot \frac{2 \cdot A_z}{h_{k-1}^{t+\Delta t} + h_k^{t+\Delta t}} \cdot u_{L-1}^{t+\Delta t} + \left(B_L \cdot \left(h_L^{t+\Delta t} + \Delta t \cdot \left(\frac{2 \cdot A_z}{h_{k-1}^{t+\Delta t} + h_k^{t+\Delta t}} + C_D \cdot \left| u_L^t \right| \right) \right) \right) \cdot u_L^{t+\Delta t} =$$

(Equation B.17)

$$B_L \cdot h_L^{t+\Delta t} \cdot \left(u_L^t - g \cdot \frac{\eta_{end}^{t+\Delta t} - \eta_{begin}^{t+\Delta t}}{\Delta x} \cdot \Delta t \right)$$

Equation B.13 represents the friction whereas Equation B.14 is the boundary condition for the velocity. The eddy viscosity A_z can be calculated by a number of formulae. The steps of the solution algorithm are simple and straightforward:

- Step 1: Solve equation B.6 for each cell to calculate $\eta_{Cell}^{t+\Delta t}$

- Step 2: Solve equation B.7 for each cell to channel in each layer to calculate $u_L^{t+\Delta t}$

As seen by the general form of discretized momentum equation (Equation B.7), $u_L^{t+\Delta t}$ depends on $u_{k-1}^{t+\Delta t}$ and $u_{k+1}^{t+\Delta t}$. In other words, the velocity of a layer at the next time steps depends on the velocities on the upper and lower layers. This means that the momentum equations for all the layers in a channel have to be solved simultaneously. Another issue is that, the horizontal density differences should be taken into account. If the density currents are important then, the water surface elevation terms $\eta_{begin}^{t+\Delta t}$ and $\eta_{end}^{t+\Delta t}$ must be corrected with pressure gradient terms calculated at the centre of each layer. A free form Fortran source code listing, that would construct the coefficient matrix and constants vector a for a channel is given below:

```fortran
do k = 1, NUM_LAYERS
    C_UP   = 2.0 * A_Z(i,k-1) / (H(i,k-1,2) + H(i,k,2))
    C_DOWN = 2.0 * A_Z(i,k)   / (H(i,k,2) + H(i,k+1,2))
    if(k .eq. 1) C_UPPER = 0.0D0
    if(k .eq. NUM_LAYERS) C_LOWER = 0.0D0

    !Bands of the coefficient matrix C:Subdiagonal, D:Diagonal, E:Super diagonal
    C(k) = (-B(i,k) * DT * C_UPPER)
    D(k) = B(i,k) * H(i,k,2) +  DT * B(i,k) * (C_UPPER + C_LOWER)
    E(k) = (-B(i,k) * DT * C_LOWER)
    LEVEL_GRAD = ITA  (C_END,2) - ITA  (C_BEGIN,2)
    PRESS_GRAD = PRESS(C_END,k) - PRESS(C_BEGIN,k)

    !Constant vector
    F(k) = (B(i,k) * H(i,k,2) * U(i,k,1)) - &
           (B(i,k) * H(i,k,2) * G * ((LEVEL_GRAD + PRESS_GRAD) / DX) * DT)
    if(k.eq.NUM_LAYERS) D(k) = D(k) + (B(i,k) * DT * C_D * dabs(U(i,k,1)))
end do
```

The three-banded matrix can then easily be solved using the Thomas algorithm.

As one can see in the source code listing, pressure gradient terms should be known before solving the momentum equation. Pressure depends on density that depends on salinity and temperature. On the other hand, salinity and temperature depend on the hydrodynamic transport. This means that a mass balance equation must be solved for salinity (Equations B.18 to B.20). Unlike the continuity equation, a negative flow direction is much more important here, because the flow from opposite direction will completely change the amount of salt

mass inflow and outflow, since salinity is expected to change in horizontal and vertical directions. Therefore, before solving Equation B.18 for a time step, the upstream and downstream channels for a cell must be determined by checking the velocities. Any channel that causes an inflow is an upstream channel (subscripted as ups), and any channel that causes an outflow is a downstream channel (subscripted as dws).

$$
\frac{\partial S_{i,k}}{\partial t} = \frac{1}{V_{i,k}} \left(\sum_{ups=1}^{\substack{\text{Number of}\\\text{inflowing}\\\text{channels}}} u_{ups,k} \cdot h_{ups,k} \cdot B_{ups,k} \cdot S_{ups,k} - \sum_{dws=1}^{\substack{\text{Number of}\\\text{outflowing}\\\text{channels}}} u_{dws,k} \cdot h_{dws,k} \cdot B_{dws,k} \cdot S_{i,k} + \right.
$$
$$
w_{upper,ups,k} \cdot A_{surf,k} \cdot S_{i,k-1} - w_{upper,dws,k} \cdot A_{surf,k} \cdot S_{i,k} +
$$
$$
\left. w_{lower,ups,k} \cdot A_{surf,k+1} \cdot S_{i,k+1} - w_{lower,dws,k} \cdot A_{surf,k+1} \cdot S_{i,k} + Svdisp + Shdisp \right)
$$

(Equation B.18)

$$
Svdisp = \frac{\partial}{\partial z}\left(K_z \cdot A_{int,v} \cdot \frac{\partial S}{\partial z} \right)
$$

(Equation B.19)

$$
Shdisp = \frac{\partial}{\partial x}\left(K_x \cdot A_{int,h} \cdot \frac{\partial S}{\partial x} \right)
$$

(Equation B.20)

The terms used in Equations B.18 to B.20 are listed below:

i	: Index for cell no
k	: Index for layer no
S	: Salinity $[M \cdot L^{-3}]$
$w_{upper,ups,k}$	: Downwelling velocity from upper layer (considered as inflow) $[L \cdot T^{-1}]$
$w_{upper,dws,k}$	: Upwelling velocity to upper layer (considered as outflow) $[L \cdot T^{-1}]$
$w_{lower,ups,k}$	: Upwelling velocity from upper layer (considered as inflow) $[L \cdot T^{-1}]$
$w_{lower,dws,k}$	: Downwelling velocity to lower layer (considered as outflow) $[L \cdot T^{-1}]$
$Svdisp$	: Exchange of salt mass by vertical dispersion $[M \cdot T^{-1}]$
$Shdisp$	: Exchange of salt mass by horizontal dispersion $[M \cdot T^{-1}]$
K_z	: Vertical eddy diffusivity $[L^2 \cdot T^{-1}]$
K_x	: Horizontal eddy diffusivity $[L^2 \cdot T^{-1}]$
$A_{int,v}$	: Vertical interface area $[L^2]$
$A_{int,H}$	: Horizontal interface area $[L^2]$

The vertical dispersion term is discretized as below:

$$\text{Svdiff} = \left(DS_{upper} \cdot \left(S_{i,k\text{-}1} - S_{i,k} \right) - DS_{lower} \cdot \left(S_{i,k} - S_{i,k+1} \right) \right) \qquad \text{(Equation B.21)}$$

$$DS_{upper} = \frac{2 \cdot K_z \cdot A_{surf,i,k}}{h_{k\text{-}1} + h_k} \qquad \text{(Equation B.22)}$$

$$DS_{lower} = \frac{2 \cdot K_z \cdot A_{surf,i,k+1}}{h_k + h_{k+1}} \qquad \text{(Equation B.23)}$$

Substitution of Equation 21 into Equation 18 and rearrangements yield Equation B.24 that is the spatially and temporally discretized salt mass balance

$$-\left(\frac{\Delta t \cdot \left(w_{upper,ups,k} \cdot A_{surf,k} \right) + DS_{upper}}{V_{i,k}} \right) \cdot S_{i,k\text{-}1}^{t+\Delta t} +$$

$$\left(\frac{\Delta t \cdot \left(w_{upper,dws,k} \cdot A_{surf,k} + w_{lower,dws,k} \cdot A_{surf,k+1} + DS_{upper} + DS_{lower} \right)}{V_{i,k}} + 1 \right) \cdot S_{i,k}^{t+\Delta t}$$

$$-\left(\frac{\Delta t \cdot \left(DS_{lower} + w_{lower,ups,k} \cdot A_{surf,k+1} \right)}{V_{i,k}} \right) \cdot S_{i,k+1}^{t+\Delta t} = \qquad \text{(Equation B.24)}$$

$$S_{i,k}^{t} + \frac{\Delta t}{V_{i,k}} \cdot \left(\overset{\substack{\text{Number of}\\\text{inflowing}\\\text{channels}}}{\underset{ups=1}{\sum}} u_{ups,k} \cdot h_{ups,k} \cdot B_{ups,k} \cdot S_{ups,k}^{t} - \overset{\substack{\text{Number of}\\\text{outflowing}\\\text{channels}}}{\underset{dws=1}{\sum}} u_{dws,k} \cdot h_{dws,k} \cdot B_{dws,k} \cdot S_{i,k}^{t} + \overset{\substack{\text{Number of}\\\text{neighbouring}\\\text{cells}}}{\underset{n=1}{\sum}} \text{Shdiff}_n \right)$$

As seen in Equation B.24, all layers in a cell must be solved simultaneously resulting in a linear system of equations to be solved. Like for the momentum equations, a three-banded coefficient matrix is solved. The free formatted Fortran source code listing illustrates the generation and solution of the equation system is given below.

The detailed solution algorithm is given in Figure B.1. The full version of the algorithm as a Fortran program can be made available upon request from the author

```fortran
!Generate right hand sides
do i = 1, NUM_CELLS
    do k = 1, NUM_LAYERS
        SALT_FS(i,k) = SALT(i,k,1)
    end do
end do

do i = 1, NUM_LINKS
    C_BEGIN = BEGIN_CELL_NOS(i)
    C_END   = END_CELL_NOS  (i)

    do k = 1, NUM_LAYERS
        if (U(i,k,2) >= 0.0D0) then
            H_UPSTREAM   = C_BEGIN
            H_DOWNSTREAM = C_END
        else
            H_DOWNSTREAM = C_BEGIN
            H_UPSTREAM   = C_END
        end if

        FLOW_RATE = dabs(U(i,k,2) * H(i,k,2) * B(i,k)) !Horizontal advection

        !Horizontal dispersion
        HS_DISP   = ((K_X * H(i,k,2) * B(i,k)) / LENGTHS(i)) * &
                    (SALT(H_UPSTREAM,k,1) - SALT(H_DOWNSTREAM,k,1))

        if (H_UPSTREAM > 0) SALT_FS(H_UPSTREAM,k) = &
            SALT_FS(H_UPSTREAM,k) - ((DT/VOLS(H_UPSTREAM  , k)) * (FLOW_RATE * &
                SALT(H_UPSTREAM,k,1) + HS_DISP))

        if (H_DOWNSTREAM > 0) SALT_FS(H_DOWNSTREAM,k) = &
            SALT_FS(H_DOWNSTREAM,k) + ((DT/VOLS(H_DOWNSTREAM, k)) * (FLOW_RATE * &
                SALT(H_UPSTREAM,k,1) + HS_DISP))
    end do
end do

do i = 1, NUM_CELLS    !Generate the coefficient matrix
    C = 0.0D0
    D = 0.0D0
    E = 0.0D0
    F = 0.0D0
    W(i,1) = 0.0D0
    W(i,NUM_LAYERS+1) = 0.0D0

    do k = 1, NUM_LAYERS !Generate the matrix for salt mass balance equation
        DS_UPPER = 2.0 * K_Z(i,k-1) / (H(i,k-1,2) + H(i,k,2))
        DS_LOWER = 2.0 * K_Z(i,k)   / (H(i,k,2)   + H(i,k+1,2))

        if (W(i,k+1) >= 0.0D0) then
            W_LOWER_UPS = dabs(W(i,k+1))
            W_LOWER_DWS = 0.0D0
        else
            W_LOWER_UPS = 0.0D0
            W_LOWER_DWS = dabs(W(i,k+1))
        end if

        if (W(i,k) >= 0.0D0) then
            W_UPPER_DWS = dabs(W(i,k))
            W_UPPER_UPS = 0.0D0
        else
            W_UPPER_DWS = 0.0D0
            W_UPPER_UPS = dabs(W(i,k))
        end if

        if(k.eq.1) DS_UPPER = 0.0D0
        if(k.eq.NUM_LAYERS) DS_LOWER = 0.0D0
        C(k) = (-DT * (W_UPPER_UPS * A_SURFS(i,k)) + DS_UPPER) / VOLS(i,k)

        D(k) = ((DT * ((W_UPPER_DWS * A_SURFS(i,k))   + &
                       (W_LOWER_DWS * A_SURFS(i,k+1))+ &
                        DS_UPPER + DS_LOWER)) / VOLS(i,k)) + 1.0D0

        E(k) = (-DT * (W_LOWER_UPS * A_SURFS(i,k+1)) + DS_LOWER) / VOLS(i,k)
        F(k) = SALT_FS(i,k)
    end do

    INFO = 0
    call SOLVE_MATRIX_THOMAS(NUM_LAYERS, C, D, E, F, INFO)     !Solve the matrix

    do k = 1, NUM_LAYERS    !Get the solution vector
        SALT(i,k,2) = F(k)
    end do
end do
```
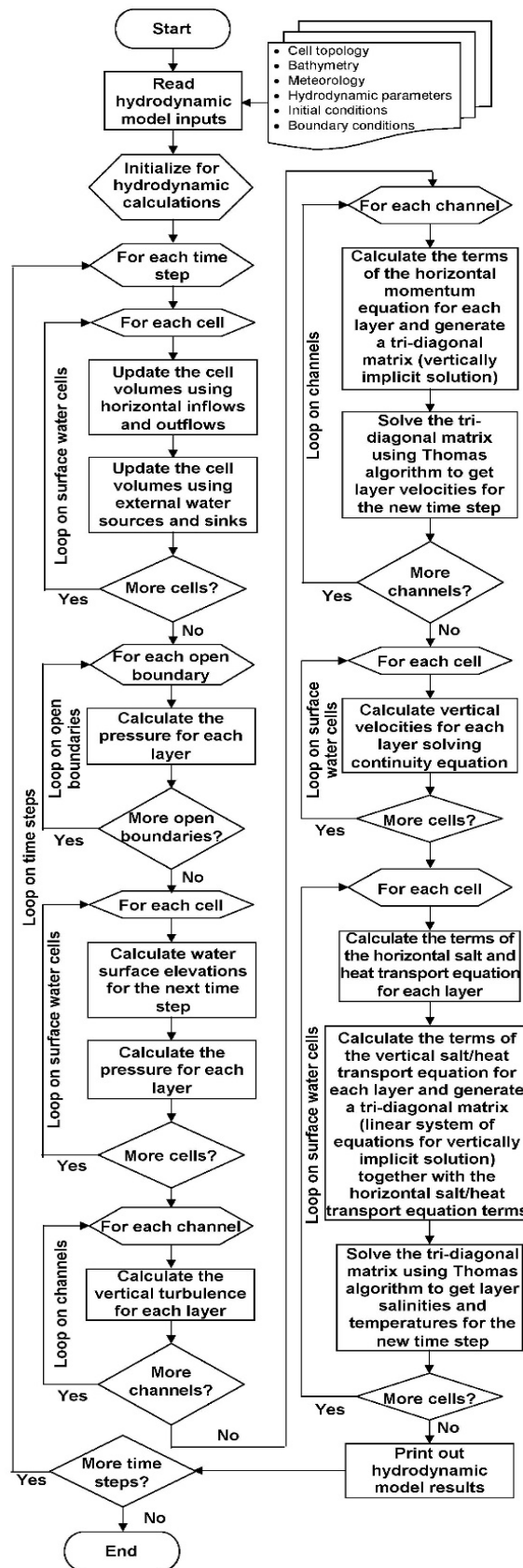
Figure B.1. Solution algorithm for the example hydrodynamic model

Instructions to Authors

The editorial and publication processes of the journal are shaped in accordance with the guidelines of the Committee on Publication Ethics (COPE), the European Association of Science Editors (EASE), the International Council of Medical Journal Editors (ICMJE), and National Information Standards Organization (NISO). The journal conforms to the Principles of Transparency and Best Practice in Scholarly Publishing (https://doaj.org/bestpractice).

Originality, high scientific quality, and citation potential are the most important criteria for a manuscript to be accepted for publication. Manuscripts submitted for evaluation should not have been previously presented or already published in an electronic or printed medium. The journal should be informed of manuscripts that have been submitted to another journal for evaluation and rejected for publication. The submission of previous reviewer reports will expedite the evaluation process. Manuscripts that have been presented in a meeting should be submitted with detailed information on the organization, including the name, date, and location of the organization.

Manuscripts submitted to "**Aquatic Research**" will go through a double-blind peer-review process. Each submission will be reviewed by at least two external, independent peer reviewers who are experts in their fields in order to ensure an unbiased evaluation process. The editorial board will invite an external and independent editor to manage the evaluation processes of manuscripts submitted by editors or by the editorial board members of the journal. The Editor in Chief is the final authority in the decision-making process for all submissions.

An approval of research protocols by the Ethics Committee in accordance with international agreements (World Medical Association Declaration of Helsinki "Ethical Principles for Medical Research Involving Human Subjects," amended in October 2013, www.wma.net) is required for experimental, clinical, and drug studies. If required, ethics committee reports or an equivalent official document will be requested from the authors.

For manuscripts concerning experimental research on humans, a statement should be included that shows the written informed consent of patients and volunteers was obtained following a detailed explanation of the procedures that they may undergo. Information on patient consent, the name of the ethics committee, and the ethics committee approval number should also be stated in the Materials and Methods section of the manuscript. It is the authors' responsibility to carefully protect the patients' anonymity. For photographs that may reveal the identity of the patients, signed releases of the patient or of their legal representative should be enclosed.

"**Aquatic Research**" journal requires experimental research studies on vertebrates or any regulated invertebrates to comply with relevant institutional, national and/or international guidelines. The journal supports the principles of Basel

Declaration (https://www.basel-declaration.org/) and the guidelines published by International Council for Laboratory Animal Science (ICLAS) (http://iclas.org/). Authors are advised to clearly state their compliance with relevant guidelines.

"**Aquatic Research**" journal advises authors to comply with IUCN Policy Statement on Research Involving Species at Risk of Extinction and the Convention on the Trade in Endangered Species of Wild Fauna and Flora for research involving plants.

All submissions are screened by a similarity detection software (iThenticate by CrossCheck).

In the event of alleged or suspected research misconduct, e.g., plagiarism, citation manipulation, and data falsification/ fabrication, the Editorial Board will follow and act in accordance with COPE guidelines.

Each individual listed as an author should fulfil the authorship criteria recommended by the ICMJE. The ICMJE recommends that authorship be based on the following 4 criteria:

1. Substantial contributions to the conception or design of the work; or the acquisition, analysis, or interpretation of data for the work; AND

2. Drafting the work or revising it critically for important intellectual content; AND

3. Final approval of the version to be published; AND

4. Agreement to be accountable for all aspects of the work in ensuring that questions related to the accuracy or integrity of any part of the work are appropriately investigated and resolved.

In addition to being accountable for the parts of the work he/she has done, an author should be able to identify which co-authors are responsible for specific other parts of the work. In addition, authors should have confidence in the integrity of the contributions of their co-authors.

All those designated as authors should meet all four criteria for authorship, and all who meet the four criteria should be identified as authors. Those who do not meet all four criteria should be acknowledged in the title page of the manuscript.

"**Aquatic Research**" journal requires corresponding authors to submit a signed and scanned version of the authorship contribution form (available for download through **http://scientificwebjournals.com/AquatRes/AquatResCopyright andAuthorContributionForm2019.pdf**) during the initial submission process in order to act appropriately on authorship rights and to prevent ghost or honorary authorship. If the editorial board suspects a case of "gift authorship," the submission will be rejected without further review. As part of the submission of the manuscript, the corresponding author should also send a short statement declaring that he/she accepts to undertake all the

responsibility for authorship during the submission and review stages of the manuscript.

"**Aquatic Research**" journal requires and encourages the authors and the individuals involved in the evaluation process of submitted manuscripts to disclose any existing or potential conflicts of interests, including financial, consultant, and institutional, that might lead to potential bias or a conflict of interest. Any financial grants or other support received for a submitted study from individuals or institutions should be disclosed to the Editorial Board. To disclose a potential conflict o f interest, the ICMJE Potential Conflict of Interest Disclosure Form should be filled in and submitted by all contributing authors. Cases of a potential conflict of interest of the editors, authors, or reviewers are resolved by the journal's Editorial Board within the scope of COPE and ICMJE guidelines.

The Editorial Board of the journal handles all appeal and complaint cases within the scope of COPE guidelines. In such cases, authors should get in direct contact with the editorial office regarding their appeals and complaints. When needed, an ombudsperson may be assigned to resolve cases that cannot be resolved internally. The Editor in Chief is the final authority in the decision-making process for all appeals and complaints.

When submitting a manuscript to "**Aquatic Research**" journal, authors accept to assign the copyright of their manuscript to **ScientificWebJournals**. If rejected for publication, the copyright of the manuscript will be assigned back to the authors. "**Aquatic Research**" journal requires each submission to be accompanied by a Copyright Transfer Form (available for download at **http://scientificwebjournals.com/AquatRes/AquatResCopyright andAuthorContributionForm2019.pdf.** When using previously published content, including figures, tables, or any other material in both print and electronic formats, authors must obtain permission from the copyright holder. Legal, financial and criminal liabilities in this regard belong to the author(s).

Statements or opinions expressed in the manuscripts published in "**Aquatic Research**" journal reflect the views of the author(s) and not the opinions of the editors, the editorial board, or the publisher; the editors, the editorial board, and the publisher disclaim any responsibility or liability for such materials. The final responsibility in regard to the published content rests with the authors.

MANUSCRIPT PREPARATION

The manuscripts should be prepared in accordance with ICMJE-Recommendations for the Conduct, Reporting, Editing, and Publication of Scholarly Work in Medical Journals (updated in December 2017 - http://www.icmje.org/icmje-recommendations.pdf). Authors are required to prepare manuscripts in accordance with the CONSORT guidelines for randomized research studies, STROBE guidelines for observational studies, STARD guidelines for studies on diagnostic accuracy, PRISMA guidelines for systematic reviews and meta-analysis, ARRIVE guidelines for experimental animal studies, TREND guidelines for non-randomized studies, and COREQ guidelines for qualitative studies.

Manuscripts can only be submitted through the journal's online manuscript submission and evaluation system, available at http://dergipark.gov.tr/journal/2277/submission/start

Manuscripts submitted to the journal will first go through a technical evaluation process where the editorial office staff will ensure that the manuscript has been prepared and submitted in accordance with the journal's guidelines. Submissions that do not conform to the journal's guidelines will be returned to the submitting author with technical correction requests.

Authors are required to submit the following forms during the initial submission.

- Copyright Transfer Form,

- Author Contributions Form (one form for copyright and contributions available in **http://scientificwebjournals.com/AquatRes/AquatResCopy rightandAuthorContributionForm2019.pdf**)

- ICMJE Potential Conflict of Interest Disclosure Form (should be filled in by all contributing authors) Download this form from **http://www.icmje.org/conflicts-of-interest/** fill and save. Send this to the journal with your other files.

Preparation of the Manuscript

Title (should be clear, descriptive and not too long)

Full Name(s) and Surname (s) of author(s)

ORCID ID for all author (s) (http://orcid.org/)

Address (es) of affiliations and e-mail (s)

Complete correspondence address and e-mail

Abstract

Key words (indexing terms), normally 3-6 items

Introduction

Material and Methods

Results and Discussion

Conclusion

Compliance with Ethical Standard

Conflict of interests: When you (or your employer or sponsor) have a financial, commercial, legal or professional relationship with other organizations or people working with them, a conflict of interest may arise that may affect your research. A full description is required when you submit your article to a journal.

Ethics committee approval: Ethical committee approval is routinely requested from every research article based on experiments on living organisms and humans. Sometimes, studies from different countries may not have the approval of the ethics committee, and the authors may argue that they do not need the approval of their work. In such situations, we consult COPE's "Guidance for Editors: Research, Audit and Service Evaluations" document and evaluate the study at the editorial board and decide whether or not it needs approval.

Financial disclosure: If there is any, the institutions that support the research and the agreements with them should be given here.

Acknowledgment: Acknowledgments allow you to thank people and institutions who assist in conducting the research.

References

Tables

Figures

Manuscript Types

Original Articles: This is the most important type of article since it provides new information based on original research. The main text should contain Introduction, "Materials and Methods", "Result and Discussion" and Conclusion sections.

Statistical analysis to support conclusions is usually necessary. Statistical analyses must be conducted in accordance with international statistical reporting standards. Information on statistical analyses should be provided with a separate subheading under the Materials and Methods section and the statistical software that was used during the process must be specified.

Units should be prepared in accordance with the International System of Units (SI).

Review Articles: Reviews prepared by authors who have extensive knowledge on a particular field and whose scientific background has been translated into a high volume of publications with a high citation potential are welcomed. These authors may even be invited by the journal. Reviews should describe, discuss, and evaluate the current level of knowledge of a topic in researches and should guide future studies. The main text should start with Introduction and end with Conclusion sections. Authors may choose to use any subheading in between those sections.

Short Communication: This type of manuscript discusses important parts, overlooked aspects, or lacking parts of a previously published article. Articles on subjects within the scope of the journal that might attract the readers' attention, particularly educative cases, may also be submitted in the form of a "Short Communication" Readers can also present their comments on the published manuscripts in the form of a "Short Communication". The main text should contain Introduction, "Materials and Methods", "Result and Discussion" and Conclusion sections.

Table 1. Limitations for each manuscript type

Type of manuscript	Page	Abstract word limit	Reference limit
Original Article	≤25	180	40
Review Article	no limits	180	60
Short Communication	≤5	150	20

Tables

Tables should be included in the main document, presented after the reference list, and they should be numbered consecutively in the order they are referred to within the main text. A descriptive title must be placed above the tables. Abbreviations used in the tables should be defined below the tables by footnotes (even if they are defined within the main text). Tables should be created using the "insert table" command of the word processing software and they should be arranged clearly to provide easy reading. Data presented in the tables should not be a repetition of the data presented within the main text but should be supporting the main text.

Figures and Figure Legends

Figures, graphics, and photographs should be submitted as separate files (in TIFF or JPEG format) through the submission system. The files should not be embedded in a Word document or the main document. When there are figure subunits, the subunits should not be merged to form a single image. Each subunit should be submitted separately through the submission system. Images should not be labelled (a, b, c, etc.) to indicate figure subunits. Thick and thin arrows, arrowheads, stars, asterisks, and similar marks can be used on the images to support figure legends. Like the rest of the submission, the figures too should be blind. Any information within the images that may indicate an individual or institution should be blinded. The minimum resolution of each submitted figure should be 300 DPI. To prevent delays in the evaluation process, all submitted figures should be clear in resolution and large (minimum dimensions: 100 × 100 mm). Figure legends should be listed at the end of the main document.

All acronyms and abbreviations used in the manuscript should be defined at first use, both in the abstract and in the main text. The abbreviation should be provided in parentheses following the definition.

When a drug, product, hardware, or software program is mentioned within the main text, product information, including the name of the product, the producer of the product, and city and the country of the company (including the state if in USA), should be provided in parentheses in the following format: "Discovery St PET/CT scanner (General Electric, Milwaukee, WI, USA)"

All references, tables, and figures should be referred to within the main text, and they should be numbered consecutively in the order they are referred to within the main text.

Limitations, drawbacks, and the shortcomings of original articles should be mentioned in the Discussion section before the conclusion paragraph.

References

Reference System is APA 6th Edition

In-text Citation with APA

The APA style calls for three kinds of information to be included in in-text citations. The **author's last name** and the work's **date of publication** must always appear, and these items must match exactly the corresponding entry in the references list. The third kind of information, the page number, appears only in a citation to a direct quotation.

....(Crockatt, 1995).

Direct quote from the text

"The potentially contradictory nature of Moscow's priorities surfaced first in its policies towards East Germany and Yugoslavia," (Crockatt, 1995, p. 1).

Major Citations for a Reference List in Table 2.

Note: All second and third lines in the APA Bibliography should be indented.

REVISIONS

When submitting a revised version of a paper, the author must submit a detailed "Response to the reviewers" that states point by point how each issue raised by the reviewers has been covered and where it can be found (each reviewer's comment, followed by the author's reply and line numbers where the changes have been made) as well as an annotated copy of the main document. Revised manuscripts must be submitted within 30 days from the date of the decision letter. If the revised version of the manuscript is not submitted within the allocated time, the revision option may be cancelled. If the submitting author(s) believe that additional time is required, they should request this extension before the initial 30-day period is over.

Accepted manuscripts are copy-edited for grammar, punctuation, and format. Once the publication process of a manuscript is completed, it is published online on the journal's webpage as an ahead-of-print publication before it is included in its scheduled issue. A PDF proof of the accepted manuscript is sent to the corresponding author and their publication approval is requested within 2 days of their receipt of the proof.

Table 2.

Material Type	Reference List/Bibliography
A book in print	Baxter, C. (1997). *Race equality in health care and education.* Philadelphia: Ballière Tindall, p. 110-115, ISBN 4546465465
A book chapter, print version	Haybron, D.M. (2008). Philosophy and the science of subjective well-being. In M. Eid & R. J. Larsen (Eds.), *The science of subjective well-being* (p. 17-43). New York, NY: Guilford Press. ISBN 4546469999
An eBook	Millbower, L. (2003). *Show biz training: Fun and effective business training techniques from the worlds of stage, screen, and song.* p. 92-90. Retrieved from http://www.amacombooks.org/ (accessed 10.10.2015)
An article in a print journal	Carter, S. & Dunbar-Odom, D. (2009). The converging literacies center: An integrated model for writing programs. *Kairos: A Journal of Rhetoric, Technology, and Pedagogy,* 14(1), 38-48.
Preview article in a journal with DOI	Gaudio, J.L. & Snowdon, C.T. (2008). Spatial cues more salient than color cues in cotton-top tamarins (*Saguinus oedipus*) reversal learning. *Journal of Comparative Psychology,* https://doi.org/10.1037/0735-7036.122.4.441
Websites - professional or personal sites	*The World Famous Hot Dog Site.* (1999, July 7). Retrieved January 5, 2008, from http://www.xroads.com/~tcs/hotdog/hotdog.html (accessed 10.10.2015).
Websites - online government publications	U.S. Department of Justice. (2006, September 10). Trends in violent victimization by age, 1973-2005. Retrieved from http://www.ojp.usdoj.gov/bjs/glance/vage.htm (accessed 10.10.15).
Photograph (from book, magazine or webpage)	Close, C. (2002). *Ronald.* [photograph]. Museum of Modern Art, New York, NY. Retrieved from http://www.moma.org/collection/object.php?object_id=108890 (accessed 10.10.2015).
Artwork - from library database	Clark, L. (c.a. 1960's). *Man with Baby.* [photograph]. George Eastman House, Rochester, NY. Retrieved from ARTstor.
Artwork - from website	Close, C. (2002). *Ronald.* [photograph]. Museum of Modern Art, New York. Retrieved from http://www.moma.org/collection/browse_results.php?object_id=108890 (accessed 10.10.2015).